Development of an environmentally friendly lithium-ion battery recycling process

By

Bruce Musariri

Thesis presented in partial fulfilment
of the requirements for the Degree

Of

MASTER OF ENGINEERING
(EXTRACTIVE METALLURGICAL ENGINEERING)

In the Faculty of Engineering
At Stellenbosch University

Supervisor
Prof. G. Akdogan

Co-Supervisors
Prof. C. Dorfling
Prof. S. Bradshaw

April 2019

DECLARATION

By submitting this thesis electronically, I declare that the entirety of the work contained therein is my own, original work, that I am the sole author thereof (save to the extent explicitly otherwise stated), that reproduction and publication thereof by Stellenbosch University will not infringe any third party rights and that I have not previously in its entirety or in part submitted it for obtaining any qualification.

Date: April 2019

PLAGIARISM DECLARATION

1. Plagiarism is the use of ideas, material and other intellectual property of another's work and to present is as my own.

2. I agree that plagiarism is a punishable offence because it constitutes theft.

3. I also understand that direct translations are plagiarism.

4. Accordingly all quotations and contributions from any source whatsoever (including the internet) have been cited fully. I understand that the reproduction of text without quotation marks (even when the source is cited) is plagiarism.

5. I declare that the work contained in this assignment, except where otherwise stated, is my original work and that I have not previously (in its entirety or in part) submitted it for grading in this module/assignment or another module/assignment.

Initials and surname: B. Musariri

Date: April 2019

Abstract

The main aim of this work was to evaluate the technical feasibility of using organic acids as lixiviants for Co, Li and Ni recovery from lithium-ion batteries (LIBs) and to recover the metals from the resulting pregnant leach solution (PLS).

Batch leaching tests to investigate the effects of H_2O_2 addition, temperature and acid concentration on metal dissolution were performed in a glass jacketed reactor with 300 ml working volume, using citric acid and DL-malic acid as lixiviants. Initial tests to investigate the effects of H_2O_2 addition indicated that it speeds up the leaching kinetics, hence it was included in successive leaching tests. Leaching tests were performed to investigate the effect of temperature and acid concentration on metal dissolution. Temperature levels of 30℃, 60℃ and 95℃ were used and acid concentration levels of 1 M, 1.25M and 1.5 M were used, with the H_2O_2 concentration and pulp density being kept constant at 2 % v/v and 20g/L, respectively. Results revealed that the performances of both acids were almost similar with over 95% metal dissolution within 30 minutes, using 1.5M citric acid and 1M DL-malic acid in the presence of 2% v/v H_2O_2 at 95℃ and 20g/L pulp density. After considering the cost of each acid, citric acid was selected as the more suitable lixiviant and was used in successive tests.

Batch solvent extraction tests were performed, with the aim of separating Mn and Al from Co, Li and Ni in the PLS, using D2EHPA as extractant in kerosene diluent. The following variables at the given levels were investigated: D2EHPA concentration (10% v/v and 20% v/v), pH (2.5, 3.0 and 3.5) and organic/aqueous phase ratio (O/A) (1, 2, 3, 4, and 5). The best separation results were obtained using 10% v/v D2EHPA at pH 2.5 and organic phase/aqueous phase O/A ratio 5, where 94% Mn was extracted within 15 minutes, with 47% Al, 7% Co, 9% Li and 3% Ni co-extraction, in one stage. The McCabe-Thiele method was employed under the optimum conditions and it predicted that over 99% Mn can be extracted in two stages. This was verified experimentally and 99% Mn and 89% Al were extracted in two stages, with 13% Co, 17% Li and 6% Ni co-extraction.

Metal precipitation tests were carried out at 50℃, 60℃, 70℃ and 80℃ using NaH_2PO_4 as precipitating agent. The results revealed that the solubility of Li_3PO_4 decreases with temperature increase, while the solubilities of $Co_3(PO_4)_2$, $Mn_3(PO_4)_2$ and $Ni_3(PO_4)_2$ were not

affected, in the investigated temperature range. Five scenarios for the recovery of metals from solution were considered and the proposed separation order in each scenario was experimentally investigated. For each scenario a flowsheet was constructed and mass balances were performed. Comparisons were made based on the mass balances, and the flowsheet in scenario four was selected as the most efficient one. It involves Mn and Al extraction from PLS using D2EHPA, followed by phosphate precipitation at 50℃ (targeting Co and Ni) and subsequent phosphate precipitation at 80℃ (targeting Li). This yields three products: a 93% pure Mn product, a Co-Ni product with 42 wt. % Co and 57 wt. % Ni and a Li product with 89 wt. % Li.

Opsomming

Die hoofdoel van hierdie werk was om die tegniese uitvoerbaarheid van die gebruik van organiese sure as loogmiddels vir Co, Li en Ni-herwinning uit lithium-ion batterye (LIBs) te evalueer en om die metale van die resulterende pregnant loogsifoplossing (PLS) te herwin.

Lotlogingstoetse om die effek van H_2O_2-aanvulling, temperatuur en suurkonsentrasie op metaaldissolusie te ondersoek, is uitgevoer in ’n glasomhulselreaktor met 300 ml werkende volume, deur sitroensuur en DL-appelsuur as loogmiddels te gebruik. Aanvanklike toetse om die effek van H_2O_2-aanvulling te ondersoek, het gewys dat dit die loging-kinetika versnel, en is dit dus ingesluit in opeenvolgende logingstoetse. Logingstoetse is uitgevoer om die effek van temperatuur en suurkonsentrasie op metaaldissolusie te ondersoek. Temperatuurvlakke van 30 °C, 60 °C en 95 °C is gebruik en suurkonsentrasievlakke van 1 M, 1.25 M en 1.5 M is gebruik, met die H_2O_2-konsentrasie en pulpdigtheid wat konstant gehou is by 2% v/v en 20 g/L, onderskeidelik. Resultate het bekendgemaak dat die doeltreffendheid van beide sure amper soortgelyk was met meer as 95% metaaldissolusie binne 30 minute, deur 1.5 M sitroensuur en 1 M DL-appelsuur te gebruik in die teenwoordigheid van 2% v/v H_2O_2 by 95 °C en 20 g/L pulpdigtheid. Nadat die kostes van elke suur in ag geneem is, is sitroensuur gekies as die meer gepaste loogmiddel en is in opeenvolgende toetse gebruik.

Lotoplosmiddelekstraksietoetse is uitgevoer, met die doel om Mn en Al van Co, Li en Ni in die PLS te skei, deur D_2EHPA as ekstraheermiddel in keroseenverdunner te gebruik. Die volgende veranderlikes by die gegewe vlakke is ondersoek: D_2EHPA-konsentrasie (10% v/v en 20% v/v), pH (2.5, 3.0 en 3.5) en organiese/waterige-verhouding (1, 2, 3, 4 en 5). Die beste skeiding resultate is verkry deur 10% v/v D_2EHPA by pH 2.5 en O/A-verhouding 5 te gebruik, waar 94% Mn binne 15 minute geëkstraheer is, met 47% Al, 7% Co, 9% Li en 3% Ni koëkstrahering in een stadium. Die McCabe-Thiele-metode is gebruik met die optimale kondisies en dit het beraam dat meer as 99% Mn in twee stadia geëkstraheer kan word. Dis eksperimenteel geverifieer, en 99% Mn en 89% Al is geëktraheer in twee stadia, met 13% Co, 17% Li en 6% Ni koëkstrahering.

Metaal presipitasietoetse is uitgevoer by 50 °C, 60 °C, 70 °C en 80 °C deur NaH_2PO_4 as neerslagmiddel te gebruik. Die resultate het bekendgemaak dat die oplosbaarheid van Li_3PO_4

afneem met temperatuur wat toeneem, terwyl die oplosbaarheid van $CO_3(PO_4)_2$, $Mn_3(PO_4)_2$ en $Ni_3(PO_4)_2$ nie geaffekteer is in die temperatuurbestek wat ondersoek is nie. Vyf scenario's vir die herwinning van metale uit oplossing is oorweeg en die voorgestelde skeidingsorde in elke scenario is eksperimenteel ondersoek. Vir elke scenario is 'n vloeidiagram saamgestel en massabalanse is uitgevoer. Vergelykings is gemaak gebaseer op die massabalanse, en die vloeidiagram in scenario vier is gekies as die mees doeltreffende een. Dit sluit in Mn en Al ekstrahering uit PLS deur D_2EHPA te gebruik, gevolg deur fosfaatneerslag by 50 °C (gerig op Co en Ni) en daaropvolgende fosfaatneerslag by 80 °C (gerig op Li). Hierdie lewer 'n opbrengs van drie produkte: 'n 93% suiwer Mn-produk, 'n Co-Ni-produk met 42 wt. % Co en 57 wt. % Ni, en 'n Li-produk met 89 wt. % Li.

Acknowledgements

I would like to express my gratitude to the individuals and organizations listed below:

My supervisor, Prof. Guven Akdogan and co-supervisor, Prof. Christie Dorfling, for their support. Their technical advice and guidance was instrumental in the completion of this project.

The technical and administrative staff at the Department of Process Engineering, Stellenbosch University, for their assistance.

My parents. Because of their love and financial support, I was able to study Metallurgical Engineering at the University of Zimbabwe, which enabled me to do my MEng in Extractive Metallurgy at the University of Stellenbosch.

The Department of Science and Technology, Waste RDI Roadmap, for their financial support.

Table of contents

List of figures

List of tables

Nomenclature

AAS	Atomic Absorption Spectrometry
ICP-OES	Inductively Coupled Plasma Optical Emission Spectrometry
LIBs	Lithium Ion Batteries
NMP	N-methyl-2-pyrrolidone
PLS	Pregnant Leach Solution
PTFE	Poly-Tetra-Fluoro-Ethylene
PVDF	Polyvinylidene Fluoride
SEAF	Submerged Electric Arc Furnace
UHT	Ultra High Temperature
VOCs	Volatile Organic Compounds
VTR	Vacuum Thermal Treatment

Chapter 1: Introduction

1.1 Background

Lithium-ion batteries are made up of an anode, a cathode, plastic separator and an organic electrolyte. The most common commercially used cathodic active materials used in LIBs are $LiN_{1/3}Co_{1/3}Mn_{1/3}O_2$, $LiNiO_2$, $LiCoO_2$ and $LiMn_2O_4$ (Wang *et al.*, 2009).

$LiCoO_2$ is the most common cathodic material for use in commercial LIBs, even though it has disadvantages such as high cost and limited Co deposits. (Hayashi *et al.*, 2009).

End of life LIBs are generally disposed as domestic waste, which does not conform to environmental protection standards. Recycling, incineration and landfilling have been reported as the most adequate methods of treating these waste batteries (Karnchanawong & Limpiteeprakan, 2009).

During incineration, metal oxides may be reduced to their metallic form, which results in the accumulation of heavy metals (Cu, Fe, Li and Co) in the environment and pollution of water sources (Grimes *et al.*, 2000).

In landfills, heavy metals can also slowly leach into the soil and eventually reach the water table, resulting in the pollution of ground water and even surface water sources. In upcoming years, the safe disposal of LIB waste is expected to become more expensive due limited storage capacity in these specialized dumpsites and the large numbers of LIBs that are being produced every year (Karnchanawong & Limpiteeprakan, 2009).

The recovery of metals from spent LIB components is therefore, beneficial, not only for environmental protection but also for the provision of expensive raw materials such as Co, Ni and Li for further LIB manufacturing.

Among other process routes, hydrometallurgy and pyro-metallurgy are used for LIB recycling. The main steps in the hydrometallurgical route are dismantling, size reduction, physical separation and leaching. Solvent extraction and ion exchange resins are used for the purification and upgrading of the resulting pregnant leach solutions and electrometallurgy or chemical precipitation can be used for converting them into a saleable form (Gaines, 2014).

In recent years, research has shifted towards the use of more environmentally friendly leaching reagents for the recovery of valuable metals from LIBs. This research focuses on environmentally friendly metal extraction process routes for the extraction of valuable metals such as Co, Li and Ni from LIBs, while preventing pollution of the environment and reducing the threat to human health, posed by the presence of heavy metals and other toxic compounds from waste LIBs in the environment.

1.2 Problem statement

LIBs are widely used in electronic devices such as cellular phones, laptops as well as in electric cars, due to their favorable properties such as relatively lower weight to volume ratio, higher voltage, lower self-discharge rate and higher energy density. The use of LIBs in the world is increasing due to high volumes of consumer electronics. Because of this, gradual rise of LIB waste is expected in upcoming years, especially with the newly introduced electric vehicles (EVs). LIBs contain valuable metals such as Co, Li and Ni as well as toxic compounds. The current LIB recycling processes cause a lot of harm to the environment, and for the sustainable management of natural resources and reduction of environmental pollution, less environmentally harmful recycling processes should be used for metal extraction from LIBs.

1.3 Aims and Objectives of Research

The main aim of this project was to investigate the development of an environmentally friendly metal extraction process for metal recovery from end-of-life LIBs, to recover Co, Li and Ni for further battery manufacture.

The research objectives were to:

i. Evaluate the effectiveness of organic acids as leaching reagents, with regard to Co, Li and Ni recovery, using citric and DL-malic acid as competitors.
ii. Select the most appropriate organic acid with regard to leaching performance and cost, and subsequently investigate the recovery metals from the pregnant leach solution using solvent extraction and/or selective precipitation.
iii. Propose a metal extraction process flowsheet based on the results from the leaching and metal extraction tests.

1.4 Research approach

This project was divided into two parts. The first part was on the leaching of metals from LIB cathodic material, using citric and DL-malic acid as lixiviants. The second part involved the recovery of metals from the resulting pregnant leach solution.

The leaching studies were completed in three phases:

- Phase one involved dismantling of batteries to module level and discharging them through immersion in NaCl solution. This was necessary to eliminate the residual charge in the batteries and prevent short circuiting and ignition during handling. Further dismantling was carried out to separate the anodes and cathodes.
- In phase two, the cathodic material was separated from the Al foils through leaching of the cathodes with 10 wt. % NaOH solution. The NaOH selectively dissolved the Al foils, leaving behind the cathodic material as a residue. After filtration, washing and drying, the cathodic material was ground to further liberate the metal particles before the leaching tests.
- Phase three involved reductive leaching of the cathodic material with citric acid and DL-malic acid at fixed pulp density. Initially, leaching tests were performed to investigate the effect of H_2O_2 addition on metal recovery, and a decision on its inclusion in subsequent leaching tests was made based on the results from the initial tests. After the necessity of H_2O_2 during the leaching process had been ascertained, a full factorial experimental design was used to investigate the effect of temperature and acid concentration on metal dissolution. Citric and DL-malic acid were compared and the more suitable lixiviant was selected, based on leaching performance and cost.

To investigate metal recovery from the pregnant leach solution, a bulk stock pregnant solution was prepared through leaching the cathodic material under the optimum conditions that had been determined by the leaching tests, using the lixiviant that had been selected as the suitable one. Solvent extraction experiments were performed on the PLS, with the aim of investigating the extraction of Mn and Al from the pregnant leach solution. A full factorial experimental design was used to investigate the effects of extractant concentration, pH and

O/A ratio on the separation process and the optimum conditions were determined. Batch phosphate precipitation tests were conducted on the PLS to investigate the effect of temperature on solubilities of the different metal phosphates. Once the effect of temperature on the precipitation of metal phosphates from solution had been established, successive tests were carried out with the aim of separating metals using solvent extraction and the differences in the solubilities of metal phosphates at different temperatures. Flowsheets for 5 different metal recovery options were drawn, and mass balances were performed for each flowsheet, based on the experimental results. The flowsheets were compared and the most efficient process route was selected.

1.5 Document outline

Section 2 provides an overview on metal extraction from LIBs and a literature survey on existing hydrometallurgical metal extraction processes for treatment of LIBs. This is followed by literature on leaching theory and the existing knowledge around the leaching of metals from LIBs using organic acids, as well as solvent extraction chemistry and previous work done on the recovery of metals from LIB leach solutions. The experimental methodology and equipment is discussed in Section 3. Experimental results are discussed in section 4. Section 5 comprises of the various flowsheets developed together with the corresponding mass balances. Section 6 has the conclusions and recommendations.

Chapter 2: Literature review

2.1 Introduction

LIBs are used as sources of power in modern life equipment. Their performance is better than that of conventional batteries, which have aqueous electrolytes.(Castillo *et al.*, 2002; Lee & Rhee, 2002). There are significant differences between lithium batteries and lithium-ion rechargeable batteries (LIBs) (Bernardes *et al.*, 2004).

Lithium batteries consist of a cathode made out of Li. However, Li is very reactive and must not come into contact with moisture during cell corrosion, to avoid explosions. On the other hand, LIBs do not have metallic lithium, but contain lithium oxide compounds at the cathode and graphite at the anode. $LiCoO_2$, $LiNiO_2$ and $LiMn_2O_4$ are some of the oxides that are used at as cathodic material. Another main feature of LIBs is a flammable and toxic organic electrolyte, which consists of dissolved compounds such as $LiClO_4$, $LiBF_4$ and $LiPF_6$ (Wang *et al.*, 2009).

Batteries typically contain organic electrolytes and binders, heavy metals and polymers in the proportion of 27.5% Li oxides, 24.5% Ni/Steel, 14.5% Cu/Al, 16%C, 17.5% polymers and other organic compounds (Shin *et al.,* 2005).

By the year 2000, about 500 million LIBs had been produced worldwide. From these numbers, 200-500Mt of LIB waste is estimated every year, with 6-16wt. % Co and 3-8wt. % Li. Automobile and industrial applications are expected to rise to about 40 billion USD by 2020 which is approximately half of the battery market share worldwide (Lee & Rhee, 2003).

In LIBs, the pressing of the cathode, anode and separator layers against each other makes the required electric contacts. The anode is a thin copper sheet coated with graphite, and the PVDF binder is used for binding the graphite to the copper sheet. The cathode is an Al plate sheet coated with the cathodic material and a mixture of electric conductor, polyvinylidene fluoride (PVDF) binder and other components. The common cathodic active material for almost all commercialized LIBs is $LiCoO_2$ (Li *et al.,* 2010).

One of the main objectives of recycling LIBs is Co and Li extraction. Cobalt is a limited resource and is more expensive than most of the metals found in LIBs. Lithium is a very expensive and strategic metal, used in many industrial applications (Conard, 1992).

2.2 LIB chemistry and design

The main constituents of an LIB are the anode, cathode, electrolyte, plastic separator and casing. Li salts that are dissolved in organic chemicals make up the electrolytes. $LiPF_6$, $LiBF_4$, $LiClO_3$ and $LiSO_2$ are some of the most common Li salts, while propylene carbonate and ethylene carbonate are used as solvents (Al-Thyabat *et al.,* 2013). Since Li salts are not stable in water based solutions, organic solutions are used instead. Micro perforated plastics such as polypropylene are used for making the separators, while steel or plastic is used for making the casings. The typical composition of LIBs is displayed in Table 1.

Table 1: Typical composition of lithium ion batteries (Knights & Sallojee, 2015)

Component	Composition (Mass %)
$LiCoO_2$	27
Ni/steel	25
Al/	14
C	16
Electrolyte	4
Polymers	14

2.3 Process routes for metal extraction from LIBs

Mechanical, hydrometallurgical and pyro-metallurgical routes are mainly used during metal extraction from LIBs. Usually a combination of two or more of these approaches is employed to ensure complete metal recovery. In the past two decades, hydrometallurgy has contributed the most to metal extraction from LIBs, followed by mechanical treatment and lastly pyro-metallurgy (Zeng *et al.,* 2014).

2.3.1 Mechanical routes

LIBs are shredded and crushed to reduce the particles to a suitable size, and then mechanically separated. Mechanical separation techniques separate materials using their differences in

density, conductivity and magnetic behavior. Density separation methods can be used to separate the lighter fractions from the rest of the material using shaking tables or froth flotation. Magnetism is used for the separation of ferrous metals from the mixture. Crushing is usually followed by grinding to liberate the cathode material. After liberation, standard mineral processing operations are used for concentrating the material (Al-Thyabat *et al.*, 2013).

2.3.2 Pyro metallurgical routes

They involve the recovery of metals through application of high temperatures. Specialised gas trapping and purification systems are required to control the emission of harmful gasses such as SO_x and NO_x associated gasses, Cl and volatile metals (e. g. zinc and mercury) that are produced during the process (ELI BAMEV, 2014). When heat is applied at low temperatures, reactions are characterized by changes in structure and phase transformations, while chemical reactions dominate at high temperatures. At high temperatures, smelting of batteries takes place and slag forming agents can be added to form the metal phase, slag fraction and gases that are emitted. Pyro-metallurgical routes have fast and simple steps, with no risk of exposure to electrolyte. During the process, plastics, organic material and carbonates combust and supply some of the heat for smelting and this reduces fuel consumption. Due to the high temperatures that are employed, pyro-metallurgical processes require large amounts of energy. They cannot recover Li since it is oxidized and reports to the slag phase, and often hydrometallurgy is used for its recovery from the slag after pyro-metallurgical processes. A lot of gasses (CO_2, CO, SO_2, VOCs and dust) are emitted at the high temperatures used, requiring expensive specialized gas purification equipment to control the emissions, which adds to the operational costs. Ignoble metals report to the slag and the organics are combusted before being used as reductants (Bernardes *et al.*, 2004; Georgi-Maschler *et al.,* 2012).

2.3.3 Hydrometallurgical routes

Hydrometallurgy involves the extraction of metals in an aqueous environment, whereby the value metal is transferred from the solid phase (feed) to the aqueous phase. The metal bearing solution is then concentrated and purified before the value metal is extracted from the concentrated solution and converted to solid form. During recycling of LIBs, battery material is dissolved and selectively separated whilst in solution, and the different process

streams are purified and the target metals are obtained. Before dissolution, there is usually liberation of the metals through shredding, crushing and grinding. Many processing plants also incorporate mechanical treatment in combination with hydrometallurgy. Due to its chemical specifity and unique applications in processes that are considered uneconomic, hydrometallurgy is fast becoming the preferred metal extraction technology. Some of the advantages of applying hydrometallurgy in metal extraction from LIBs are high metal recoveries, high purity, very low gas emissions and low energy consumption. Liquid effluents are also produced, but they are easier and cheaper to contain than gas emissions. Hydrometallurgy offers high selectivity which makes the extraction of several metals at high efficiencies possible. It also has the ability to extract lithium (Jha *et al.,* 2013).

Leaching, precipitation, ion exchange, solvent extraction and electrochemistry are some of the hydrometallurgical processes that are used. Table 2 summarizes the advantages and disadvantages of the different process routes in metal extraction from LIBs.

Table 2: Summary of the advantages and disadvantages of the available LIB recycling process routes

Process route	Advantages	Disadvantages
Mechanical	❖ Composition of the material is not altered.	❖ Risk of explosions during battery shredding. ❖ Uniform feed composition is required, since separation of components is difficult. ❖ High energy requirements for crushing and milling.
Hydrometallurgy	❖ More precise and easier to control ❖ Relatively lower energy requirements. ❖ High metal recoveries and high purity product streams. ❖ Very low gas emissions and less environmentally harmful.	❖ Liquid effluents produced ❖ High sensitivity to input of the process.
Pyro-metallurgy	❖ Simple operation. ❖ No sorting required. ❖ Ability to handle high input volumes in any proportions.	❖ Inability to recover lithium. ❖ Inability to recover plastics and other organic material. ❖ Energy intensive ❖ High operating costs due to requirement of sophisticated gas extraction systems to control gas emissions.

2.4 Current commercial LIB recycling processes

2.4.1 Sony Sumitomo process

It was developed by Sony of Japan in conjunction with Sumitomo Metals Mining Company and it mainly recovers cobalt from LIBs. Batteries are heated in a furnace, to 1000℃, which causes the cells to open up and combust inflammables like plastics, leaving behind a residue of copper, iron and aluminium pieces, which are removed from the mixture using magnetism. The remaining material is a mixture of the cathodic active material and graphite powders. Cobalt is recovered from this powder by hydrometallurgy (Sonoc *et al.,* 2015).

2.4.2 Recupyl process

Treats both primary Li and secondary Li-ion batteries. Batteries are shredded and ground into smaller particles in an inert enclosure filled with carbon dioxide and argon to prevent the violent reaction of lithium with air and moisture. Ground material is then separated into different fractions using gravity and magnetic separation techniques. The fractions produced are: the fines fraction (cathodic active material and carbon), magnetic fraction with steel casings, heavy fraction (copper and aluminium) and the low weight fraction (plastics and paper). The fines fraction is added to water at a controlled rate with vigorous mixing in a low oxygen atmosphere and there is reaction of Li with water to produce LiOH and H_2. Phosphoric acid or sodium carbonate is added to the lithium hydroxide rich water and lithium is recovered as lithium phosphate or lithium carbonate, respectively. The rest of the metals are also recovered by hydrometallurgy (Sonoc *et al.*, 2015).

2.4.3 Toxco process

The Toxco process utilizes both mechanical and hydrometallurgical techniques to recover valuable metals from LIBs. Before shredding and milling in lithium brine, the batteries are rendered inert by cryogenic cooling to -200℃ using liquid nitrogen. The lithium-containing solution is separated from the undissolved product using a screw press and filtered to produce a metal oxide cake (fluff). Using a shaking table, the cake is separated into heavy Co-Cu and light steel plastic streams, which are bagged and sold. The Li solution is pumped to dewatering tanks to increase the concentration of the lithium salts (LiCl, Li_2CO_3 and $LiSO_3$) until they precipitate. The solution from the dewatering tanks is filtered and purified with an electrolytic membrane. Sulfuric acid is used for dissolving the metal salts in the cake. Li^+ ions permeate

through the membrane and precipitate as LiOH. CO_2 is then used for converting the LiOH into Li_2CO_3, which is then filtered, washed, dried and packed (Gaines, 2014).

2.4.4 Accurec GmbH process

Electrode material is extracted by mechanical processes and then there is subsequent recovery of Co-Mn alloy by pyro metallurgical treatment and recovery of LiCl using hydrometallurgy. The batteries are subjected to vacuum thermal treatment (VTR) and pyrolysis to eliminate organic electrolytes and then crushed. Sieving and magnetism are then used to separate Al, Cu, steel and organic binder from the rest of the material. Organic binder is used to agglomerate the cathodic active material which is moulded into briquettes. The briquettes are fed into the furnace and smelted to form a metallic Co-alloy and a slag fraction. The Li reports to the slag and is leached out a LiCl (Sonoc *et al.*, 2015).

2.4.5 Falconbridge International Ltd- Canada

LIBs are fed to a partial pyro-metallurgical treatment process in Canada to produce a Cu, Co and Ni alloy. The alloy is shipped to Norway where it is pulverized and further treated by hydrometallurgical means. A chloride leach process is used to leach the value metals and the leach solutions are concentrated and purified using solvent extraction and the metals in different process streams are converted to their metallic form by electro-winning (Kushnir, 2015).

2.4.6 Batrec Industrie AG- Switzerland

The first step is crushing in an inert environment and then mechanical separation to produce different fractions, namely, Ni-scrap (Ni-chrome-steel), Co-Mn oxides and plastics. The cobalt fraction also contains lithium. The products are shipped to material producing companies where they are further processed (Georgi-Maschler *et al.*, 2012).

2.4.7 Umicore process

In the Umicore process, LIBs are charged into an ultra-high temperature (UHT) smelter after dismantling of large battery cases. Slag forming agents including battery production byproducts are added to the furnace and three fractions are produced, namely, a metal alloy fraction(Co, Ni, Cu, Fe), a slag fraction (Al, Li, Mn, REE) and a gas fraction with flue dust (Worrell & Reuter, 2014). 30-50% battery scrap should be in the feed so that the product will contain an economically acceptable Co and Ni content. (Cheret & Santen, 2011). The furnace

consists of three zones, at different temperatures. These include the preheating zone (<300℃), the plastic pyrolysing zone (700℃) and the smelting zone (1200-1450℃) (Cheret & Santen, 2011). Combustible compounds from the batteries heat the smelter to a temperature high enough to avoid emission of volatile organic compounds (VOCs), with a scrubbing system. The alloy is further refined using hydrometallurgy for Co and Ni recovery for further battery manufacturing and other uses. Li is oxidized and reports to the slag, and its recovery is currently uneconomic. Slag is used in the construction industry (Knights & Sallojee, 2015; Sonoc *et al.*, 2015).

2.4.8 Akkuser OY-Finland

In the Akkuser process, there are no chemicals added and a dry process is used. Before mechanical treatment, batteries are thoroughly sorted as it is important for the process to have a feed with uniform chemistry and composition. After sorting, there is crushing and milling of batteries into a very fine dust, with close monitoring of gasses emissions. The dust is mechanically separated into different fractions with the lighter plastics and paper fraction being separated first. The metal fractions are also separated into different classes according to composition and magnetic properties. The recovered material is then sold to battery manufactures (Kushnir, 2015).

A list of the current commercial processes that are being used to recycle end of life LIBs is shown in Table 3.

Table 3: Current commercial LIB recycle processes (Knights & Sallojee, 2015)

Company/Process	**Location**	**Metals recycled**	**Capacity**
Sony and Sumitomo Metals	Japan	Li-ion only	150
Dowa Eco-System Co. Ltd.	Japan	All Lithium Batteries	1 000
Toxco	Canada	All Lithium Batteries	4 500
Umicore	Belgium	Li-ion only	7 000
Batrec AG	Switzerland	Li-ion only	200
Recupyl	France	All Lithium Batteries	110
SNAM	France	Li-ion only	300
Xstrata	Canada	All Lithium Batteries	7 000
Inmetco	USA	All Lithium Batteries	6 000
JX Nippon Mining & Metals Co.	Japan	Unknown	5 000
Chemetall	Germany	Unknown	5 000
Accurec	Germany	Unknown	6 000
Stiftung Gemeinsames	Germany	Unknown	340
G & P Batteries	UK	Li-ion only	145
SARP	France	Li-ion only	200
Revatech	Belgium	Li-ion only	3 000
Shenzhen Green Eco-manufacturer			
Hi-Tech Co.	China	Li-ion only	20 000
Fuoshan Bangpu Ni/Co High-Tech	China	Li-ion only	3 600
TES-AMM	Singapore	Li-ion only	1 200
BDT	USA	All Lithium Batteries	350
Metal-Tech Ltd	Israel	All Lithium Batteries	
Akkuser Ltd	Finland	All Lithium Batteries	4000
		Total	70 595

2.5 Leaching theory

Leaching involves the transfer of the target metal from the solid feed into the aqueous phase. In most cases there is selective dissolution of the mineral of interest when the solid feed is contacted with a leaching reagent/lixiviant. The unwanted material in the feed must not be affected by the leaching reagent and should remain in the solid phase if the leaching is to be selective. The unreacted solids are filtered from the solution and the remaining solution is known as a pregnant leach solution. The solid phase must generally be permeable, to allow penetration of the leaching reagent into the solid, increasing the surface area for chemical reaction(Liley *et al.*, 1997).

2.5.1 Leaching mechanism

The shrinking core model is widely used for describing the physical phenomenon of leaching. It is based on the idea that initially the leaching reaction takes place on the exterior surface of a mineral particle and the leaching zone progresses towards the particle center, leaving behind inert material, which is referred to as ash. This means that during leaching, there is always a core of unreacted material that is progressively shrinking in size (Levenspiel, 1999). Figure 1 is an illustration of how leaching progresses according to the shrinking core model.

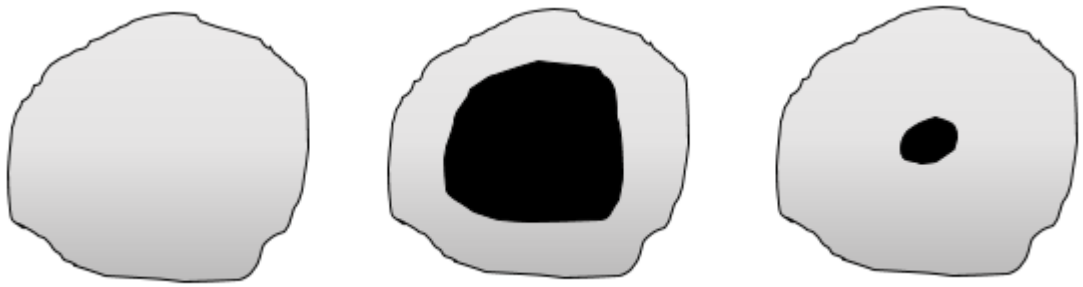

Figure 1: Illustration of the shrinking core model, applied to leaching [Adapted from (Levenspiel, 1999)*]*

For a spherical particle of unchanging size, leaching takes place in five steps (Levenspiel, 1999):

1. Diffusion of dissolved lixiviant reactant from the bulk solution through the boundary layer surrounding the particle to the solid surface.

2. Diffusion of the dissolved lixiviant reactant through inert material or porous product to the reaction surface at the core.
3. Reaction of the dissolved lixiviant reactant with the solid at the reaction surface
4. Diffusion of dissolved product through the inert layer to the outer surface of solid particle
5. Diffusion of the dissolved product through the boundary layer into the bulk solution.

The individual rates at which each of these steps progress may differ and the slowest step controls the overall leaching rate. Any effort to speed up the leaching process by speeding up any one of these steps, will only be successful if it is the rate limiting step (Levenspiel, 1999).

Figure 2 shows the features of a particle which follows the shrinking core model during leaching in more detail.

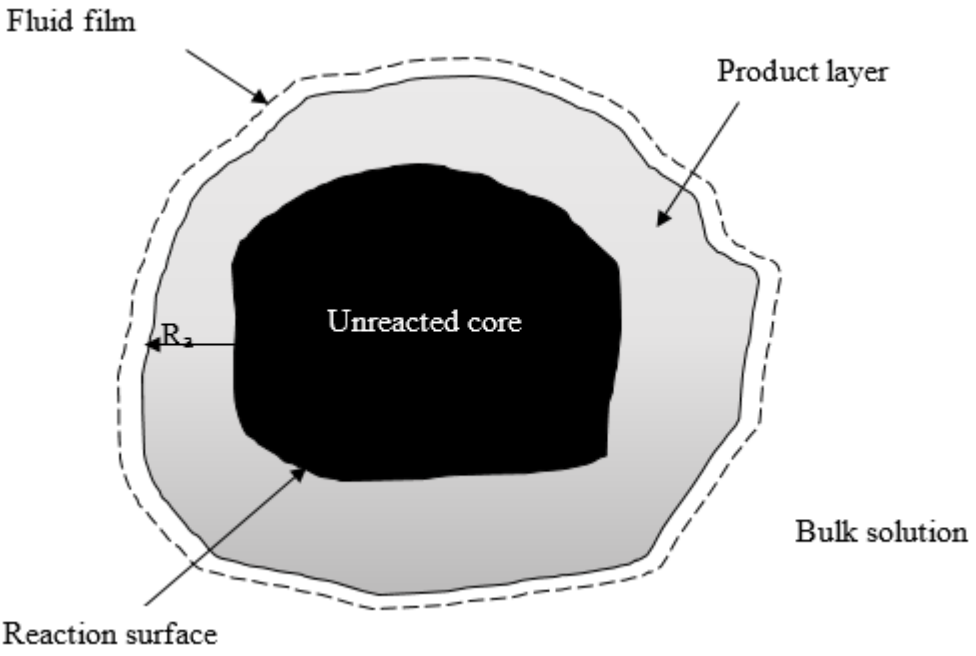

Figure 2: Schematic diagram of a topo-chemically reacted particle, as described by the shrinking core model (Pecina, Franco, Castillo & Orrantia, 2008)

2.5.2 Leaching kinetics

Leaching economics is a function of leaching rate due to the impact equipment has on leaching efficiency. Leaching is generally a slow process, hence leaching extent is not only determined by thermodynamic factors but also by the kinetics. How long the leaching process takes to reach equilibrium and how long the operation permits it to do so become crucial. If

the kinetics are understood, then the most suitable leaching conditions can be rationally determined. Equation 1 is used for developing the shrinking core model.

$$\mathrm{A(in\ fluid) + bB(in\ solid) \rightarrow C(product\ in\ fluid) + porous\ residue} \quad [1]$$

Where b = number of moles of B consumed per mole of A that reacts.

In the shrinking core model, leaching rate can be controlled by any one or a combination of the following mechanisms (Levenspiel, 1999):

- Diffusion of the dissolved lixiviant reactant and/or dissolved product through the boundary layer surrounding the solid mineral.
- Diffusion of dissolved lixiviant reactant and/or dissolved product through the product layer.
- Chemical reactions at the surface of the unreacted mineral solid.

The kinetic models for describing different rate limiting mechanisms are represented by the equations below, according to (Levenspiel, 1999).

For a surface chemical reaction controlled leaching process, Equation 2 is the suitable mathematical model to describe its leaching kinetics.

$$1 - (1 - X_B)^{\frac{1}{3}} = k_r t \quad [2]$$

$$\text{Where } k_r = \frac{bkC_{Ab}}{\rho R} \quad [3]$$

k = first order rate constant (ms^{-1})

C_{Ab} = concentration of A (dissolved lixiviant reactant) in the bulk solution ($mol.m^{-3}$)

ρ = molar density of B (solid reactant) ($mol.m^{-3}$)

R = radius of solid particle (m)

t = time (s)

X_B = fraction of the dissolved solid particle (B)

The mathematical model for an internal diffusion controlled leaching process shown in equation 4:

$$1 - 3(1 - X_B)^{\frac{2}{3}} + 2(1 - X_B) = k_d t \quad [4]$$

Where $k_d = \frac{6bD_eC_{Ab}}{\rho R^2}$ [5]

D_e = effective diffusion coefficient of A (dissolved lixiviant reactant) through product layer ($m^2. s^{-1}$)

If it is a mixed control leaching process (diffusion in product layer and chemical reaction), Equation 6 is suitable for describing the kinetics.

$$\left[1 - 3(1 - X_B)^{\frac{2}{3}} + 2(1 - X_B)\right] + a\left[1 - (1 - X_B)^{\frac{1}{3}}\right] = k_d t \quad [6]$$

Where $a = \frac{6D_e}{Rk}$ [7]

The values of k_r and k_d are usually found experimentally through curve fitting, even though they are functions of the characteristics of the material.

Table 4 is a summary of the guidelines for determining the rate limiting step for a leaching process. R is the reaction rate, while D represents the initial particle size, and E_a, the activation energy.

Table 4: Guidelines for determining rate limiting step in a leaching process

Mechanism	E_a **(KJ/mol)**	**Order of reaction**	**Agitation effect**	**Effect of D**
Chemical reaction	>40	Any	No	$R \propto 1/D$
Boundary layer diffusion	<20	First	Yes	$R \propto 1/D$
Porous layer diffusion	<20	First	No	$R \propto 1/D^2$

2.5.3 Leaching thermodynamics

Often, the thermodynamics of a system give an indication of the extent to which leaching takes place, including the solubility of the dissolved species in solution. Pourbaix diagrams

give the relative stabilities of metal species in aqueous solutions by showing the most common species at equilibrium and providing information on equilibria involved in leaching of ores. In order to select appropriate leaching conditions, it is important to know the various soluble species that will exist in a system. If one or more forms of the metal ions form in solution, then the conditions at which the metal ions remain in solution should be identified. Let's say the general leaching reaction is represented by Equation 11:

$$[MC]_{(s)} \leftrightarrow M^{+}{}_{(aq)} + C^{-}{}_{(aq)} \quad [8]$$

Where MC is the mineral with metal M.

If the leaching reaction is feasible, the forward reaction is favored. At equilibrium the concentration of MC must be very small and the solubility of MC should be high. The leaching is said to be selective if the dissolution reaction for the target mineral only is feasible (Havlík, 2008).

2.5.4 Factors affecting leaching

2.5.4.1 Particle size

The degree of exposure of mineral surfaces is a very important factor that seriously needs to be considered if total dissolution of a mineral from the ore is desired. In general, leaching rate increases with decreasing grind size. The feed size must be small enough for a large surface area of the valuable mineral to be exposed to the lixiviant (Havlík, 2008).

2.5.4.2 Diffusion rates

Diffusion of reactants from the bulk solution, through the boundary layer to the reaction surface plays a crucial role in the leaching process. It is largely dependent on the difference in concentration between reactants in the bulk solution and reactants at the reaction surface, as it acts as the driving force for diffusion through the boundary layer. Figure 3 illustrates the difference between reactant concentration at the reaction surface and concentration of reactant in the bulk solution as a function of the distance from the solid-solution interface.

Applying Fick's first law of diffusion and assuming that the concentration gradient through the boundary layer is linear, we get the Nerst model, represented by Equation 9:

$$(\frac{dn}{dt})_R = \frac{D_R A(C_R - C_{RO})}{\delta} \quad [9]$$

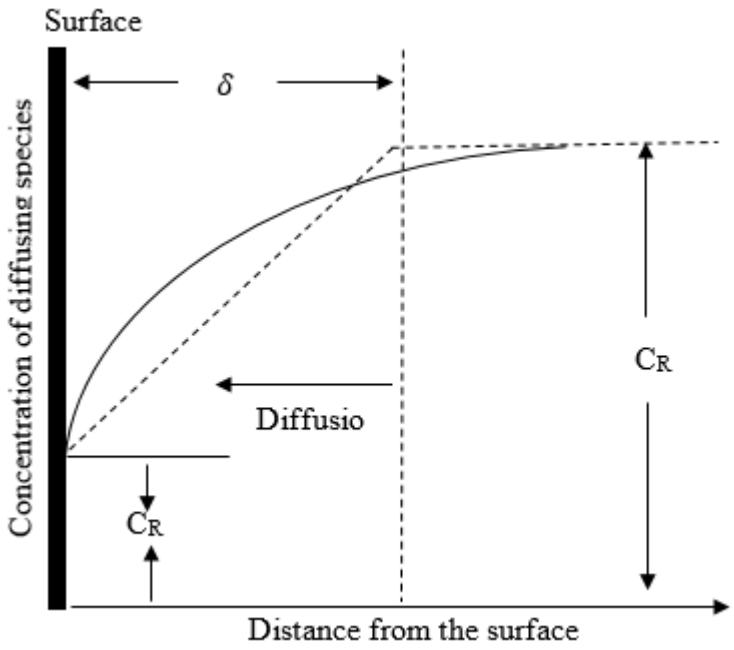

Figure 3: Concentration gradient as a function of the distance from the solid-liquid interface [Redrawn from (Jackson, 1986)*]*

Where $(\frac{dn}{dt})_R$ is the diffusion rate of reactant R through boundary layer with thickness δ, diffusion coefficient D_R and interfacial area A. C_R and C_{RO} are the reactant concentrations in the bulk solution and at the reaction surface, respectively.

$$D_R = \frac{k_B T}{6\pi r \eta} \quad [10]$$

Equation 10 is known as the Stokes-Einstein equation, where T is the solution temperature, η is the viscosity of solution, r is the molecular radius and k_B is the Boltzmann constant. From Equation 10, it can be seen that D_R is directly proportional to the temperature and inversely proportional to the viscosity of solution. D_R decreases with increasing lixiviant concentration, since the viscosity is increased.

For a process that is controlled by diffusion through the boundary layer, the concentration of reactant at the reaction surface (C_{RO}) can be assumed to be zero. This because the relatively faster chemical reaction at the surface rapidly consumes all the reactant that is presented to the reaction surface. In this scenario, Equation 9 becomes:

$$\left(\frac{dn}{dt}\right)_R = \frac{D_R A C_R}{\delta} \quad [11]$$

From Equation 11, the diffusion rate can be increased by; increasing agitation which decreases the boundary layer thickness, increasing interfacial area through particle size reduction and increasing concentration of the dissolved reactant in the bulk solution(C_R).

The Nerst model can similarly be applied to the diffusion of products from the reaction surface into the bulk solution through the boundary layer as shown in Equation 12 (Jackson, 1986):

$$\left(\frac{dn}{dt}\right)_P = \frac{D_P A (C_{PO} - C_P)}{\delta} \quad [12]$$

Where P is a specific product. When fresh lixiviant is used, for example, at the beginning of a leaching reaction the concentration of product in the bulk solution (C_P) will be zero, hence the diffusion driving force will be at its highest.

When the diffusion rate of reactants from the bulk solution to the mineral surface and products from the mineral surface to the bulk solution is slow, increasing the agitation rate speeds up the diffusion rate of species in solution. That is if diffusion of species through the boundary layer is rate controlling. If leaching rate is controlled by diffusion through a product layer around the mineral particle or through fissures, changing the agitation speed will not have a huge effect on leaching rate. In such cases, further particle size reduction or increasing temperature and lixiviant concentration would be the only options available to speed up the leaching rate. If chemical reaction conditions are dominant, increase in agitation speed will not speed up the leaching process, provided there is sufficient agitation (Jackson, 1986).

2.5.4.3 Rate of chemical reaction

Chemical reaction controlled processes are largely dependent on surface area and temperature, while independent of agitation. The rate of chemical reactions that take place on the mineral surface can be speeded up by increasing the surface area of the mineral that is exposed to the lixiviant, increasing temperature or introducing a catalyst. The reaction rate constant is defined by the Arrhenius equation and the rate constant increases exponentially with an increase in temperature, as shown by Equation 13.

$$k = \mathrm{A}e^{\frac{-\mathrm{E_a}}{\mathrm{RT}}} \quad [13]$$

Where A is the pre-exponential factor, R is the ideal gas constant, T is the absolute temperature and E_a is the specific activation energy.

For diffusion controlled leaching, leaching rate increases linearly with temperature and it is not as remarkable as that in chemical reaction controlled leaching (Havlík, 2008).

2.5.4.4 Lixiviant concentration

Increase in lixiviant concentration results in an increase in in leaching rate to a certain extent. Varying the lixiviant concentration may result in in a change in the rate limiting step (Havlík, 2008).

2.5.4.5 Pulp density

Generally, decreasing the pulp density increases leaching rate. There will be more leaching reagent per unit volume of pulp, and this means that most of the mineral particles are leached at the same time, which results in more metal dissolution per unit time. On the other hand, increasing the solid content results in less leaching reagent per unit volume of pulp and this increases competition for the leaching reagent among particle. The probability of some mineral particles not getting sufficient contact with the leaching reagent rises, which results in poor and slow leaching. Due to the high contribution of leaching reagents to the production costs in a processing plant, it is critical to optimize pulp density and leaching reagent consumption (Pérez & Hillier, 2003).

2.5.4.6 Insoluble product

In some cases, insoluble reaction product may form during leaching. If the product is porous, it will slightly affect the leaching rate. However in the case of a non-porous product, the leaching rate drops (Havlík, 2008).

2.6 Experimental hydrometallurgical metal extraction processes from LIBs

There have been numerous studies that have been conducted on laboratory scale, with the aim of continuously improving existing LIB recycling processes and to also develop alternative and less environmentally harmful ones.

Metals from spent LIB cathodic active material are conventionally recovered by leaching with mineral acids like H_2SO_4, HCl and HNO_3. The highest Co leaching efficiencies are obtained

using HCl at temperatures around 80°C (Zhang, et al., 1998). However, the production of chlorine gas (Cl_2) from HCl reaction results in extra costs due to the requirements of sophisticated gas capturing and containment equipment as well as serious environmental problems. It was reported that when H_2SO_4 or HNO_3 were used as lixiviants in $LiCoO_2$ leaching, with H_2O_2 as a reductant, higher Co and Li recoveries were obtained. It has also been reported that increase in metal recoveries was observed when acid concentration, temperature, and H_2O_2 concentration were increased and when pulp density was decreased (Lee & Rhee, 2003).

Bio-hydrometallurgical metal extraction processes are slowly becoming more popular than hydrometallurgical ones because they are more efficient, cost less and have less industrial requirements (Brandl & Faramarzi, 2006). If Bio-hydrometallurgical processes are used for the treatment of waste LIB residues, there will be less demand for resources like energy, landfill space and ores. Acidithiobacillus ferro-oxidants draw their energy from elemental sulfur and ferrous ions and produce metabolites such as ferric iron and sulfuric acids in the leaching reagents to extract Co from the LIBs. However, the bio-hydrometallurgical technologies that are currently being used are not yet mature in their application in metal extraction from LIBs and are still in the research phase (Mishra *et al.,* 2008).

2.7 Environmentally friendly metal extraction processes

In order to sustainably manage natural resources and to protect the environment, alternative metal extraction processes that are less harmful to the environment should be developed. Recent studies have shown that organic acids can be used in the hydrometallurgical extraction of Co, Li and nickel as less environmentally harmful lixiviants.

2.7.1 Leaching of spent LIBs with organic acids

In recent years, a considerable amount of research on the leaching of spent LIB cathodic active material with organic acids has been done. The most common organic acids, are aspartic acid, formic acid, lactic acid, succinic acid, oxalic acid, tartaric acid, DL-malic acid and citric acid. Some of the studies were briefly discussed to help with the selection of conditions that were used in the leaching experiments.

In a study by Li *et al.*, 2009 Li and Co were leached from $LiCoO_2$ cathodic material using citric acid with H_2O_2 as a reductant. After leaching under the optimum conditions: 1.25M acid

concentration, 1% v/v H_2O_2 concentration, 20 g/L pulp density at 90°C, about 93% Co and 99% Li recoveries were achieved within 30 minutes. The batteries were dismantled into anodes and cathodes. The cathodes were treated with NMP to dissolve the polyvinylidene fluoride (PVDF binder), recovering Al and Cu in their metallic form. After separating the cathodic active material, it was heated at 700°C for 5 hours in a muffle to burn off the acetylene black and the PVDF binder and cooled at room temperature. After cooling, the material was milled for 120 minutes to a particle size less than106μm before being fed to the leaching tests.

Three carboxyls are contained in one citric acid ($C_6H_8O_7$) molecule and theoretically, 1M of $C_6H_8O_7$ dissociates in water to produce three H^+ ions, not all the H^+ ions are released into the solution. The leaching of $LiCoO_2$ with $C_6H_8O_7$ can be described as a three-tier reaction. Equations 14, 15 and 16 represent the proposed series of reactions that take place during the leaching of $LiCoO_2$ with a $C_6H_8O_7$ according to Li *et al.*, 2010.

$$6H_3Cit_{(aq)} + 2LiCoO_{2(s)} + H_2O_{2aq} \rightarrow 2Li^+{}_{(aq)} + 2Co^{2+}{}_{(aq)} + 6H_2Cit^-{}_{(aq)} + 4H_2O_{(l)} + O_{2(g)} \quad [14]$$

$$6H_2Cit^-{}_{(aq)} + 2LiCoO_{2(s)} + H_2O_{2(aq)} \rightarrow 2Li^+{}_{(aq)} + 2Co^{2+}{}_{(aq)} + 6HCit^{2-}{}_{(aq)} + 4H_2O_{(l)} + O_{2(g)} \quad [15]$$

$$6HCit^{2-}{}_{(aq)} + 2LiCoO_{2(s)} + H_2O_{2(aq)} \rightarrow 2Li^+{}_{(aq)} + 2Co^{2+}{}_{(aq)} + 6Cit^{3-}{}_{(aq)} + 4H_2O_{(l)} + O_{2(g)} \quad [16]$$

Li *et al.*, 2010 investigated Li and Co recovery from waste $LiCoO_2$, with DL malic acid as lixiviant. The batteries were discharged by submersion in a 5 wt. % NaCl solution for 24 hours and dismantled into anodes, cathodes, steel casings and plastic separators. The cathodic material was separated from Al foils by submerging the cathodes in NMP for 1 hour at 100°C to dissolve PVDF binder. After filtration and drying, the cathodic powder was heat treated using a method similar to the one used by Li *et al.*, 2009, before being ground to a particle size less than 106 μm. Leaching were performed to investigate the effects of DL-malic acid concentration, H_2O_2 concentration, temperature and pulp density on Co and Li dissolution and to find the optimum leaching conditions. The four variable were investigated in the following ranges: DL-malic acid concentration (0.5-3M), H_2O_2 concentration (0-2.5% v/v),

temperature (20-100°C) and pulp density (17-33 g/L). After leaching under the optimum conditions (1.5M DL-malic acid concentration, 2% v/v H_2O_2 concentration, 90°C and 20g/ pulp density), over 93% Co and 99% Li recoveries were achieved within 40 minutes.

The proposed reactions for Co and Li dissolution in DL-malic acid are represented by Equations 17, 18, 19 and 20 (Li *et al.*, 2010):

With H_2O_2 absent;

$$4LiCoO_{2(s)} + 12C_4H_6O_{5(aq)} \rightarrow 4LiC_4H_6O_{5(aq)} + 4Co(C_4H_5O_5)_{2(aq)} + 6H_2O_{(l)} + O_{2(g)} \quad [17]$$

$$4LiCoO_{2(s)} + 12C_4H_5O_5{}^-{}_{(aq)} + 4Li^+{}_{(aq)} + 4Co^{2+}{}_{(aq)} \rightarrow 4Li_2C_4H_4O_{5(aq)} + 8CoC_4H_4O_{5(aq)}H_2O_{(l)} + O_{2(g)} \quad [18]$$

With H_2O_2 present

$$2LiCoO_{2(s)} + 6C_4H_6O_{5(aq)} + H_2O_2 \rightarrow 2LiC_4H_5O_{5(aq)} + 2Co(C_4H_5O_5)_{2(aq)} + 4H_2O_{(l)} + O_{2(g)} \quad [19]$$

$$2LiCoO_{2(s)} + 6C_4H_5O_5{}^-{}_{(aq)} + 2Li^+{}_{(aq)} + 2Co^{2+}{}_{(aq)} + H_2O_2 \rightarrow 2Li_2C_4H_4O_{5(aq)} + 4CoC_4H_4O_{5(aq)} + 4H_2O_{(l)} + O_{2(g)} \quad [20]$$

From the work done by Li *et al.,* 2012, the leaching of Co and Li from waste $LiCoO_2$ with ascorbic acid was investigated. The batteries were discharged and manually dismantled. The electrodes were treated with NMP using an ultrasonic cleaning vessel for 20 minutes, using 100 W electric power, at 40 Hz ultrasonic frequency. This separated the cathodic material from the Al foil and graphite from the copper foil, recovering aluminium and copper in their metallic form. After filtration and drying, the cathodic powder was roasted for 1 hour at 450°C to burn off carbon and polyvinylidene fluoride (PVDF) binder. Leaching tests were performed to investigate the effects of ascorbic acid concentration (0.3-1.75M), temperature (20-90°C) and pulp density (15-50 g/L) on metal dissolution. After leaching at optimum conditions: 1.25M ascorbic acid at 70°C and 300 rpm stirring speed, for 20 minutes, up to 95% Li and 99% Co leaching was achieved. There was no mention of grinding the cathodic material. No H_2O_2 was used. Ascorbic acid was being used as a leaching reagent and reducing agent at the same time due to its reducing power. It can undergo double oxidation to the more stable

dehydroascorbic acid ($C_6H_6O_6$). Initially, there is dissolution of $LiCoO_2$ to produce the soluble $C_6H_6O_6Li_2$. The reduction of Co^{3+} to Co^{2+} and oxidation of ascorbic acid to dehydroascorbic acid then takes place at the same time. It was reported that theoretically, there are several possible Co^{2+} containing products with different structures. However, thermodynamic calculations indicated that $C_6H_6O_6Co$ is thermodynamically favored. Equation 21 represents the reaction for $LiCoO_2$ leaching with ascorbic acid.

$$4C_6H_8O_{6(aq)} + 2LiCoO_{2(s)} \rightarrow C_6H_6O_{6(aq)} + C_6H_6O_6Li_{2(aq)} + 2C_6H_6O_6Co_{(qa)} + 4H_2O_{(l)} \quad [21]$$

In another study by Li *et al.,* 2013, three organic acids were compared, based on their leaching performance. The leaching power of aspartic acid, citric acid and DL-malic acid was compared, with regard to Co and Li leaching from $LiCoO_2$. Prior to leaching, batteries underwent the same pretreatment process as the one used by Li *et al.*, 2009 and Li *et al.*, 2010. Organic acid and hydrogen peroxide concentration were varied from 0.5M to 2M and 0% v/v to 6% v/v, respectively, while pulp density was varied from 5g/L to 30g/L and the temperature from 25°C to 90°C.

From the results, citric and DL-malic acid leaching yielded about 93% Co and 99% Li recoveries, while a maximum of 60% Co and Li leaching was obtained with aspartic acid. This was due to the weaker acidity of aspartic acid. Higher recoveries (93-99%) were achieved within shorter periods of time (30-40 minutes) when citric and DL-malic acid were used, while around 60% metal recoveries were achieved after 120 minutes with aspartic acid. The optimum pulp density was determined to be 20g/L for citric and DL-malic acid, while 10g/L was the optimum for aspartic acid. Further increasing pulp density from the optimum resulted in a drop in metal recoveries. The optimum hydrogen peroxide concentration was found to be 1% v/v, 2% v/v and 4% v/v for citric, DL-malic and aspartic acid, respectively. Although relatively larger quantities of hydrogen peroxide were supplied to the aspartic acid system, metal recoveries did not go beyond 60%.

Li *et al.,* 2014 investigated Li and Co recovery from $LiCoO_2$ using ultrasound assisted leaching with one organic acid (citric acid) and two mineral acids (H_2SO_4 and HCl). Spent LIBs were discharged, dismantled and the $LiCoO_2$ was separated from Al foils using the NMP treatment method. The cathodic material was calcined in a muffle at 700°C for 5 hours and ground in a ball mill for 2 hours. Leaching tests were carried out in an ultrasonic cleaning machine under

the following conditions: pulp density (25g/L), ultrasonic power (60W, 90W and 120W), temperature (20℃, 40℃ and 60℃) and residence time (2hours, 3.5 hours, 5 hours and 6 hours).

Results revealed that Co extraction was significantly influenced by the type of acid and the highest recoveries were obtained from citric acid leaching. Li extraction was similar for all three leaching reagents. These observations were believed to be because Li leaching depends on the concentration of H^+ ions which are generated by acid dissociation during leaching. The dissociation of citric acid is a three- tier reaction, as previously mentioned by Li *et al.*, 2009 and the dissociation constants are ($K_{a1} = 7.4 \times 10^{-4}$; $K_{a2} = 1.7 \times 10^{-5}$; $K_{a3} = 4 \times 10^{-7}$). This generates an H^+ concentration that is as high as that from mineral acids, therefore Li dissolution will be high. Cobalt leaching depends on both acid concentration and type of chelating agent. After reduction to the lower state, Co^{2+} needs to chelate with the acid anion to ensure high leaching rate and extent. It was also observed that HCl yields faster leaching kinetics than H_2SO_4, and this is due to the high reducing power of HCl. H_2SO_4 leaching involves two steps, dissolution of $LiCoO_2$ and reduction of Co^{3+} to Co^{2+}, and these steps take simultaneously in HCl. Overall, citric acid was found to be a better performing and less environmentally harmful leaching reagent than HCl and H_2SO_4, with more than 96% Co and 99% Li recoveries. The optimum citric acid leaching conditions were: 2M citric acid concentration, 0.55M H_2O_2 concentration, 25 g/L pulp density, 60℃, 5 hours residence time and 90W ultrasonic power. The high leaching efficiencies obtained were attributed to the cavitation action of ultrasonic waves.

Nayaka *et al.*, 2015 investigated Co and Li leaching from $LiCoO_2$ using a mixture of citric and ascorbic acid, ascorbic acid being the reductant and citric acid being the chelating agent. Cell phone LIBs were discharged, dismantled and the cathodic active material was manually scrubbed off the cathodes. After a heat treatment process similar to the one used by Li *et al.*, 2010, XRD analysis revealed that 90% of the material was $LiCoO_2$. SEM-EDX confirmed the presence of residual carbon after calcination, and it was believed to be due to acetylene black electrolyte and PVDF binder. 0.2g of the material was added to 100ml of 0.1M citric acid and 0.02M ascorbic acid and leaching was performed at 80℃. After 6 hours, 99% Co and Li recoveries were achieved and this was through a reductive complexation. From the results, dissolution kinetics speeded up when the citric acid/ascorbic acid (C/A) ratio was increased.

Recording of UV-Vis spectra of the leach solution was used to confirm the presence of Co (II)-citrate which was produced due to the reduction of Co (III). The maximum adsorptions (λ_{max}) for Co (II)-citrate and Co (III)-citrate were found to be 350nm and 512nm respectively. Initially, only the adsorption peaks for Co (III) were visible, indicating that it was the dominating species. As time went on, the intensity of Co (II) increased rapidly, and may have been attributed the reduction of Co (III)-citrate to Co (II)-citrate. After leaching, cobalt was recovered from solution as cobalt oxalate using 0.1M oxalic acid, while lithium was precipitated as LiF using 0.1M NH_4F.

The study conducted by Sun & Qiu, 2012 involved the use of oxalate as both leaching reagent and precipitating agent for Co and Li recovery from $LiCoO_2$. After discharging and manually dismantling of batteries, the cathodes were placed in a vacuum calcination system with a furnace and pump. The furnace was heated at a rate of 10℃/minute until the temperature reached 600℃ and it was held constant for 30 minutes, keeping the system pressure lower than 1kPa. The condensation temperature of the cold trap was kept at -10℃. The aim of this step was to peel off the cathodic active material from the Al foil. There was no mention of grinding of the material prior to leaching. Leaching was performed on the cathodic powder under optimum conditions: 1M Oxalate, 80℃, 50g/L pulp density, 120 minutes residence time and 300 rpm agitation speed. Under these conditions, 98% Co and Li recoveries were obtained. The concentration of H_2O_2 did not have a heavy impact on metal recovery. This was believed to be because of the oxidation of oxalate, which releases carbon dioxide and facilitates the forward reaction, even though the Co-O chemical bond in waste $LiCoO_2$ is extremely strong.

In a study by Li *et al.*, 2015, Co and Li recovery from waste $LiCoO_2$ using succinic acid as lixiviant was investigated. The same battery pretreatment process as from Li *et al.*, 2009 and Li *et al.*, 2010 was used. The effects of the following variables on leaching were investigated: succinic acid concentration (0.25-2M), H_2O_2 concentration (0-6% v/v), pulp density (5-30 g/L), reaction time (10-60 min) and temperature (50-90℃). Nearly 100% Co and 96% Li leaching was achieved under optimum conditions: succinic acid concentration (1.5M), H_2O_2 concentration (4% v/v), pulp density (15 g/L), temperature (70℃) and reaction time (40 min)]. The $LiCoO_2$ undergoes reductive leaching and it is believed that three possible comlexes are produce ($Li_2C_4H_4O_4$, $CoC_4H_4O_4$ and $CoC_8H_{10}O_8$). However, thermodynamic simulation indicated that

$CoC_4H_4O_4$ is thermodynamically favoured. It is easier to form and has more stability since it has a closed loop structure with atomic species symetrical on both sides of Co^{2+} ion, this explains the higher Co recovery. Leaching data was fitted to the shrinking core kinetic models to determine the rate limiting steps at different leaching stages and conditions. It was found that during the first 20 minutes, the process is chemical reaction controlled. After about 20 minutes there was a change in the rate limiting mechanism and diffusion through a porous product layer became the rate limiting step. This was due to the build up of ash around the particles as the the lixiviant selectively dissolved Co and Li, leaving behind porous inert residue.

Another study worth mentioning was by He *et al.*, 2017. An investigation on Co, Li, Ni and Mn recovery from scrap cell phone LIBs, using tartaric acid as lixiviant, was conducted. After discharging, dismantling and separation of electrodes, ultrasonic cleaning was performed on the cathodes in a solvent under the following conditions: cleaning temperature 70℃, 1:10 solid/liquid ratio, 240W ultrasonic power, 40 kHz frequency and 90 minutes residence time. XRD analysis revealed that there were three compound phases in the cathodic material, namely, carbon, $LiCoO_2$ and $LiNi_{0.5}Co_{0.2}Mn_{0.3}O_2$ and it was believed that the $LiNi_{0.5}Co_{0.2}Mn_{0.3}O_2$ peak came from the mixture of different NCM cathodic material, which have different metal proportions but the same XRD pattern. The particles in the cathodic active material had a low degree of agglomeration due to the dispersive effect of ultrasound and total dissolution of PVDF binder in NMP. This increased the surface area that was exposed to the lixiviant, hence enhancing the leaching process. SEM-EDS analysis also revealed that the leach residue mainly comprised carbon and fluorine, which were believed to be from PVDF binder since they do not dissolve in acid but remain behind as ash. Leaching was carried out in a 250ml glass reactor in a water bath, varying the H_2O_2 concentration from 0-5% v/v and L-tartaric acid concentration from 0.25M to 2.5 M. Pulp density and temperature ranges of 14-33 g/L and 40-80℃ were investigated, respectively and the residence time was 300 minutes. The optimum conditions were as follows: 4% v/v H_2O_2 concentration, 2M tartaric acid concentration, 17 g/L pulp density, 70℃ and 30 minutes residence time. Under these conditions, over 98% Co, Li, Mn and Ni recoveries were obtained.

In a more recent study by Li *et al.*, 2017, Co, Li, Mn and Ni recovery from waste $LiN_{1/3}Co_{1/3}Mn_{1/3}O_2$, using lactic acid with H_2O_2 was investigated. Batteries were dischaged

using a saturated saline solution and dismantled into separate elctrodes and plastic separators. NaOH leaching was used for separating cathodic material from the Al foils. The cathodes were treated with 10M NaOH solution at room temperature for 2h and after filtration and washing, the the residue was dried at 60°C for 24 hours. The material was calcined at 610°C for 5h in a muffle, before being milled for 30 minutes. Leaching experiments were performed in a 100 ml thermostatic pyrex reactor using a water bath for temperature control, with a condenser pipe to prevent water loss, with a stirrer set at 300 rpm. The effects of lactic acid concentration (0.25-2M), pulp density (10-40 g/L), temperature (40-90°C), H_2O_2 concentration (0-3% v/v) and residence time (10-60 min) were investigated, in the given ranges. More than 98% metals recoveries were achieved within 20 minutes under the optimum conditions: 1.5M lactic acid concentration, 70°C, 0.5% v/v H_2O_2 concentration and 20 g/L pulp density. Kinetic analysis was performed with basis on the shrinking core model and the Avrami equation (Equation 22). The leaching data did not fit into the shrinking core models and the Avrami equation was used to describe the leaching kinnetics.

$$\ln[-\ln(1-x)] = \ln k + n \ln t \qquad [22]$$

Where x is the metal extraction fraction, k is the rate constant (min^{-1}), n is a suitable parameter and t is the reaction time in minutes. Plots of $\ln[-\ln(1-x)] = \ln k + n \ln t$ produced linear relationships with regression coefficients higher than 0.96. The leaching mechanism was described as a two-step reaction; the first step being the reduction of high valence Co, Mn and Ni to Co^{2+}, Mn^{2+} and Ni^{2+}, which promoted the solubilisation of $LiN_{1/3}Co_{1/3}Mn_{1/3}O_2$. The second step was the chelation of Co^{2+}, Li^{+}, Mn^{2+} and Ni^{2+} with the lactate anion, and the overall dissolution reaction is shown by Equation 23

$$3LiNi_{1/3}Co_{1/3}Mn_{1/3}O_{2(s)} + 9C_3H_6O_{3(aq)} + \frac{1}{2}H_2O_{2(l)} \rightarrow 2LiC_3H_5O_{3(aq)} + Ni(C_3H_5O_3)_{2(aq)} + Co(C_3H_5O_3)_{2(aq)} + Mn(C_3H_5O_3)_{2(aq)} + 5H_2O_{(l)} + O_2 \qquad [23]$$

Gao *et al.*, 2017 also investigated the extraction of Co, Li, Mn and Ni from waste $LiN_{1/3}Co_{1/3}Mn_{1/3}O_2$, using formic acid as a leaching reagent, in the presence of H_2O_2. After discharging and dismantling, the cathodes were cut into small pieces ($1cm \times 1cm$), and digested with aqua regia. The metal content of the solution was analysed using ICP-OES and the material was found to contain 18.32% Ni, 18.65% Co, 17.57% Mn, 6.15% Li and 7.86% Al.

The cathode pieces were directly leached with formic acid solution to selectively leach the Co, Li, Mn and Ni in the cathodic powder, leaving behind pieces of Al foil. The effects of formic acid concentration (1.0-4.5M), temperature (30-90°C), pulp density (30-90 g/L) and H_2O_2 concentration (2-12% v/v) on metal dissolution were investigated. The acid dissociation equation for formic acid is illustrated by Equation 24

$$HCOOH_{(aq)} \leftrightarrow HCOO^-_{(aq)} + H^-_{(aq)} \qquad pK_a = 3.77, 25°C \qquad [24]$$

Besides being a weak acid, formic acid can also act as a reductant during metal leaching due to its aldehyde. It has the ability to selectively dissolve Li, Co, Mn and Ni from the cathodes, leaving behind the Al foil and organic solvents (binder and electrolyte). The reaction for the dissolution of $LiN_{1/3}Co_{1/3}Mn_{1/3}O_2$ in formic acid is shown in Equation 25.

$$6LiNi_{1/3}Co_{1/3}Mn_{1/3}O_{2_{(s)}} + 21HCOOH_{(aq)} \rightarrow 2NiC_2H_2O_{4_{(aq)}} + 2CoC_2H_2O_{4_{(aq)}} + 2MnC_2H_2O_{4_{(aq)}} + 6LiCHO_{2_{(aq)}} + 3O_{2_{(g)}} + 12H_2O_{(l)} \qquad [25]$$

Small amounts of Al also dissolve along with the target metals and the reaction is illustrated by Equation 26.

$$2Al_{(s)} + 6HCOOH_{(aq)} \rightarrow 2C_3H_3AlO_{6_{(aq)}} + 3H_{2_{(g)}} \qquad [26]$$

Addition of H_2O_2 enhances the leaching of cathodic active material by acting a reductant converting Co^{3+} and Mn^{4+} to Co^{2+} and Mn^{2+} respectively. In the presence of a reductant, Co, Li, Mn and Ni leaching was observed to be rapid, reaching equilibrium within 20 minutes. After 20 minutes, there was a drop in metal concentration in solution and it was believed to be due to the formation of metal hydroxide precipitates. There was an increase in metal dissolution when formic acid concentration was increased, but the Al extraction never exceeded 10%. Formic acid had an insignificant effect on Al leaching, indicating that it is suitable for selectively leaching Co, Li, Mn and Ni from cathodes, leaving the Al foils behind. The reaction for the leaching of $LiN_{1/3}Co_{1/3}Mn_{1/3}O_2$ with formic acid in the presence of hydrogen peroxide is shown by Equation 27.

$$6LiNi_{1/3}Co_{1/3}Mn_{1/3}O_{2_{(s)}} + 18HCOOH_{(aq)} + 3H_2O_{2_{(aq)}} \rightarrow 2NiC_2H_2O_{4_{(aq)}} + 2CoC_2H_2O_{4_{(aq)}} + 2MnC_2H_2O_{4_{(aq)}} + 6LiCHO_{2_{(aq)}} + 3O_{2_{(g)}} + 12H_2O_{(l)} \qquad [27]$$

Results indicated that Al leaching is not affected by H_2O_2 concentration, but over 99% Co, Li, Mn and Ni recoveries were obtained at optimum H_2O_2 concentration. It was therefore conclude that the cleanest Al foils are obtained when H_2O_2 is utilized. Kinetic analysis was also carried out based on the shrinking core models and it indicated that the leaching process was chemical reaction controlled.

From the studies that have been discussed, the separation of cathodic material from the Al prior to organic acid leaching is an important step. Most of the publications have indicated the use of NMP as the preferred method to achieve this separation (He *et al.*, 2017; Li *et al.*, 2013, 2010, 2009, 2012, 2015, 2014). However, NMP is very expensive and its use in the separation of cathodic material from Al foils on an industrial scale will lower the economic feasibility of the operation. Li *et al.*, 2017 used NaOH solution to selectively dissolve the Al foils, leaving behind the cathodic material as a residue. Successive organic acid leaching tests were carried out and high metal recoveries were obtained. There are lower costs associated with the NaOH route, and it produces results that are just as good as the NMP route. For these obvious economic reasons, the NaOH route was employed in this work.

2.7.2 Variables affecting the rate and extent of LIB leaching

2.7.2.1 Acid concentration

Li *et al.*, 2010 and Li *et al.*, 2009 investigated the effect of DL-malic acid and citric acid concentration on Li and Co extraction. Acid concentration was varied from 0.3 to 2M, and 1.5M was found to be the optimum for DL-malic acid leaching, while 1.25M was found to be the optimum citric acid concentration, with up to 93 % Co and 99 % Li recoveries. Further increase in the citric and DL-malic acid concentration resulted in a decrease in Co and Li recoveries. This was believed to be attributed to a decrease in conductivity of the solution as the amount of acid molecules in solution is increased, and this had a negative effect on the leaching extent.

Gao *et al.*, 2017 varied the acid concentration from 1M to 4.5M, and an increase in leaching efficiency with increase in acid concentration up to 4.5M was observed. However, due to economic considerations and for of optimisation of acid consumption, 2M was chosen as the most suitable acid concentration.

In studies by He *et al.*, 2017 and Li *et al.*, 2012, 2017, it has been reported that as the acid concentration is increased, there is an initial increase in leaching rate and extent up to a certain point, further increase in the amount of acid results in no change in the leaching efficiency and in some cases, it ends up having a negative effect on leaching. This is usually due to loss in solubility when the amount of acid molecules in the system is increased.

2.7.2.2 Temperature

Li *et al.*, 2010 investigated the effect of temperature on Co and Li leaching with DL-malic acid, while Li *et al.*, 2009 investigated the effect of temperature on $LiCoO_2$ dissolution using citric acid as leaching reagent. From both studies, it was observed that there is a remarkable increase in Co and Li dissolution when temperature is increased from 30℃ to 90℃. At 30℃, less than 50% metal recoveries were obtained after 2h. When the temperature was increased to 90℃, over 93% Co and 99 % Li recoveries were achieved within 30 minutes. However, further increase in temperature from 90℃ did not cause any significant increase in dissolution rate or extent.

The importance of temperature on metal dissolution using organic acids has also been investigated in many other studies. In all of these studies, it has been reported that leaching rate and extent increases with an increase in temperature up to a certain optimal temperature, further increase in temperature shows no significant increase in metal dissolution (Gao *et al.*, 2017; He *et al.*, 2017; Li *et al.*, 2012, 2015, 2014; Nayaka *et al.*, 2015; Sun & Qiu, 2012; Zeng *et al.*, 2014).

2.7.2.3 H_2O_2 Concentration

Li, *et al.*, 2010 reported that when leaching $LiCoO_2$ with DL-malic, Co and Li dissolution rate increased with an increase in H_2O_2 concentration. After leaching with 1.5M acid at 20 g/L pulp density and 90℃ with no H_2O_2, only 37 % Co and 54% Li dissolved after 2h. When 2% v/v H_2O_2 was included in the system, 93% Co and 99% Li recoveries were obtained within 30 minutes. Further increase in H_2O_2 from 2.0% v/v to 2.5% v/v resulted in no further increase in metal dissolution rate.

Similarly, Li *et al.*, 2009 investigated the effect of H_2O_2 on Co and Li recovery from $LiCoO_2$ using citric acid lixiviant. The H_2O_2 concentration was varied from 0 to 2% v/v while the following

conditions were kept constant: citric acid concentration at 1.25M, pulp density at 20 g/L, residence time at 30 minutes, temperature at 90°C. An increase in Co and Li dissolution rate was also observed as the H_2O_2 concentration was increased. Co dissolution increased from 25% to 91%, while Li dissolution increased from 54% to 99% when H_2O_2 was increased from 0% v/v to 1% v/v. However, increase in H_2O_2 to 1.5% v/v did not increase metal dissolution any further.

Li *et al.*, 2010, 2009 and Golmohammadzadeh *et al.*, 2017 reported that H_2O_2 decomposes at high temperatures according to Equation 28 and the decomposition rate increases with increase in temperature.

$$H_2O_{2(l)} \rightarrow H_2O_{(l)} + \frac{1}{2}O_{2(g)} \quad [28]$$

There is significant interaction between the type of acid used and H_2O_2 concentration. For example, Golmohammadzadeh *et al.*, 2017 reported that there is increase in metal dissolution with increase in H_2O_2 concentration up to a certain limit, beyond that limit, further increase in H_2O_2 results in a drop in metal dissolution. This is because excessive amount of hydrogen peroxide results in a change in the role of the H_2O_2 from being a reductant to being an oxidant (Golmohammadzadeh *et al.*, 2017).

Ferreira *et al.,* 2009 investigated the effect of H_2O_2 concentration on Co and Li recovery from $LiCoO_2$ using sulphuric acid as a lixiviant. It was reported that the dissolution of $LiCoO_2$ involves the reduction of Co^{3+} to Co^{2+} and during dissolution, Co_3O_4 is produced as an intermediate oxide and remains in the solid phase. Without H_2O_2, the dissolution of Co_3O_4 is very slow and requires excess amount of acid to be converted into the more soluble $CoSO_4$. The sequential reaction scheme for the mechanism with no H_2O_2 is represented by Equations 29 and 30, and the overall reaction is represented by Equation 31.

$$4LiCoO_{2(s)} + 3H_2SO_{4(aq)} \rightarrow Co_3O_{4(s)} + 2Li_2SO_{4(aq)} + CoSO_{4(aq)} + 3H_2O_{(l)} + \frac{1}{2}O_{2(g)} \quad [29]$$

$$Co_3O_{4(s)} + 3H_2SO_{4(aq)} \rightarrow 3CoSO_{4(aq)} + 3H_2O_{(l)} + \frac{1}{2}O_{2(l)} \quad [30]$$

$$4LiCoO_{2(s)} + 6H_2SO_{4(aq)} \rightarrow 2Li_2SO_{4(aq)} + 4CoSO_{4(aq)} + 6H_2O_{(l)} + O_{2(g)} \quad [31]$$

Equations 32 and 33 show the reaction scheme when H_2O_2 is present and Equation 34 shows the overall reaction.

$$4LiCoO_{2(s)} + 3H_2SO_{4(aq)} + H_2O_{2(l)} \rightarrow Co_3O_{4(s)} + 2Li_2SO_{4(aq)} + CoSO_{4(aq)} + 4H_2O_{(l)} + O_{2(g)} \quad [32]$$

$$Co_3O_{4(s)} + 3H_2SO_{4(aq)}H_2O_{2(l)} \rightarrow 3CoSO_{4(aq)} + 4H_2O_{(l)} + O_{2(l)} \quad [33]$$

$$4LiCoO_{2(s)} + 6H_2SO_{4(aq)} + 2H_2O_{2(l)} \rightarrow 2Li_2SO_{4(aq)} + 4CoSO_{4(aq)} + 8H_2O_{(l)} + 2O_{2(g)} \quad [34]$$

Zou, 2012 also proposed that H_2O_2 has the same effect of reducing Ni^{3+} and Mn^{3+} to Ni^{2+} and Mn^{2+} during $LiMn_2O_4$ and $LiNiO_2$ leaching, respectively, the Li dissolution being promoted since Li and Co, Mn or Ni are in the same oxide compound.

Another study worth mentioning is the one by Gao *et al.*, 2017, from which the effect of H_2O_2 concentration on Co, Li, Mn and Ni leaching from $LiNi_{1/3}Mn_{1/3}Co_{1/3}O_2$ was investigated using formic acid as a lixiviant. It was reported that H_2O_2 assists with $LiNi_{1/3}Mn_{1/3}Co_{1/3}O_2$ dissolution by reducing Co^{3+} and Mn^{4+} into the more soluble Co^{2+} and Mn^{2+}, Ni and Li dissolution being promoted as well, since they are contained in the same oxide compound. It was concluded that metal dissolution from LIB cathodic material is dependent on H_2O_2 concentration.

2.7.3 Selection of leaching reagents

From the previous studies on metal recovery from LIBs that have been discussed, it seems as if most of the mentioned organic acids are good leaching reagents, capable of yielding over 90% metal recoveries under optimum conditions. However in this study two acids were selected based on acid strength, ability to act as a chelating agent and cost.

Table 5 shows a list of the most common organic acids with their associated pKa values. pKa is a measure of acidity, the lower the pKa value, the stronger the acid.

Table 5: pKa values of the most common organic acids (Serjeant & Dempsey, 1979)

Acid	**pKa_1**	**pKa_2**	**pKa_3**
Ascorbic acid	4.10	11.79	15.89
Citric acid	3.14	4.77	6.39
Formic acid	3.75	-	-
Lactic acid	3.08	-	-
DL-malic acid	3.4	5.11	-
Oxalic acid	1.23	4.19	-
Succinic acid	4.16	4.61	-
Tartaric acid	2.98	4.34	-

From Table 5 the strength of acidity decreases in the order; oxalic acid, tartaric acid, lactic acid, citric acid and DL-malic acid, based on the first dissociation constants. Oxalic acid is a strong organic acid and its dissociation involves two steps. However, it forms cobalt oxalate precipitates and this makes it an unfitting leaching reagent for this study. Citric acid dissociation involves three steps as discussed in the study by Li *et al.*, 2014. One mole of citric acid generates three moles of H^+ ions and this means citric acid is capable of producing an adequate concentration of H^+ ions in solution (Golmohammadzadeh, *et al*, 2017). High H^+ ion concentration promotes Co and Li dissolution. Citric acid is also an excellent chelating agent and since the extraction of Co involves reduction to Co^{2+} and then chelating with the acid anion to ensure high leaching rates and extents, citric acid would be an excellent choice for a leaching reagent (Li *et al.*, 2014). Lactic acid has only one pKa value which means one mole of lactic acid supplies one mole of H^+ ions. This means it generates a lower concentration of H^+ ions than DL-malic and tartaric acid which generate two moles of H^+ ions from one acid molecule. However DL-malic acid has a relatively higher affinity for Co (Golmohammadzadeh

et al., 2017) and is cheaper than tartaric acid, which also makes it a good choice for a leaching reagent.

In addition to the discussion above, the use of citric acid and DL-malic acid for the dissolution of metals from LIB cathodic material has already been justified by Golmohammadzadeh *et al.*, 2017. For these reasons, citric acid and DL-malic acid were selected as leaching reagents in this work.

2.9 Solvent extraction theory

Solvent extraction is a method used for the extraction of metals from solution by contacting the pregnant solution with an immiscible organic extracting agent. The extracting agent being the organic phase and the leach solution being the aqueous phase. During agitation of the dispersion, there is contact between the two phases and the metal cation is transferred from the aqueous phase to the organic phase and an organometallic complex is formed. After equilibrium, the two phases are separated. Usually, extractants are diluted with water immiscible diluents and not used in their pure form. These diluents enhance the extracting capabilities of extractants by altering their physical properties. Mineral acids like HCl or H_2SO_4 are used for stripping the metals from the organic phase and they are then recovered in the aqueous phase and the extractant is also recycled. During extraction, H^+ ions in the organic extractant are exchanged with metal cations from the aqueous solution and during stripping, H^+ ions from the acid (stripping agent) replace metal ions in the organic extractant. This regenerates the organic extractant for further reuse in extraction. The metal species is recovered as a salt which is further processed to obtain the metal (Habashi, 1999).

2.8.1 Extracting agents

For every solvent extraction operation, it is important to select a suitable extractant that is capable of forming the relevant metal complex that can be extracted. The distribution coefficient, separation factor and percentage extraction are the key performance indicators of the process and they can also be used for quantifying the performance of extractants. The higher the distribution coefficient (D), the greater the ease with which metal ions can be extracted from the aqueous phase. The relative distribution coefficient (β) or separation factor tells us about the selectivity of the extractant towards metals that are being extracted

from aqueous solutions. The larger the relative distribution coefficient the greater the selectivity (Habashi, 1999).

$$D_A = \frac{Concentration\ of\ metal\ A(organic)}{Concentration\ of\ metal\ A(aqueous)} \quad [35]$$

$$\beta = \frac{D_A}{D_B} \quad [36]$$

$$E_A = \frac{N_{AO} - N_A}{N_{AO}} \quad [37]$$

Where:

D_A and D_B = Distribution coefficients of metals A and B, respectively, at equilibrium

β = Distribution coefficient of metal A relative to B

E_A = Percentage of metal A extracted

N_{AO} = Initial number of moles of metal A in the aqueous phase

N_A = Number of moles of metal A in aqueous phase after extraction

Selective extraction of metals is greatly impacted by aqueous solution pH. Metal species are extracted at different pH values, therefore it is important to find the pH that generates the largest separation factor of one is to achieve selective extraction. A suitable extractant should have the ability to extract two different metal species at two totally different pH values, and there should be a large difference in the distribution coefficients between the two different metals at specific pH. The pH_{50} value, which is the pH at which 50% of the metal is extracted to the organic can also be used for measuring the performance of an extractant. A large difference in pH_{50} values between two metals is an indicator of easy separation (Devi *et al.*, 1998).

Extractants that are commonly used on industrial scale can be divided into 3 main classes: basic extractants (anion exchangers), solvation extractants and acidic extractants (cation exchangers) (Xie *et al.,* 2014). However this study focuses on the separation of Mn from a Co, Ni and Li solution and from previous work done, cationic exchangers have been used (Chen & Ho, 2018; Chen *et al.*, 2015; Chen & Zhou, 2014). Table 6 shows cationic exchangers that are commonly used for Ni, Fe, Mn and Co separation.

Table 6: Popular organophosphorus extractants used for Co, Fe, Mn and Ni separation (Chen & Ho, 2018; Flett, 2005).

Type	Name	Commercial uses
Alkyl phosphinic acids	Cyanex 272, Ionquest 290, LIX 272/$(C_8H_{17})_2$ P(O)OH Cyanex 302/$(C_8H_{17})_2$P(S)OH Cyanex 301/$(C_8H_{17})_2$P(S)SH	Rare earths and Co/Ni separation; zinc and iron extraction
Alkyl phosphoric acids	DEHPA/$C_{16}H_{35}O_4$ P	Co/Ni separation; Zn, U and rare earth extraction
Alkyl phosphonic acids	PC-88A or Ionquest 801/ $C_{16}H_{35}O_4P$	Co/Ni and rare earth separation

2.8.2 Diluents

As discussed before, extracting agents are mixed with diluents before use. There are many different types of aliphatic and aromatic diluents and their molecules can range from complex molecules to simple ones. Diluents influence the extracting power of the extractant and this is related to the bonding and interactions between the extractants and diluents. There are some diluents that can polymerize the extractant, strengthening the forces between the hydrogen atom that is supposed to be exchanged and the extractant, which affects the cation exchange process (Bhattacharyya *et al.*, 2007; Rydberg *et al.*, 2004).

Some common examples of diluents used in solvent extraction are: n-hexane, Carbon tetrachloride, 1, 2 dichloroethane, Cyclohexane, Benzene, Toluene, Nitrobenzene and kerosene, Xylene, Chloroform, Dichloromethane (Gandhi *et al.*, 1993).

2.8.3 Phase separation and third phase formation

During solvent extraction a third phase can be formed, which is caused by solubility issues in the organic phase and this is a very serious challenge. During separation of the organic phase from the aqueous solution, a third phase develops between these two phases. This is because this new phase has intermediate properties that are between the organic and aqueous phase. The third phase formed is rich in metal-organic complexes. A lot of work has been done to try and understand this third phase, and the following findings have been made with regard to third phase formation (Foust *et al.*, 2008):

- Third phase formation is dependent on temperature. The third phase disappears with temperature increase because the organic-aqueous solubility decreases with temperature increase.
- If the extractant is loaded with too much amount of metal, a third phase can form
- Suspended solids usually cause phase separation problems.
- It mostly happens when aliphatic diluents are used.
- The challenges can be surmounted by adding a third phase modifier.

Typical examples of third phase modifiers are TBP (tri-n-butyl-phosphate), p-nonyl phenol, TOA (tri-octyl-amine), 2-ethylhexanol and iso-decanol. Previous studies have shown that third phase modifiers are not chosen in a random manner, an investigation is carried experimentally before a modifier is selected. In numerous studies conducted, TBP and TOA have been used as third phase modifiers (3-5 vol. % being added) (Devi *et al.*, 1998; Reddy *et al.*, 2006; Rodrigues & Mansur, 2010; Sarangi *et al.*, 1999; Tsakiridis & Agatzini, 2004).

2.8.4 Solvent Extraction and Stripping Chemistry

During solvent extraction a cation exchange reaction takes place whereby a metal species is extracted from the aqueous phase and transferred to the organic phase. A general cation exchange reaction is shown in Equation 38 (Tsakiridis & Agatzini, 2004). The interactions between diluents and extractants have not been considered:

$$(\mathrm{M^{n+}})_{\mathrm{aq}} + (\mathrm{nLH})_{\mathrm{org}} \leftrightarrow (\mathrm{ML_n})_{\mathrm{org}} + (\mathrm{nH^{+}})_{\mathrm{aq}} \quad [38]$$

M^{n+} is a valence n metal cation and LH is an organic extractant with proton H. Species in the aqueous phase are denoted by aq, while species in the organic phase are denoted by org. Equation 38 can be rewritten in terms of Mn extraction with D2EHPA to produce Equation 39.

$$(\mathrm{Mn^{2+}})_{\mathrm{aq}} + (2\mathrm{LH})_{\mathrm{org}} \leftrightarrow (\mathrm{MnL_2})_{\mathrm{org}} + (2\mathrm{H^+})_{\mathrm{aq}} \quad [39]$$

During solvent extraction, hydrogen ions are released into the aqueous solution and this causes the pH of solution to decrease. The recovery of many metal species is strongly dependant on pH. As a result, the pH has to be controlled using NaOH or NH_4OH which add OH^- to the system. This prevents excess H^+ build-up which would force Equation 38 to favour the backward reaction (Nogueira *et al.*, 2009). A modified equation for reaction 38 where NaOH is the base titrant is shown in Equation 40:

$$(\mathrm{M^{n+}})_{\mathrm{aq}} + (\mathrm{nLH})_{\mathrm{org}} + (\mathrm{nNaOH})_{\mathrm{aq}} \leftrightarrow (\mathrm{ML_n})_{\mathrm{org}} + (\mathrm{nH_2O})_{\mathrm{aq}} + (\mathrm{nNa^+})_{\mathrm{aq}} \quad [40]$$

A more general representation of the reaction that takes place during metal extraction with Cyanex 272 or D2EHPA is shown by Equation 41 (Flett, 2005).

$$(\mathrm{M^{n+}})_{\mathrm{aq}} + ((\mathrm{n+x})\mathrm{LH})_{\mathrm{org}} \leftrightarrow (\mathrm{MR_n.xLH})_{\mathrm{org}} + (\mathrm{nH^+})_{\mathrm{aq}} \quad [41]$$

When NaOH is used as a base titrant, the general metal extraction reaction Equation 41 can be rewritten as shown in Equation 42:

$$(\mathrm{M^{n+}})_{\mathrm{aq}} + ((\mathrm{n+x})\mathrm{LH})_{\mathrm{org}} + (\mathrm{nNaOH})_{\mathrm{aq}} \leftrightarrow (\mathrm{ML_n.xLH})_{\mathrm{org}} + (\mathrm{nH_2O})_{\mathrm{aq}} + (\mathrm{nNa^+})_{\mathrm{aq}} \quad [42]$$

Equation 43 represents the general reaction for extraction of divalent metals with Cyanex 272 and D2EHPA (Chen & Ho, 2018; Sahu *et al.*, 2004).

$$(\mathrm{M^{2+}})_{\mathrm{aq}} + ((1+\mathrm{x})\mathrm{LH})_{\mathrm{org}} \leftrightarrow (\mathrm{ML_2.x(LH)_2})_{\mathrm{org}} + (2\mathrm{H^+})_{\mathrm{aq}} \quad [43]$$

The nature of the organometallic complex $\mathrm{ML_2.x(LH)_2}$ can be determined by a method called Slope analysis. This can be done using the equilibrium constant shown in Equation 44:

$$K = \frac{[H^+]^2[ML_2.x(LH)_2]}{[M^{2+}][(1+x)(LH)_2]} \quad [44]$$

After rearranging Equation 44 and taking the logarithm, Equation 45 is obtained.

$$\mathrm{logD_M} - 2\mathrm{pH} = \mathrm{logK} + \mathrm{xlog[(LH)_2]} \quad [45]$$

Where [(LH) $_2$] is the concentration of the organic extractant and D_M is the distribution coefficient of metal M and. Plotting ($logD_M$–2pH) against log [(LH) $_2$] yields a straight line with intercept logK and gradient x. The nature of the organometallic complex $ML_2.x(LH)_2$ can be identified if x is known. Nogueira *et al.*, 2009 reported $ML_2.x(LH)_2$ as being $CoL_2.(LH)_2$ for Co extraction and $NiL_2.2(LH)_2$ for Ni extraction. For example, when x is known, for Ni extraction, Equation 43 becomes Equation 46.

$$(Ni^{2+})_{aq} + (3(LH)_2)_{org} \leftrightarrow (NiL_2.3(LH)_2)_{org} + (2H^+)_{aq} \quad [46]$$

A saponified form of the extractants can also be used instead of the acidic form (Cyanex 272 and D2EHPA), which is basically the sodium or ammonia salt of the extractant, and this is done before metal extraction. This reduces the amount of NaOH or NH_4OH that needs to be added to the system for controlling pH. Equations 47 and 48 show the reactions involved during extraction of a divalent metal with saponified Cyanex 272/D2EHPA. (Kang *et al.*, 2010):

$$((Na, NH_4)OH)_{aq} + {}^1/_2\,((LH)_2)_{org} \leftrightarrow ((Na, NH_4)L)_{org} + (H_2O)_{aq} \quad [47]$$

$$(M^{2+})_{aq} + (2(Na, NH_4)L)_{org} + (x(LH)_2)_{org} \leftrightarrow (MR_2.x(LH)_2)_{org}(2(Na^+, {NH_4}^+))_{aq} \quad [48]$$

When the saponified form of extractant is used, the metal species that is extracted is replaced by Na^+ or NH_4^+ instead of H^+, but extraction still occurs through cation exchange. This is shown in equation 48. This technique significantly reduces large drops in pH (caused by an increase in the amount of H^+) as a function of extraction, thereby reducing the amount of alkali that is required during the extraction process. (Kang *et al.*, 2010).

Due to interactions between diluents and extractants and dimerization of extractants, solvent extraction chemistry is more complex than what is shown in the general equations.

2.8.5 Scrubbing

In most cases during solvent extraction, the wanted metal is extracted along with the unwanted one. The unwanted metal is co-extracted to a certain extent. The unwanted metal can be scrubbed from the organic phase by mixing it with an aqueous solution containing the wanted metal.

For example, during Co and Ni extraction with Cyanex 272, the co-extracted Ni is scrubbed from the organic phase by mixing it with a Co containing aqueous solution and the Co contained in aqueous solution is exchanged with Ni in organic, as shown by Equation 49.

$$(\mathrm{NiL_2}.2(\mathrm{LH})_2)_{\mathrm{org}} + (\mathrm{Co}^{2+})_{\mathrm{aq}} \leftrightarrow (\mathrm{CoL_2}.(\mathrm{LH})_2)_{\mathrm{org}} + ((\mathrm{LH})_2)_{\mathrm{org}} + (\mathrm{Ni}^{2+})_{\mathrm{aq}} \quad [49]$$

In order for this to work, there must be greater chemical attraction between the extracting agent and the wanted metal than that between the extractant and unwanted co-extracted metal, hence it will be able to displace the co-extracted metal from the extractant and out of the organic phase. The lower the pH at which a metal is extracted by an extractant, the greater the chemical attraction between the metal species and the extractant. This means that the metals that are extracted at lower pH are able to scrub those that are extracted at higher pH (Nogueira *et al.*, 2009).

2.8.7 Stripping

A metal species can be recovered from the organic phase by a process known as stripping. Basically, stripping is the reverse of extraction, whereby the organic phase loaded with metal is agitated together with a strong acid and the metal species is removed from the organic phase and goes into the aqueous phase (Flett, 2005). The general reaction for stripping is represented by Equation 50:

$$(\mathrm{ML_n}.\mathrm{xLH})_{\mathrm{org}} + (\mathrm{nH}^{+})_{\mathrm{aq}} \leftrightarrow (\mathrm{M}^{\mathrm{n}+})_{\mathrm{aq}} + ((\mathrm{n}+\mathrm{x})\mathrm{LH})_{\mathrm{org}} \quad [50]$$

A fresh aqueous phase containing the stripped metal is generated, while the extractant is recycled back to its acidic form. Selective stripping can also be done using different acid concentrations. For two different metals that can be extracted at different pH values, a weaker acid may be employed to strip the metal that is extracted at a higher pH, followed by stripping with a stronger acid targeting the metal extracted at a lower pH than the first metal (Flett, 2005).

2.8.8 Solvent extraction kinetics

Brisk & McManamey, 1969 studied the kinetics of solvent extraction of metals using acidic organophosphorus extractants.

The dispersion of phases is important during solvent extraction and this can be facilitated by the adsorption of extractants at the interfaces, which lowers the interfacial tension. With enough adsorption of extractant at the interface, the system will become highly dispersed, and the interfacial concentration of the extractant will be higher than that in the bulk solution. This will result in reactions taking place both at the interface and in the bulk solution. In a chemical reaction controlled system, the overall extraction rate is determined by the concentration of extractant at the interface as well as the interfacial area. Interfacial concentration of the extractant is dependent on the bulk concentration, extractant molecule geometry, interfacial activity and diluent type. Increase in extractant concentration in the bulk solution results in an increase in extractant interfacial concentration up to a point whereby the solution is saturated (Flett & Spink, 1976).

2.8.9 Factors affecting solvent extraction

The ability of an extractant to effectively extract metal species from solution is dependent on a number of parameters, and these can be aqueous or organic.

2.8.9.1 Solution pH

It is one of the major factors that influence solvent extraction. The optimum operating pH can be selected depending on the type of metal being recovered. For example, the typical Co, Ni and Fe extraction pH ranges from a sulphate solution using Cyanex 272 are 5-6, 7-8 and 2-3, respectively. This means that the tendency of these metals to be extracted from the aqueous phase and report to the organic phase is in the order Fe>Co>Ni. The dependence of the extraction of various metals on pH, with a certain extractant, can be used to qualitatively predict the extraction behavior of impurities from a solution. For example, in a sulphate solution with Co, Ni and Fe as the major elements, impurities like Zn and Cu are expected to be extracted by Cyanex 272 at pH values between those of Co and Fe, with Co being extracted along with the Cu and Zn following Fe in the extraction circuit. Precision in pH control is also important to prevent co-extraction of impurities, for example, Ca and Mg in Co extraction with Cynex 272 (Habashi, 1999).

Base titrants are used for pH control during solvent extraction, NaOH and NH_4OH being the most common ones (Nogueira *et al.*, 2009).

2.8.9.2 Temperature

Solvent viscosity decreases with increase in temperature and this improves the ability of the solvent to wet the matrix and dissolve the analytes of interest. The extra energy supplied facilitates the breaking of matrix bonds and promotes the mass transfer of analytes to the surface of the matrix. There is extensive literature on the factors affecting solvent extraction, but publications with information regarding the effect of temperature are limited. Temperature affects the other factors that influence solvent extraction and the effects can be highly variable. The structure of organometallic complexes can be influenced by temperature. For example, during the separation of Co and Ni with D2EHPA, the effect of temperature can be credited to different coordination chemistries between the ligands and metal ions. Co complexes with two dimerised phosphorous acid ligands and forms both octahedral and tetrahedral complexes. The octahedral Co complex is more hydrophilic, and its stability drops at temperatures above 40℃, shifting to the tetrahedral complex which is more lipophilic. On the other hand, Ni only forms octahedral complexes with three dimerised phosphoric acid molecules. This means that Co extraction with D2EHPA is enhanced at temperatures above 40℃, while temperature does not have a significant effect on Ni extraction with D2EHPA (Preston, 1982; Rickelton, Flett & West, 1984).

2.8.9.3 Organic/Aqueous phase ratio

It refers to the relative amounts in terms of volume at which organic and aqueous phases are mixed during extraction. Plotting of metal concentrations in the organic against metal concentration in the aqueous phase at equilibrium produces extraction isotherms. The data used for the construction of these isotherms can be obtained by varying the O/A ratio at fixed pH and initial aqueous concentration and in a batch fashion (Flett, 2005). Figure 4 shows a typical extraction isotherm.

It is already known that lower metal extraction is obtained at lower O/A ratios, while higher metal extraction is obtained at higher O/A ratios. Usually, complete metal extraction is achieved in a stage wise manner using lower O/A ratios and pH values which do not achieve complete extraction in one stage (Tsakiridis & Agatzini, 2004). Figure 5 shows how this can be achieved using a multistage counter current extraction system

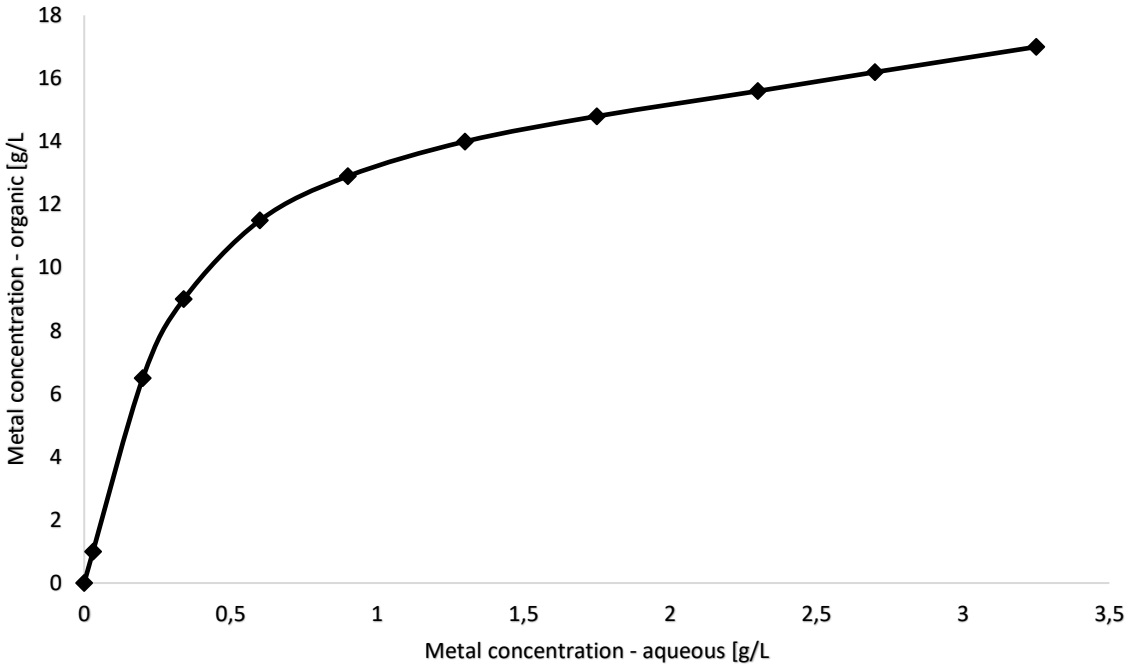

Figure 4: Typical example of an extraction isotherm [Adapted from (Rydberg *et al.*, 2004)*]*

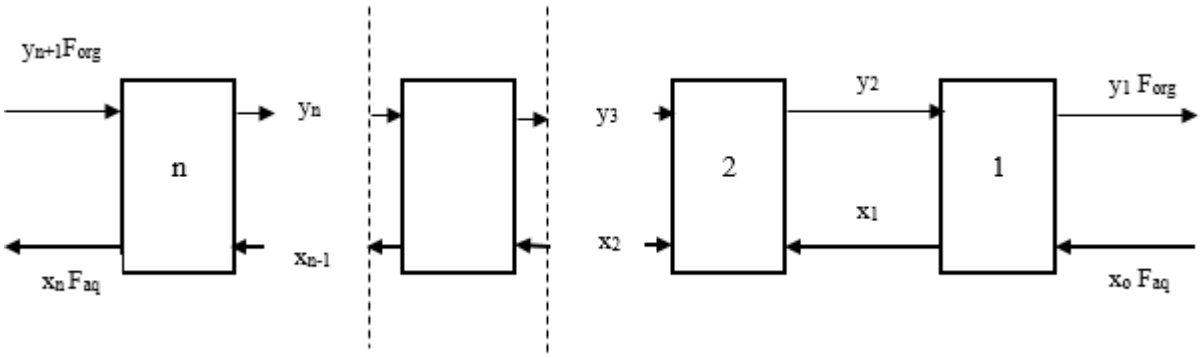

Figure 5: Multistage counter current extraction system [Adapted from (Olivier *et al.*, 2011)*]*

From Figure 5, the line represented by Equation 51 can be derived balancing of masses and some mathematical calculations (Olivier *et al.*, 2011).

$$y_1 = \frac{F_{aq}}{F_{org}}(x_o - x_n) + y_{n+1} \qquad [51]$$

Where y_1 = concentration of metal in the organic phase coming out of the system.

x_o = concentration of metal in aqueous phase going into the system.

x_n = concentration of metal in the aqueous phase coming out of the system.

y_{n+1} = concentration of metal in the organic phase going into the system.

n = Theoretical number of required stages.

F_{aq}/F_{org} = gradient of operating line (A/O ratio for the process in Figure 5)

The straight line in Equation 51 can be used together with the extraction isotherm in Figure 4 to determine the number of theoretical stages required to reduce the metal concentration in aqueous solution from x_o to x_n and increase metal concentration in the organic phase from y_{n+1} to y_1 as shown in Figure 6.

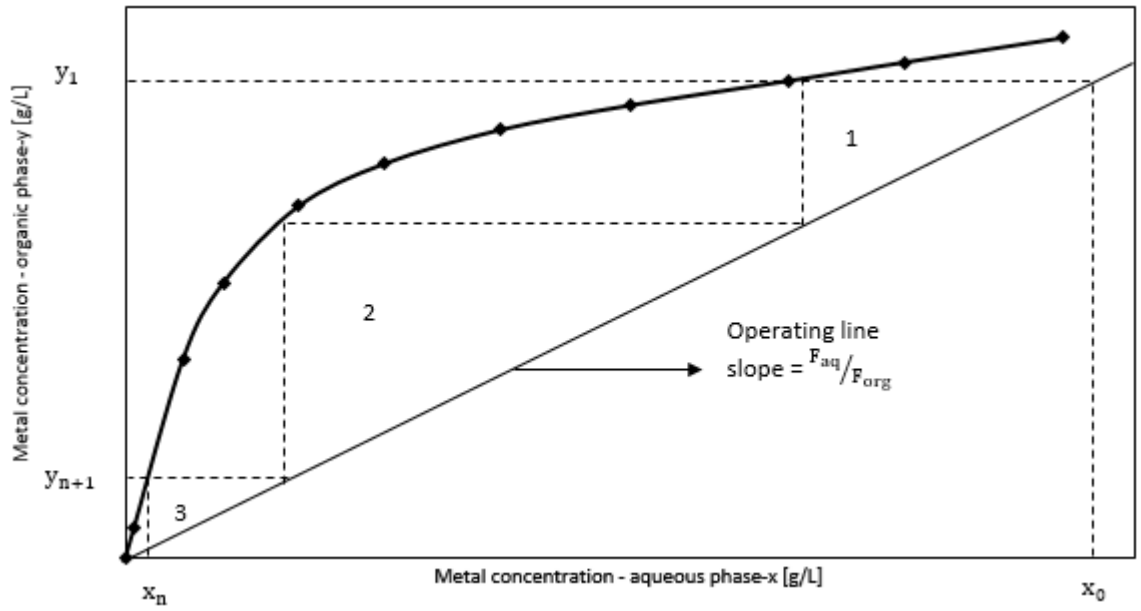

Figure 6: Typical McCabe-Thiele diagram

From Figure 6 it can be seen that, theoretically, it takes three stages to achieve the target recovery, as indicated by the dotted lines at a particular F_{aq}/F_{org}. Increase in the O/A ratio decreases the F_{aq}/F_{org} gradient on the graph, which decreases the theoretical steps needed for complete extraction. Figure 6 is a McCabe-Thiele diagram and it predicts the number of stages required for complete extraction during a solvent extraction process, at specific conditions. The McCabe-Thiele can also be similarly used to predict the theoretical number of stages in stripping.

2.8.9.4 Metal ion concentration

It is known that metal extraction increases with increase in metal ion concentration in solution. However, it has been argued that the extraction of tracer and macro amounts of metals is expected to be similar under the same equilibrium conditions, provided the solubility of extracting species in the organic phase is not exceeded (Kislik, 2012).

2.10 Solvent extraction from LIB leach solutions

Reports from previous studies have indicated that the extraction of metals from waste LIB leach solutions involves a combination of chemical precipitation and solvent extraction, with more than 98% metal recoveries being achieved. In most of the studies done, metal recovery was from sulphate solutions. This study focused on the separation of Mn from Co, Li and Ni in a citrate solution. However, literature on solvent extraction of metals from citrate solutions is limited. A literature survey on solvent extraction from both citrate and sulphate media was conducted to help with the selection of suitable conditions for the solvent extraction tests. Some of these studies are briefly discussed in this section.

In a study by Chen & Ho, 2018, Co and Mn were extracted from a sulphate leach solution using 60% saponified 0.1M Na-Cyanex 272 and they were separated by D2EHPA after stripping. The Ni left in solution was then recovered by precipitation with DMG. An actual LIB pregnant leach solution with composition: Li (0.8 g/L), Co (2.6 g/L), Ni (2.6 g/L) and Mn (1.4 g/L), was used. It was obtained after leaching $LiNi_{1/3}Mn_{1/3}Co_{1/3}O_2$ cathodic active material with Sulphuric acid. The pH was varied from 1 to 7.5 and the phases were contacted for 15 minutes. Over 98% Co and Mn was extracted at optimum pH of 6, with about 2% Ni and Li co-extraction. Above pH 6, Co started to partially precipitate as hydroxide and at pH 7, there was around 20% Ni co-extraction. After stripping, Mn was selectively extracted from the strip solution using Na-D2EHPA. The biggest challenge faced in the separation of Mn from a Ni and Co solutions, is poor separation, resulting from co-extraction of Co and Ni, if they are in high proportions (Mubarok & Hanif, 2016). However, since the proportions of Co and Ni had been reduced, the separation was more efficient. 85% Mn was extracted with 3.7% Co co-extraction using 0.2M Na-D2EHPA at equilibrium pH 2.95 and O/A ratio of 1. This was after 15 minutes of agitation. Tests on the stripping of Mn from D2EHPA were carried out and H_2SO_4 concentration (0.005-0.15M) and O/A ratio (1-80 were investigated in the given ranges. Nearly 100% Mn stripping

efficiency was achieved in one stage at optimum H_2SO_4 concentration and O/A ratio of 0.05M and 2, respectively. At O/A ratios higher than 2, there was a large drop in the percentage stripping of Mn.

Nguyen *et al.*, 2014 investigated the recovery of Co, Ni and Li from an LIB sulphate leach solution using solvent extraction and chemical precipitation. Using 0.56 mol/dm^3 of 60 % saponified Na-PC-88A, 99% Co was extracted in two counter-current stages at O/A ratio 3 and pH 4.5, after agitating for 600 seconds. This was followed by scrubbing of Ni and Li from the loaded organic using 2 g/dm^3 $CoSO_4$ solution. Over 95% Ni and 99% Li scrubbing was achieved at pH 3.65. Ni was subsequently recovered from the raffinate using solvent extraction. An organic phase of 5% v/v PC-88A was contacted with the aqueous solution at pH 6 and over 99.9% Ni was extracted with 0.01% Li co-extraction. Li was recovered by precipitation as Li_2CO_3. The Co loaded organic phase was stripped with 0.2 mol/ dm^3 H_2SO_4 and over 99.9% Co stripping was achieved in two counter-current stages at O/A ratio 1.

Chen & Zhou, 2014 investigated the recovery of Co, Li, Ni and Mn from a citric acid media. Ni and Co were first selectively precipitated using di-methyl-glyoxime ($C_4H_8N_2O_2$) and ammonium oxalate ($(NH_4)_2C_2O_4$), respectively. This was followed by Mn recovery using solvent extraction with 70-75% saponified D2EHPA as extractant. TBP (5% v/v) was used as a phase modifier and sulfonated kerosene as diluent. A 10M NaOH solution was used for saponification of the D2EHPA. The effects of pH (1-6), A/O ratio (0.25-4), D2EHPA concentration (5-30% v/v) and agitation time (30-600 seconds) on Mn extraction were investigated. It was reported that Mn extraction increased from 66% to 92% when the pH was raised from 1 to 4, with less than 0.2% Li co-extraction. However, above pH 4, there was an increase in Li co-extraction with no significant increase in Mn extraction. An increase in A/O ratio from 0.5 to 4 resulted in a drop in Mn extraction from 94% to 28%, and this was attributed to insufficient amount of extractant in the dispersion at higher A/O ratio. A maximum of about 94% Mn was extracted using 20% v/v D2EHPA, further increase in D2EHPA concentration resulted in an increase in Li co-extraction by about 1%, but with no significant increase in Mn extraction. It was determined that over 92% Mn can be extracted with 70-75% Na-D2EHPA, at pH 4 and A/O ratio 0.5 in one stage, after 300 seconds of agitation. Sulphuric acid was used for stripping Mn from the organic phase and it was recovered as $MnSO_4$. After varying the H_2SO_4 concentration from 0.01M to 0.2M, over 99% Mn was stripped in one stage

using 0.2M H_2SO_4 at A/O ratio 1 and room temperature. It was concluded that higher A/O ratios and H_2SO_4 concentrations yield higher stripping efficiencies. The D2EHPA in the organic phase was regenerated and saponified before being reused as an extractant.

In a study by Chen, *et al.*, 2015, Li, Co, Ni and Mn were recovered from a sulphuric acid pregnant leach solution using solvent extraction and precipitation. The solution was first purified by adjusting the pH to precipitate Fe using 2M NaOH solution. Ni was precipitated using di-methyl-glyoxime reagent (DMG $C_4H_8N_2O_2$), after the purification step. This was followed by Mn extraction using Co-D2EHPA and over 97% Mn extraction was achieved at pH 3.5 and O/A ratio 1, using 15 vol. % Co-D2EHPA. There was an increase in Mn extraction from 26% to 96% when the D2EHPA concentration was increased from 5-15% v/v, further increase in the extractant concentration to 30% v/v only resulted in more Co and Li co-extraction with no further increase in Mn extraction. O/A ratio was varied from 0.25 to 4 and from O/A 0.25 to 1 Mn extraction witnessed a steady increase from 15% to 97%. However, further increasing O/A ratio from 1 to 4 did not increase Mn extraction, but resulted in Co and Li co-extraction increasing from 1% about 11% and 6%, respectively. The same trend was also observed with pH, Mn extraction increased from 18% to 96% when the pH was varied from 1.5-3.5 with less than 1% Co and Li co-extraction. Mn extraction almost reached 100% from pH 3.5 to 5.5. However, there was a remarkable increase in Co and Li co-extraction from less than 1% to 16% and 7%, respectively. 5% w/v oxalic acid solution was used for scrubbing loaded Co^{2+} from the organic into the aqueous phase. It was reported that nearly 100% Co was scrubbed, while Mn was left in the organic phase. This may have been because of the ability of Co^{3+} to form stable $CoC_2O_4.2H_2O$ precipitates, unlike Mn^{2+} which cannot be precipitated in the $H_2C_2O_4$ solution. Using the McCabe-Thiele method, it was determined that two counter-current extraction stages were required to produce a raffinate containing less than 0.04 g/L Mn and over 99% Mn recoveries under the conditions stated above. Co and Li were recovered by precipitation.

From the literature survey, it is apparent that solvent extraction is capable of achieving over 98% metal extraction, and D2EHPA is the most widely used extractant for the separation of Mn from Co, Li and Ni in solution. The separation process is mainly influenced by pH, concentration of organic extractant and O/A ratio. Co, Li, Mn and Ni extraction is generally promoted by high pH, there is increase in metal extraction with increase in pH. During the

separation of Mn from Co, Li and Ni from citrate/sulphate solutions, increase in pH results in higher Mn extraction, but with more Co Li and Ni co-extraction. Mn extraction also increases with increase in the amount of extractant in the system (either by increasing the O/A ratio of the % of extractant in the organic phase) to a certain extent, further increase in the amount of extractant results in no significant increase in Mn extraction, but instead, it increases Co, Li and Ni co-extraction. It was therefore, decided that solvent extraction would be used to separate Mn from the rest of the elements in solution, using D2EHPA as extractant, in this study.

2.11 Metal precipitation from LIB leach solutions

In a study by Nguyen *et al.*, 2014, after recovery of Co and Ni using solvent extraction from a sulphate solution, Li was extracted as a carbonate precipitate. A saturated sodium carbonate (Na_2CO_3) solution was added to the solvent extraction raffinate at 100℃ to precipitate Li as lithium carbonate (Li_2CO_3). The temperature was kept constant at 100℃ to minimise Li_2CO_3 loss since its solubility decreases from 1.52 to 0.71 g/100 g of H_2O when temperature is increased from 25 to 100℃. About 92% Li was recovered as carbonate with less than 0.05% Ni co-precipitation.

Chen & Ho, 2018 also recovered Li from a sulphate solution as Li_2CO_3 using a saturated solution of Na_2CO_3 as precipitant. The remaining sodium ions were washed out from the product using hot water at 100℃. It was reported that a Li product of up to 99% purity was obtained.

In another study by Chen & Zhou, 2014, after Co, Mn and Ni recovery from a citrate solution, Li was recovered as $Li_2 PO_4$, by adding 0.5 M sodium phosphate to the leach liquor. The solubilities of Li_2CO_3 and Li_2PO_4 at 20 °C are 1.33 g/100 mL and 0.039 g/100 mL, respectively, indicating that it is more feasible to recover Li from a citrate solution as phosphate than as a carbonate. Ni and Co can also be recovered as phosphates since $Co_3(PO_4)_2$ and $Ni_3(PO_4)_2$ are classified as water insoluble. The solubility constants (K_{sp}) of $Co_3(PO_4)_2$ and $Ni_3(PO_4)_2$ in aqueous solutions at 25℃ are $2.05 \times 10^{-35}$and 4.74×10^{-32} , respectively (HSU, 1968).

As mentioned earlier by Nguyen *et al.*, 2014, the solubility of Li_2CO_3 decreases from 1.52 g/100 ml to 0.71 g/100 ml when the temperature is increased from 25℃ to 100℃. There is no

published data on the solubility of Li_3PO_4 at different temperatures, except at 20℃ where it is 0.039 g/100 ml according to Chen & Zhou, 2014. However, it can also be expected for the solubility of Li_3PO_4 to decrease with increase in temperature, just like Li_2CO_3, since they are both Li salts.

It is important to notice that in all the studies where Li was being recovered from a sulphate solution, carbonate precipitation was employed (Chen & Ho, 2018; Chen, *et al.*, 2015; Nguyen *et al.*, 2014). For Li recovery from citrate solutions, phosphate precipitation was used (Chen & Zhou, 2014; Zhou, *et al.*, 2015). Chen & Zhou, 2014 suggested that phosphate precipitation is more efficient than carbonate precipitation when recovering Li from citrate solutions. It was reported that if carbonate is used to precipitate metals from citric acid media, about 70-80% metal recoveries are obtained, but when phosphate is used, 90% metal recoveries are obtained. The first equilibrium ionization constant k_1 of phosphoric acid (7.5×10^{-3}) is greater than those of both citric acid (7.4×10^{-4}) and carbonic acid (4.2×10^{-7}), but the k_1 for citric acid is greater than the one for carbonic acid. Therefore, it can be expected for carbonate precipitation from citrate solutions media not to be as efficient as phosphate precipitation from citrate solutions. Therefore, it was decided that phosphate precipitation would be used in this work to investigate the recovery of metals from citrate solutions through precipitation.

In the studies that have been discussed, there is no mention of the pH at which metal phosphate precipitation was performed. No information could be found from literature on the relationship between Al, Co, Cu, Li, Mn and Ni phosphate precipitation and pH at different temperatures. However, Wang & Friedrich, 2015 investigated the effect of pH on Al, Co, Cu, Fe, Li, Mn and Ni carbonate precipitation from an LIB sulphate leach solution at 40 ℃. Figure 7 shows the decrease in metal concentration in solution with change in pH and a decrease in the metal content in solution from 100% is an indication of metal precipitation as a carbonate. From Figure 7, when pH is raised from 3 to 4, Fe and Al precipitation increases rapidly. At pH 5, over 97% Fe and more than 65% Al precipitates. At pH 6, nearly all the Al, precipitates and the concentration of Cu in solution is reduced by about 90%. There is a drastic increase in Co, Ni and Mn precipitation, which starts at pH 7. By the time the pH reaches 9, over 95% Co, Ni and Mn precipitates and the precipitation reaches 99% at pH 10. However, there is low Li precipitation as the pH is increased from 2 to 10 and by the time it reaches 10, only 21% Li

precipitates. This means that in order for appreciable Li precipitation to take place, a pH well above 10 should be used.

However, this investigation did not take into account the effect of temperature. Since the solubility of Li_2CO_3 decreases with an increase in temperature, it can be expected for more than 21% Li precipitation to take place at temperatures higher than 40°C.

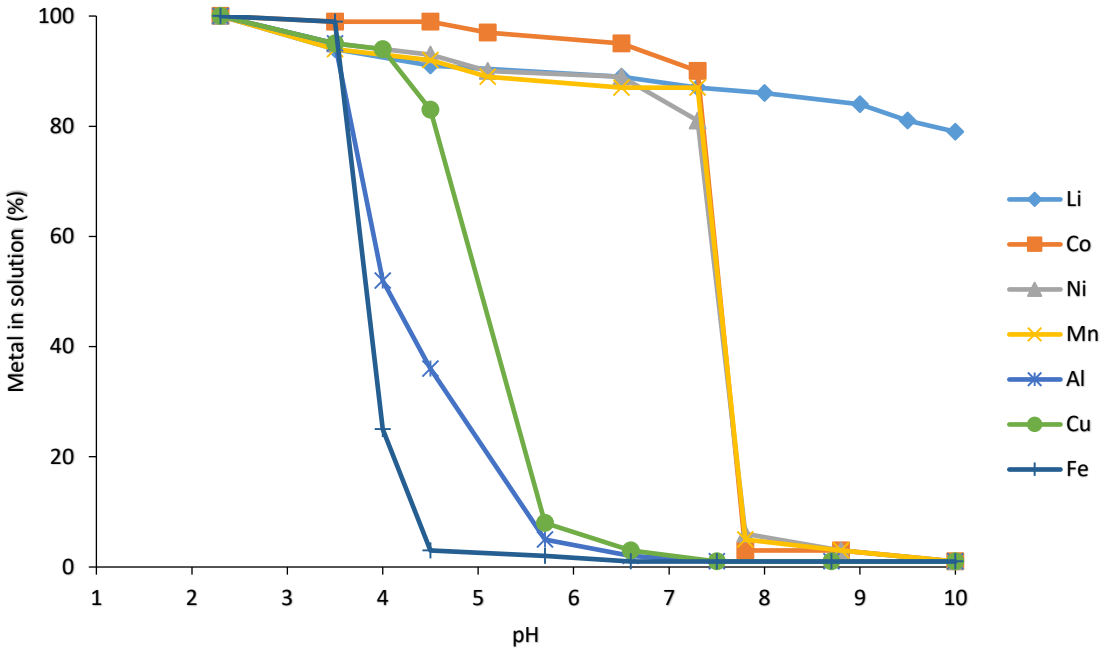

Figure 7: Metal carbonate precipitation from a sulphate solution as a function of pH at 40°C (Wang & Friedrich, 2015)

Jun SONG, 2017 investigated the recovery of Li as Li_3PO_4 from LIB waste solutions. It was reported that Li_3PO_4 precipitation takes place at in the pH range 13-14. The precipitation temperature was varied from 50°C to 100°C and it was observed that Li_3PO_4 precipitation increases with increase in temperature up to 70°C, further increase in temperature did not cause any increase in Li_3PO_4 precipitation. 70°C was selected as the optimum precipitation temperature. Reactions for the precipitation of Al, Co, Cu, Li, Mn and Ni phosphate are represented by Equations 52, 53, 54, 55, 56 and 57, respectively.

$$Al^{3+}_{(aq)} + {PO_4}^{3-}_{(aq)} \rightarrow AlPO_{4(S)} \quad [52]$$

$$3Co^{2+}_{(aq)} + 2{PO_4}^{3-}_{(aq)} \rightarrow Co_3(PO_4)_{2(s)} \quad [53]$$

$$3Cu^{2+}_{(aq)} + 2{PO_4}^{3-}_{(aq)} \rightarrow Cu_3(PO_4)_{2(s)} \quad [54]$$

$$3Li^{+}_{(aq)} + {PO_4}^{3-}_{(aq)} \rightarrow Li_3PO_{4(s)} \quad [55]$$

$$3Mn^{2+}_{(aq)} + 2{PO_4}^{3-}_{(aq)} \rightarrow Mn_3(PO_4)_{2(s)} \quad [56]$$

$$3Ni^{2+}_{(aq)} + 2{PO_4}^{3-}_{(aq)} \rightarrow Ni_3(PO_4)_{2(s)} \quad [57]$$

Chapter 3: Experimental

3.1 Discharging and dismantling

LIBs from scrap laptops were used in this study. The batteries were dismantled to individual cell level and the plastic casings were removed. To prevent ignition and short-circuiting during cutting and dismantling, batteries should be discharged; in this study, the LIBs were discharged by immersion in a 1 wt. % NaCl solution for 48 hours after which they were air dried. A voltmeter was used to check for any residual charge in the batteries. A battery was considered as discharged if it measured a voltage less than 0.5 V.

After the batteries had been discharged and dried, further dismantling was carried out. The steel casings were cut using a band saw and removed. The inner components were uncoiled, separating the anodes, cathodes and plastic separators. The copper from the anodes was recovered in its metallic form, while the cathodes were further processed.

3.2 Separation of cathodic active material from Al foils

The NaOH leaching step used by Li *et al.*, 2017 was adopted in this study for separation of the cathodic material from the aluminium foils, to obtain the feed for the cathodic material leaching tests. This significantly reduced the amount of Al in the sample that would be introduced to the leaching step, which was important since Al interferes with Co, Li and Ni extraction from solution in downstream processes.

Cathodes were treated with a 10 wt. % NaOH solution for 2 hours at room temperature and a pulp density of 100 g/L. A 5L glass vessel with an overhead stirrer was used as a reactor. Before being fed into the reactor, cathodes were cut into small pieces ($2 \times 2\text{cm}$) using scissors. The desired volume of 10 wt. % NaOH solution was added to the reactor, and the appropriate mass of cathodes was weighed and added to the reactor. The lid was then mounted and fastened onto the reactor. The overhead stirrer was switched on and set to 300 rpm and the leaching was carried out for 2 hours. At the end of the 2 hour leaching period, the pulp was filtered using a vacuum pump, filter paper, funnel and flask. The residue was washed with distilled water and after filtration the residue was dried in an oven for 24 hours at 60℃. The dried cathodic material was pulverized and a 10 way rotary splitter was used for

splitting the sample to make it as uniform as possible and to obtain smaller representative samples, which were used in aqua regia digestions and as feed to the leaching tests.

3.3 LIB cathodic active material characterization

LIBs from different laptops were used, and this results in a mixture of different types of cathodic material, with different compositions. In other studies, N-methyl-2-pyrrolidone (NMP) was used for dissolving polar binders such as Polyvinylidene Fluoride (PVDF) on the cathode, while the highly non-polar binders such as Poly-Tetra-Fluoro-Ethylene (PTFE), which do not dissolve in NMP were eliminated by calcination in a muffle furnace at 700℃. In this study, no NMP or heat treatment was done on the material and it can be assumed that there is still binder in the sample. Because of the binder, the powder forms agglomerates after size reduction.

Aqua regia digestion and analysis of the resulting leach liquor is one of the usual methods that are used to determine the metal composition in LIBs. Aqua regia solution is a mixture of HNO_3 and HCl at a molar ratio of 1:3. After sample preparation, aqua regia digestions were performed on the cathodic material to determine the metal content.

20 g samples were digested at 60℃ and pulp density of 100 g/L for 48 hours. ICP-OES was used for analysing the leach liquor and the results were used as an indication of the metal content in the cathodic material.

Scanning Electron Microscopy (SEM) backscattering analysis was done on a representative sample of the cathodic material to determine the elemental composition. Before introducing the sample to a microscope, it had to be mounted on epoxy and polished. During the mounting and polishing process, the following steps were followed:

- The powdered sample was transferred into a cylindrical stub, mounted on a glass plate with adhesive tape.
- An epoxy resin was mixed and poured into the stub.
- The stub with the sample and epoxy was placed into an oven for drying and hardening.
- After approximately 24 hours, the stub was polished using different grits in a polishing machine.

The sample was coated with gold to for conductivity and a carbon tape was stuck on the sides of the polished surface. XRD analysis was also carried out using a PANalytical Empyrean diffractometer.

3.4 Batch tests

3.4.1 Introduction

The aim of the batch experiments that were carried out was to investigate the recovery of Co, Li and Ni from LIB cathodic material. Figure 8 shows the sequence in which the experimental work was carried out.

After a review on the available organic acids, citric and DL-malic acid were selected as the most suitable leaching reagents for this study, as discussed in section 2.7.3 .The first step was to determine the optimum leaching conditions. The second step was to investigate the recovery of these metals from solution using a combination of solvent extraction and chemical precipitation.

Initial leaching tests were conducted to investigate the effect of H_2O_2 addition on metal dissolution and a decision on its inclusion in successive tests was made based on the results. After it had been ascertained that H_2O_2 was necessary, it was included in the rest of the leaching tests. More Leaching tests were performed to investigate the effects of temperature and acid concentration on metal dissolution, in the presence of H_2O_2. Citric acid and DL-malic acid were considered as leaching reagents with the aim of comparing the two on the basis of leaching performance and cost, and selecting the more suitable lixiviant. Once it had been ascertained that citric acid was more suitable, a bulk stock pregnant leach solution (PLS) was prepared for use in the solvent extraction and metal precipitation tests. This solution was obtained by leaching cathodic active material with citric acid, under the optimum conditions that had been determined by the batch leaching tests

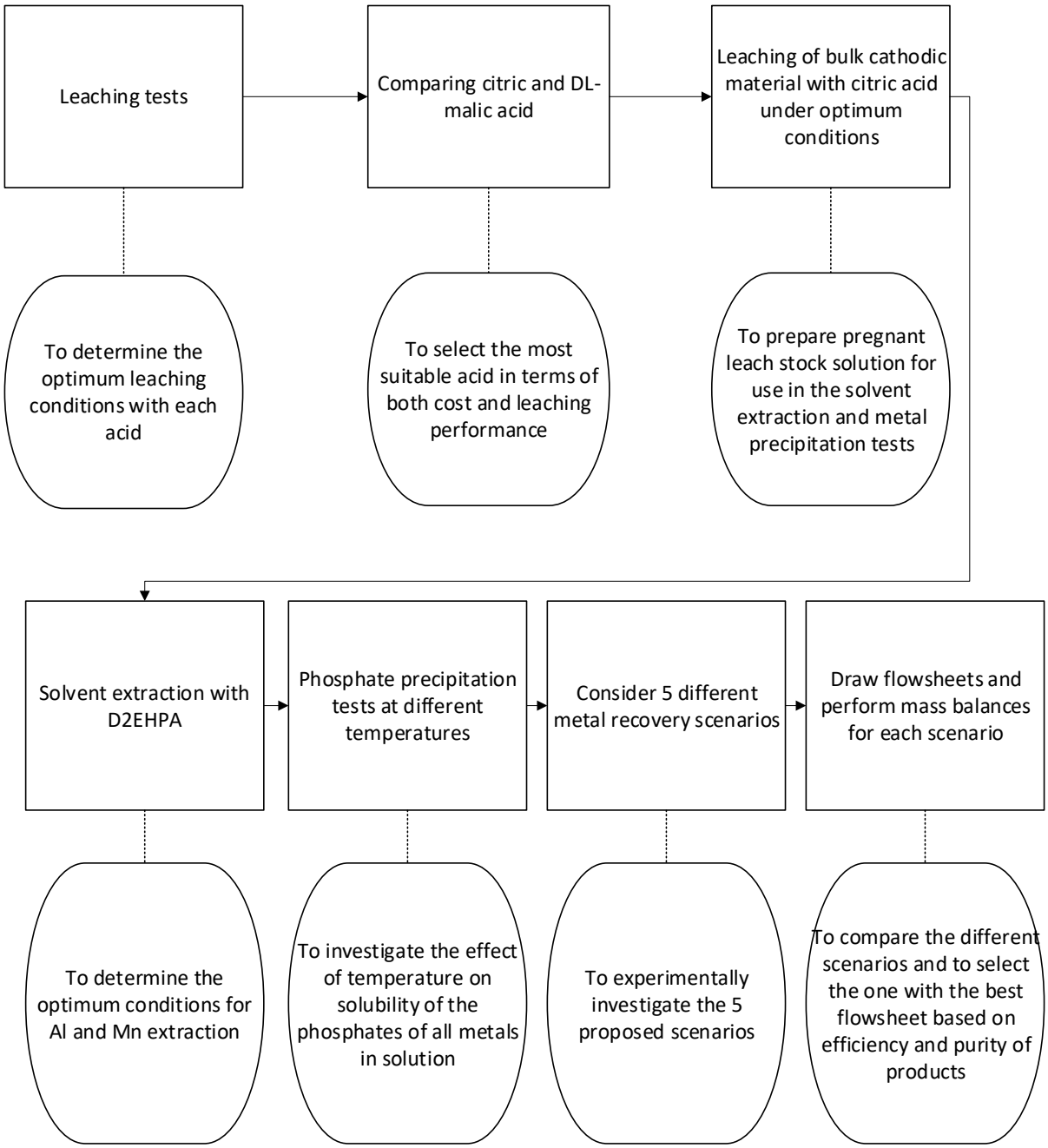

Figure 8: Schematic illustration of the order in which the experimental work was carried out

Solvent extraction tests were carried out on the PLS using D2EHPA, with the aim of finding optimum conditions for Mn and Al extraction from solution, with minimal Co, Li and Ni co-extraction. The effects of pH, O/A ratio and extractant concentration (D2EHPA) on the separation process were investigated.

Once the optimum conditions had been determined, another bulk solution (PLS1) with low Mn and Al concentrations was prepared by extracting Mn and Al with D2EHPA, using the optimum conditions that had been determined by the solvent extraction experiments. The raffinate (PLS1) was used as the feed in subsequent metal precipitation tests.

Stripping tests were carried out on the loaded organic phase and the effects of O/A ratio and H_2SO_4 concentration on Mn stripping were investigated.

Metal precipitation tests from the pregnant leach solution (PLS) were conducted, using NaH_2PO_4 as the precipitating agent. During the precipitation tests, the effects of temperature on $AlPO_4$, $Co_3(PO_4)_2$, Li_3PO_4, $Mn_3(PO_4)_2$ and $Ni_3(PO_4)_2$ solubility in aqueous solutions were investigated. The aim of the precipitation tests was to verify if Li can be separated from the rest of the metals in solution by using differences in the solubilities of their phosphates at different temperatures. Once it had been verified that the separation of Li from Co, Mn and Ni through phosphate precipitation at different temperatures was possible, different metal recovery options were drafted and 5 scenarios were considered.

Figure 9 shows a schematic illustration which describes the scenarios that were considered for metal recovery. Each scenario was experimentally investigated.

Direct phosphate precipitation at 80℃ on pregnant leach solution PLS was carried out and this was considered as scenario 1. In scenario 2, there was phosphate precipitation from PLS at 50℃, followed by phosphate precipitation at 80℃. Scenario 3 involved Mn and Al extraction with D2EHPA from PLS to produce PLS1, followed by phosphate precipitation of the remaining metals from PLS1 at 80℃. Scenario 4 involved Mn extraction with D2EHPA from PLS to produce PLS1, followed by phosphate precipitation at 50℃, then subsequent phosphate precipitation at 80℃. In scenario 5, there was Mn extraction with D2EHPA from PLS to produce PLS1, followed by carbonate precipitation using Na_2CO_3 as precipitant, then subsequent phosphate precipitation at 80℃.

For each scenario, a simple flowsheet was drawn and a mass balance was performed. The five scenarios were compared with regard to efficiencies and purity of the final product streams and the scenario that yielded the best results was selected.

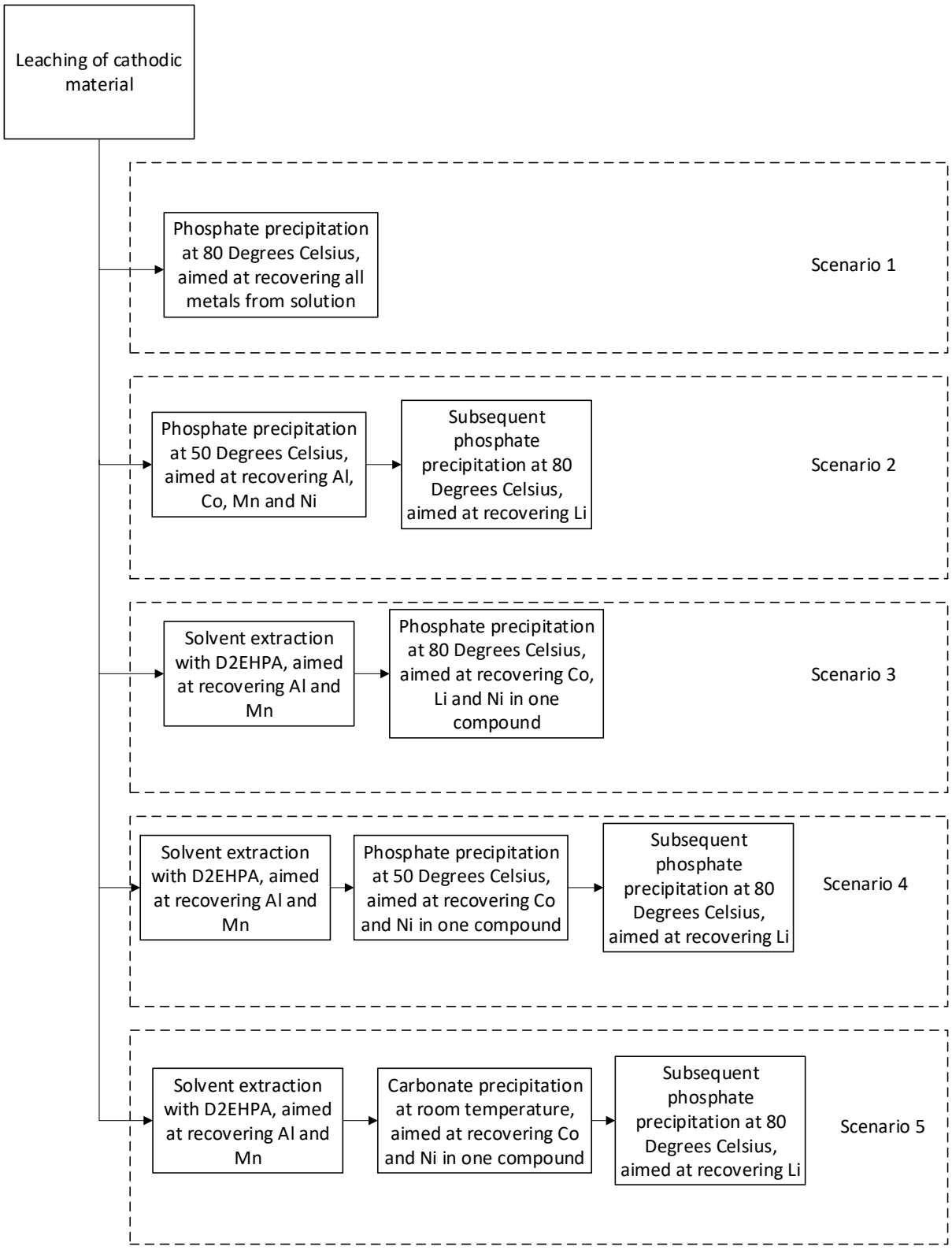

Figure 9: Schematic illustration of the 5 metal recovery scenarios that were considered

3.4.2 Experimental Design

Leaching

For the selection of a suitable leaching reagents, two of the best organic acids were compared in terms of leaching performance and cost. Citric acid and DL-malic acid were selected as the most appropriate leaching reagents for this study, as discussed in section 2.7.3 of this document. Organic acid leaching tests were conducted using citric acid and DL-malic acid as lixiviants in the presence of H_2O_2, with the aim of recovering Co, Li and Ni. Before H_2O_2 was added, preliminary tests were performed to investigate the effect of H_2O_2 on metal dissolution and to decide on its inclusion based on the results.

The effects of temperature and acid concentration on the leaching rate and extent were investigated using a 3^2 full factorial experimental design. Li *et al.*, 2009 varied the acid concentration from 0.3-1.5 M during citric acid leaching tests and determined 1.25M as the optimum acid concentration. For DL-malic acid, Li *et al.*, 2010 varied acid concentration from 0.3M to 3.0 M and determined 1.5 M as the optimum acid concentration. For this research, 1 M, 1.25 M and 1.5 M were selected as the three acid concentration levels for the full factorial experiments since these values are closer to the optimum acid concentrations that were reported from literature.

For both organic acids, 30℃, 60℃ and 95℃ were selected as the three temperature levels for the full factorial experimental designs. This is comparable to the temperature range (30-90℃) investigated by Li *et al.*, 2009 and Li *et al.*, 2010.

Furthermore, a number of studies have indicated that 20 g/L is the preferred pulp density for the leaching of cathodic material with organic acids (He *et al.*, 2017; Lee & Rhee, 2002; Li *et al.*, 2010, 2009, 2014). When the pulp density was increased from 20 g/L, there was a significant drop in metal recovery. This is because of a reduction in the leaching reagent concentration per unit volume of pulp, which increases the probability of some mineral particles not getting sufficient contact with the leaching reagent, resulting in poor leaching. When the pulp density was further lowered from 20g/L, there was no significant increase in metal recovery, therefore, 20 g/L was determined as the optimum pulp density. For these reasons, 20 g/L was used in this work during the all the leaching experiments.

From Li *et al.*, 2009, 1% v/v H_2O_2 concentration was found to be the optimum for citric acid leaching at 90°C and 20 g/L pulp density. Li *et al.*, 2010 determined 2% v/v H_2O_2 as the optimum for DL-malic acid leaching at the same pulp density and temperature. From both studies, further increase in H_2O_2 concentration from the optimum did not increase the leaching efficiency. However, for the purposes of comparison, a H_2O_2 concentration of 2% v/v was used in both citric acid and DL-malic acid leaching.

Table 7 summarizes the variables for the 3^2 full factorial experimental design for the leaching tests, with their levels. Table 8 shows the parameters that were kept constant during the leaching tests and the justification. The results from these tests were used to compare the leaching performance of citric acid and DL-malic acid. The cost of each acid was also considered, and from this comparison, the more suitable leaching reagent was selected and it was used in successive tests.

Table 7: Experimental design for organic acid leaching test

Variable	**Level 1**	**Level 2**	**Level 3**
Acid concentration (M)	1	1.25	1.5
Temperature (°C)	30	60	95

Table 8: Parameters kept constant during leaching tests

Parameter	**Set point and justification**
H_2O_2 concentration	Sufficient amount required for reductive leaching to take place from literature (2% v/v) (Li *et al.*, 2010, 2009).
Pulp density	From literature, it was reported that 20g/L is the most suitable pulp density for organic acid leaching of LIB cathodic material (Li *et al.*, 2010, 2013, 2014, 2017).
Leaching time	Leaching time will be held constant at 120 minutes to ensure maximum dissolution of metals.
Agitation speed	Minimum agitation speed required to keep all particles in suspension (750 rpm).

Solvent extraction

Extractant concentration, pH and O/A ratio were identified as the main process variables that affect the separation of Mn from Co, Li and Ni in LIB citrate leach solutions during solvent extraction with D2EHPA. A $2 \times 3 \times 5$ full factorial experimental design was used to investigate the effects of these variables on the Mn extraction process. Table 9 shows the full factorial experimental design for the solvent extraction tests, while Table 10 shows the variables that were kept constant during the tests and the justification.

Table 9: Experimental design for solvent extraction tests.

Variable	**Levels**				
D2EHPA (% v/v)	10			20	
pH	2.5		3		3.5
O/A ratio	1	2	3	4	5

Table 10: Parameters held constant during solvent extraction tests

Parameter	**Set point and justification**
Temperature	Tests were carried out at ambient temperatures (21-24℃) since it was reported in literature that the extraction takes place at room temperature (25℃) (Chen & Ho, 2018; Chen *et al.*, 2015).
Mixing time	Set to 15 minutes to make sure that reaction reached equilibrium (Chen & Ho, 2018).

Stripping

H_2SO_4 concentration and A/O ratio were identified as the most influential factors on Mn stripping from D2EHPA. A 2×5 full factorial experimental design was used to investigate the effect of H_2SO_4 concentration and A/O ratio on metal stripping. The experiments were carried out in triplicates to test for the repeatability.

Table 11 shows the parameters that were investigated for and their set points, while Table 12 shows the parameters that were kept constant and the justification.

Table 11: Experimental design for stripping tests

Variable	**Levels**				
H_2SO_4 (M)	0.5			2.0	
A/O ratio	1	2	3	4	5

Table 12: Parameters kept constant during stripping tests

Parameter	**Set point and justification**
Temperature	(21-24℃), since it was reported in literature that the stripping takes place at room temperature (Chen & Ho, 2018; Chen, *et al.*, 2015).
Mixing time	Set to 300 seconds, minimum time for complete Mn stripping from D2EHPA (Chen, *et al.*, 2015; Chen & Zhou, 2014).

Metal precipitation

The effect of temperature on metal precipitation as phosphates was investigated, using NaH_2PO_4. $2H_2O$ as a precipitating agent. Phosphate precipitation was selected as the preferred method since it is more efficient to precipitate metals from a citrate solution as phosphates than as carbonates and this is justified by the discussion in section 2.11. Precipitation tests were carried out at temperature levels of 50℃, 60℃, 70℃ and 80℃ since they fall in the range that was investigated by Jun SONG, 2017. According to Jun SONG, 2017, maximum Li_3PO_4 precipitation takes place at pH 13-14. However, no information on the precipitation of the other metals as phosphates with pH in a citrate solution was found from literature. However, it can be expected that precipitation increases with increase in pH and at pH 13, there is high probability that all the metals will precipitate. Since the aim of these precipitation tests was to investigate the effect of temperature on solubility of the phosphates of all the metals in solution, it was most reasonable to carry out the precipitation

tests at a pH value which would allow for maximum phosphate precipitation. For these reason, all the tests were performed in the pH range 13-14.

Table 13 shows the variables that were held constant and the motivation. The tests were carried out in triplicates to check for the repeatability of the experiments.

Table 13: Variables kept constant during metal precipitation tests with NaH2PO4. 2H2O

Parameter	Set point and motivation
pH	Kept in the range 13-14 for maximum precipitation of metals as phosphates.
NaH_2PO_4 concentration	Kept constant at 0.5M, at which there is about 350% (calculations shown in section 3.4.3) excess PO_4^{3-} in solution to ensure complete metal precipitation

3.4.3 Materials and reagents

Leaching

Waste LIBs from scrap computers were used for this research. The leach solution for all experiments was prepared using distilled water, 99 wt. % solid citric acid and DL-malic acid. The citric acid was supplied by Kimix and DL-malic acid was supplied by Sigma Aldrich. 50 wt. % H_20_2 supplied by Scienceworld was used as a reductant during the leaching tests

Aqua regia solution was prepared using 55 wt. % HNO_3 and 37 wt. % HCl, which were supplied by Scienceworld.

Solvent extraction

An actual LIB pregnant leach solution was used in the tests. In order to prepare the pregnant leach solution, LIB cathodic material was leached with citric acid using the optimum conditions that were determined by the leaching tests. The metal concentration in solution was determined using ICP-OES.

The D2EHPA that was used was supplied by Hong Kong Guokang Bio-Technology Co., Limited and kerosene supplied by Scienceworld was used as a diluent. NaOH pellets (Assay 98%),

supplied by Scienceworld were dissolved in distilled water to prepare the 10M NaOH solution that was used for pH control.

The H_2SO_4 (98 wt. %) that was used for the stripping tests was supplied by Scienceworld. Acid solutions of the desired concentrations were prepared by diluting the appropriate amount of concentrated H_2SO_4 with distilled water.

Metal precipitation tests

The same bulk pregnant leach solution that was prepared prior to the solvent extraction tests was also used in the metal precipitation tests. The same NaOH solution that had been prepared for pH control in the solvent extraction tests was also used for pH adjustment during metal precipitation tests

The NaH_2PO_4 and Na_2CO_3 that were used for preparing the precipitating agent were supplied by Sigma Aldrich. A 0.5M NaH_2PO_4 solution was prepared by dissolving the appropriate mass of NaH_2PO_4 in distilled water.

Assuming that all metals from a solution with 0.105 g/L Al, 2.20 g/L Co, 0.71 g/L Li, 1.85 g/L Mn and 2.5 g/L Ni, which is 0.004M Al, 0.036M Co, 0.103M Li, 0.034M Mn and 0.0425M Ni are to be precipitated. Estimating the amount of NaH_2PO_4 required to precipitate all the metals from solution was as follows:

Based on the Equations 52-57, 2 moles of PO_4^{3-} react with 3 moles of Co^{2+}, Mn^{2+} and Ni^{2+}, therefore the number of moles of PO_4^{3-} per liter required to react with 0.036M Co, 0.034M Mn and 0.043M Ni = $2/3 \times (0.036 + 0.034 + 0.043) = 0.075$ mol/L.

1 mole of PO_4^{3-} reacts with 3 moles of Li^+ and the number of moles of PO_4^{3-} per liter required to react with 0.103M Li = $1/3 \times 0.103 = 0.034$ mol/L.

1 mole of PO_4^{3-} reacts with 1 mole of Al^{3+}. The total number of moles of PO_4^{3-} per liter required to precipitate all the metals from solution = 0.075 + 0.034 + 0.004 = 0.113 mol/L. Therefore, a 0.113M PO_4^{3-} solution is required for complete metal precipitation.

However, a 0.5M solution was used and % excess PO_4^{3-} = (0.5M – 0.113M)/0.113M × 100% = 342.48%.

The saturated Na_2CO_3 solution was prepared by adding solid Na_2CO_3 to distilled water and stirring until it no longer dissolved.

3.4.4 Equipment

Leaching

The setup consisted of a glass jacketed reaction vessel with a working volume of 300mL and an overhead Teflon stirrer. A hotplate with proportional feedback control was used for heating. Cooling was controlled by manipulating the flow rate of cooling water flowing in the reactor jacket. A lid containing ports for the overhead stirrer, condenser, temperature probe and sampling, was fitted to the vessel. A schematic illustration of the experimental setup is shown in Figure 10.

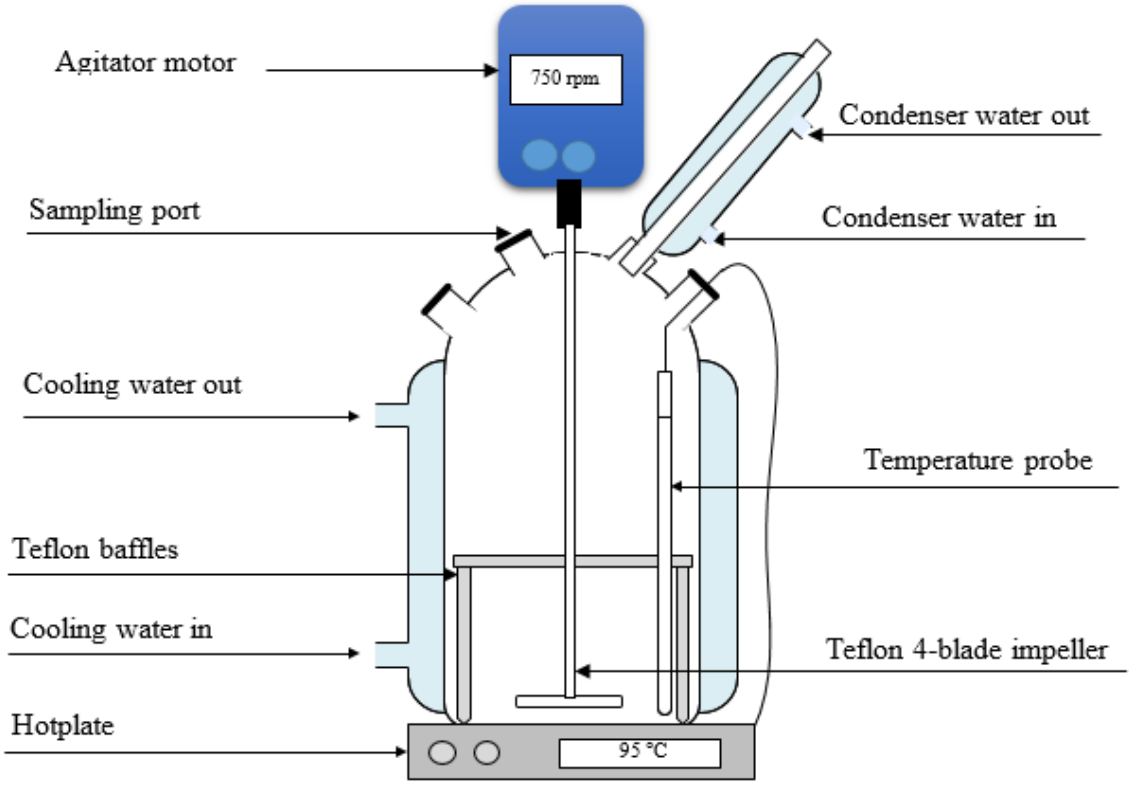

Figure 10: Setup used for leaching experiments.

Solvent extraction

From previous studies, most of the experimental work on solvent extraction and striping of LIB pregnant leach solutions was carried out in a batch manner. The organic and aqueous phases can be manually mixed by wrist action or a mechanical stirrer can be used (Darvishi *et al.*, 2005). After sufficient contacting time, the phases are allowed to separate in a separation funnel. Some publications have reported ICP-OES as the preferred method of analyzing the metal content of the aqueous solutions (Chen & Ho, 2018; Chen *et al.*, 2015), while AAS has also been reported as a good analytical method (Chen *et al.*, 2015). ICP-MS has also been used, and it is more suitable for very dilute solutions since it can detect concentrations as low as parts per billion.

In this study, 100ml and 250ml beakers were used as dispersion vessels, and mixing was achieved by means of magnetic stirrers. ICP-OES was used for analyzing the metal content in the aqueous phase.

Metal precipitation tests

There is no information from literature on the equipment that was used for the precipitation tests with Na_3PO_4 and Na_2CO_3. However, in this work, 100 ml beakers were used as vessels, for temperatures less than 60°C. For temperatures of 60°C and higher, a 200 ml glass vessel was used. A Teflon lid with a port for the temperature probe was fitted at the top to minimize water loss. Magnetic stirrer hot plates were used for agitation and for temperature control. ICP-OES was using for analyzing the metal content in the aqueous solution after filtration.

3.4.5 Methodology

Leaching

For the organic acid leaching experiments, 250mL of organic acid solution of the required concentration was added to the vessel and heated to the desired temperature. An appropriate amount of cathodic material was added to the acid solution, followed by the addition of H_2O_2. The instance when H_2O_2 was added to the solution was considered as the start of the experiment (t = 0 minutes).

2 mL samples were taken at the following time intervals from the beginning of the test run: 10, 20, 30, 60, 90, and after 120 minutes when the experiment ended. Samples were immediately filtered with a 0.22 μm syringe filter to prevent further leaching from occurring.

The remaining solid residue at the end of the leaching test was filtered, washed with de-ionized water and dried in an oven at 80℃ for 24 hours. The dried residue was weighed to determine the volume of aqua regia required and digested in aqua regia at 60 °C for 24 hours.

Solvent extraction

A certain volume of pregnant leach solution was added to a beaker with a magnetic stirrer bar. The aqueous pH was then adjusted to the desired value through NaOH addition. The appropriate amount of organic extractant was added and the mixture was agitated for 15 minutes. Every 90 seconds, the agitator was switched off to measure to pH of the aqueous solution and it would be adjusted back to the desired value by dropwise addition of NaOH. This was repeated until the pH no longer changed, indicating that equilibrium had been reached. After equilibrium had been achieved, the dispersion was added to a separation funnel and the phases were separated. The final volume of the aqueous phase was measured and a sample was collected and diluted for analysis.

For the stripping tests, a certain volume of loaded organic was added to a beaker. The appropriate amount of H_2SO_4 to make up the desired A/O ratio was added to the beaker and the magnetic stirrer was switched on. After 300 seconds, the mixture was transferred into a separation funnel and the phases were separated. A sample was taken from the aqueous phase and diluted before being analyzed for metal content.

Metal precipitation tests

The pregnant leach solution and precipitating agent were initially heated to the desired temperature. The appropriate volumes of pregnant leach solution and NaH_2PO_4 solution were measured and added to a beaker (PLS/ NaH_2PO_4 ratio =1/1), and the magnetic stirrer set to 250 rpm. The pH was adjusted to the range 13-14 by adding the appropriate amount of 10M NaOH. Using a magnetic stirrer hot plate and temperature probe for temperature control, the mixture was agitated for 120 minutes. Every 15 minutes the pH of the solution was measured and adjusted to the desired range when necessary. At the end of the experiment, the mixture

was filtered and the final filtrate volume was measured. A sample of the filtrate was collected and the metal content was analyzed.

3.4.6 Analytical methods

The concentrations of the metals in aqueous solutions during leaching, solvent extraction, metal precipitation and aqua regia digestion were analyzed using Inductively Coupled Plasma Optical Emission Spectrometry (ICP-OES). The metals analyzed for were Al, Co, Cu, Li, Mn and Ni. XRD (X-Ray Diffraction) and SEM (Scanning Electron Microscopy) were also used for characterization of the feed material.

3.4.7 Data interpretation

The leaching efficiency for the various metals from each experiment was quantified using Equation 58.

Formula for calculating metal dissolution during leaching experiments:

$$\%\ \text{Metal dissolution} = \frac{\text{Mass of metal in solution}}{\text{Mass of metal in feed}} \times 100 \qquad [58]$$

Formula for metal extraction during solvent extraction experiments is represented by Equation 59

$$\%\ \text{Extraction} = \frac{M - M_E}{M} \qquad [59]$$

$$\text{Where } M = \text{Mass of metal in the aqueous phase before extraction}$$

$$M_E = \text{Mass of metal in the aqueous phase after extraction}$$

Equation 59 can also be used for calculating metal extraction during precipitation tests:

$$\text{Where } M = \text{Mass of metal in solution before precipitation}$$

$$M_E = \text{Mass of metal in solution after precipitation}$$

Chapter 4: Results and discussion

4.1 LIB characterization

The aim of this step was to determine the average metal composition of the cathodic material. Aqua regia digestion was performed using 20g samples of the material. Ten digestions were carried out and the masses of metal leached from each digestion are shown in Table 23, (Appendix A). The average metal content in the cathodic material from these ten tests is shown in Table 14, together with the error limits. The figures are split into two parts; metal content based on the mass of metal only (metal distribution in the metallic phase) and metal content based on mass of the entire cathodic material. For a 1 Kg sample of cathodic material, there is 450g of metal which is 45 wt. %, with C and O completing the balance.

Table 14: Average metal content in LIBs

Metal	**Metal phase (%)**	**Cathodic material (g/Kg)**
Al	1.50 ± 0.0	6.75 ± 0.47
Co	29.28 ± 0.48	131.45 ± 3.32
Cu	0.11 ± 0.001	0.48 ± 0.03
Li	9.89 ± 0.40	44.41 ± 2.56
Mn	24.77 ± 0.57	111.30 ± 5.93
Ni	34.45 ± 0.41	154.70 ± 6.19

Results from XRD analysis done on the cathodic material are shown in Figure 11. In addition to the metal compositions determined by aqua regia, graphite, $LiNi_{0.05}Mn_{0.05}Co_{0.9}O_2$ and $Li_{1.2}Mn_{0.49}Ni_{0.16}Fe_{0.16}O_2$ oxides were identified as the major phases in the sample. From Figure 11, the $Li_{1.2}Mn_{0.49}Ni_{0.16}Fe_{0.16}O_2$ phase constitutes 37.82%, while $LiNi_{0.05}Mn_{0.05}Co_{0.9}O_2$ and graphite constitute 31.46% and 30.73%, respectively.

This means that the material is made up of about 30% C in the form of graphite, and metallic oxides constituting 70%. The fraction of oxygen in the material was estimated using $Li_{1.2}Mn_{0.49}Ni_{0.16}Fe_{0.16}O_2$ and $LiNi_{0.05}Mn_{0.05}Co_{0.9}O_2$, and it was determined to be 24.33% (sample calculations shown in Appendix 8.1.2). From aqua regia digestion results (Table 14), the

metallic phase constitutes 45% in the sample and this implies that oxygen constitutes 25%, which is comparable to the 24.33% estimated from the XRD results.

The phases identified by the XRD analysis seem to indicate that there is a considerable amount of Fe in the sample. However, ICP-OES analysis of the aqua regia pregnant leach solution indicated that the amount of iron in in the material was below the detection limit.

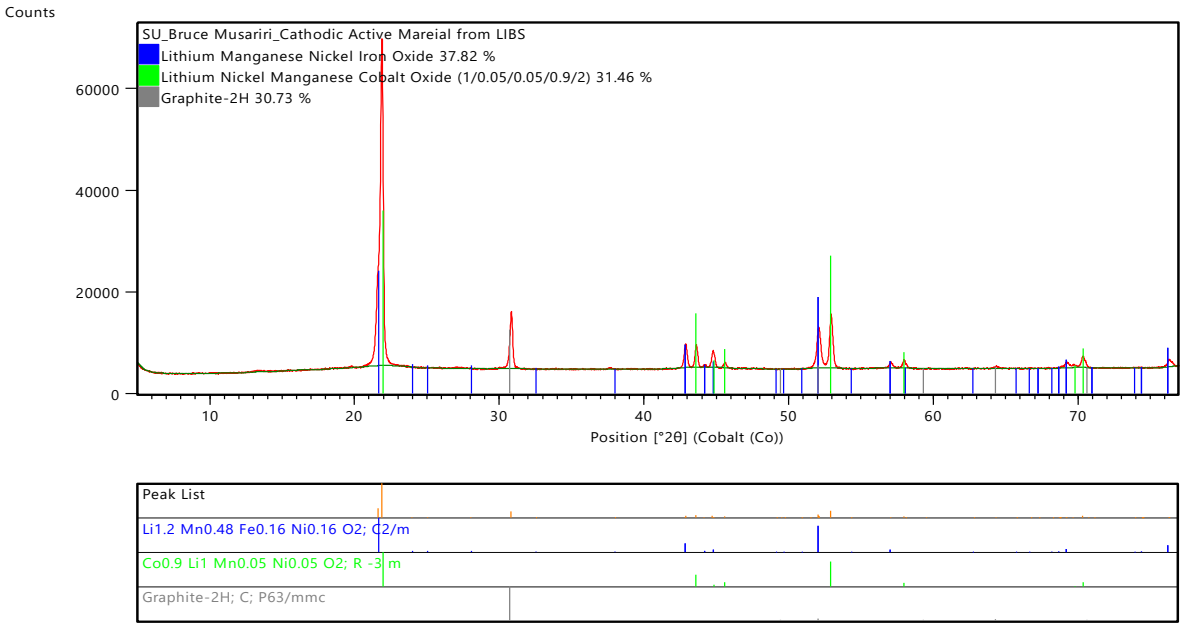

Figure 11: XRD performed on cathodic active material

SEM analysis was also performed on the sample and the results are shown in Table 15. Quantitative EDS also indicates that iron is not present in the cathodic material and there is an average of 39 wt. % C in the sample, which is comparable to the 30% C content determined by XRD. The main sources of carbon are graphite and organic compounds. According to EDS, the sample is made up of 27% oxygen, which is quite comparable to the estimated 24.33% and 25% determined by XRD and aqua regia digestion, respectively. The SEM machine that was used for analysis uses a lithium-beryllium screen and it could not detect lithium.

Figure 12 shows the spectrum for Quantitative EDS test 1 from Table 15. The spectra for the tests 2-5 are presented in Figures 38-41, Appendix A.

Table 15: Quantitative EDS (wt. %) of the cathodic active material.

Analysis	Wt. %									
	C	O	Na	Al	Mn	Fe	Co	Ni	Cu	total
1	38.60	26.48	0	1.04	8.41	0	13.71	11.76	0	100
2	38.1	27.4	0	1.13	8.66	0	12.27	12.44	0	100
3	40.47	28.85	0	1	7.73	0	10.95	11	0	100
4	39.24	27.54	0.36	1.12	8.06	0	11.97	11.71	0	100
5	38.91	27.03	0	1.04	8.09	0	12.71	11.78	0.44	100
Average	39.06	27.46	0.07	1.066	8.19	0	12.32	11.73	0.088	100

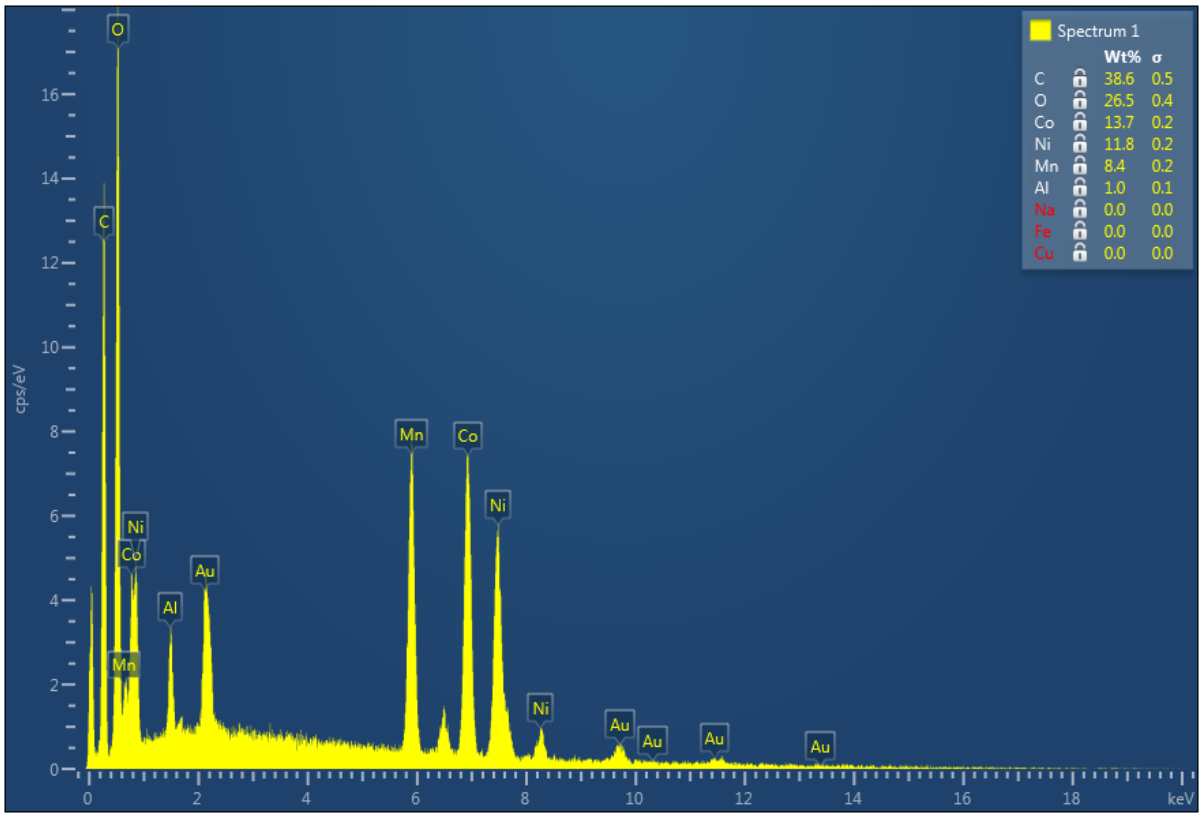

Figure 12: SEM – Spectrum for analysis 1

Some SEM images of the cathodic material before leaching are shown in Figures 13, 14 and 15. Figure 13 shows an electron image, while Figure 14 shows the associated layered map. Field analysis was carried out and these images were captured. Point analysis was also carried out and from each point a spectrum was generated, giving the composition at each point. These spectra are the ones labeled spectrum 14-18, in Figures 13 and 14.

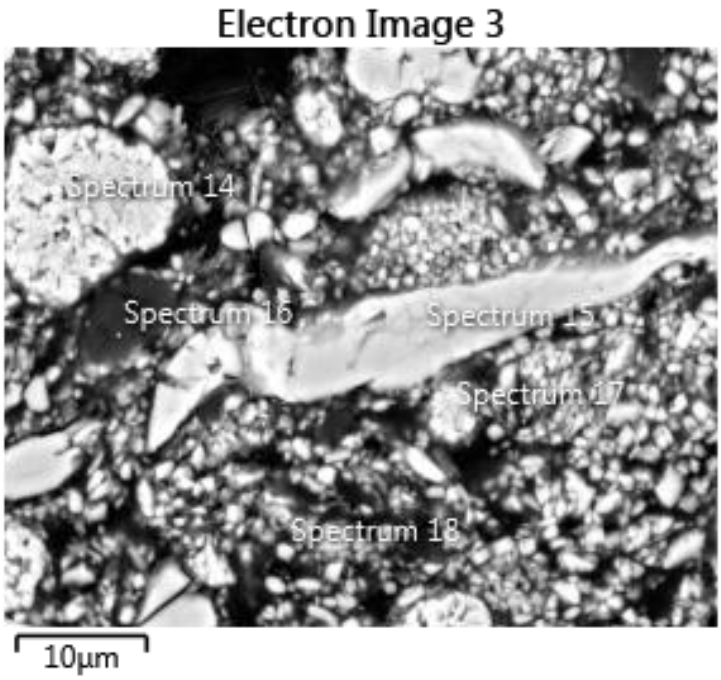

Figure 13: SEM – Electron image from cathodic material before leaching

Figure 14: SEM - EDS layered map of cathodic material before leaching

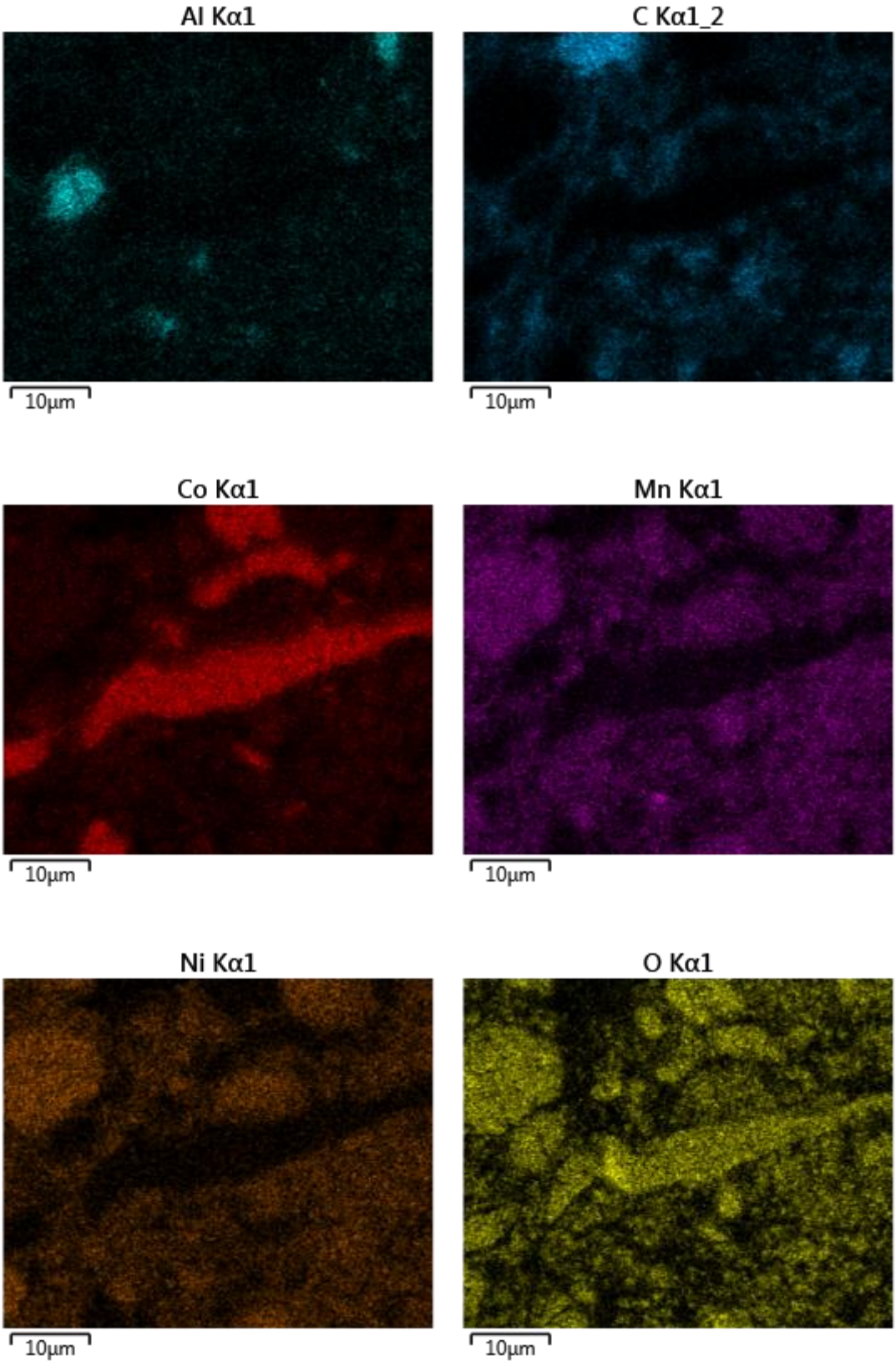

Figure 15: SEM – EDS individual element maps for Al, C, Co, Mn, Ni and O before leaching

Figure 15 shows the individual maps for Al, C, Co, Mn, Ni and O. The images show that there are significant amounts of carbon and oxygen in the feed. Generally, the oxygen is highly concentrated across the whole map as shown in Figure 15, showing that the metals in the sample are in oxide form.

4.2 Leaching

4.2.1 Effect of H_2O_2 addition

Preliminary leaching tests were carried out to investigate the effect of H_2O_2 addition on the leaching process, and to decide on its inclusion in successive leaching experiments. Figure 16 shows the effect of H_2O_2 on Co leaching with 1M citric acid at 80°C and 30°C, using 20g/L pulp density. From Figure 16, it is evident that addition of H_2O_2 to the system results in faster Co leaching kinetics. At 80°C, 48 % Co leaching is achieved after 20 minutes, with no H_2O_2 present. When H_2O_2 is included, 80 % Co leaching is achieved within 20 minutes.

Figure 17 shows the effect of H_2O_2 on Co leaching with 1 M DL-malic acid at 80°C and 30°C, using 20g/L pulp density. The same observations were made from the tests with 1M DL-malic acid. With no H_2O_2, 40 % Co leaching is achieved after 20 minutes and when H_2O_2 is included, 71 % Co leaching is achieved within 20 minutes. At lower temperatures, the inclusion of H_2O_2 also results in faster leaching kinetics; and this is observed for both citric and DL-malic acid. H_2O_2 has the same effect on Li and Ni leaching with both citric and DL-malic acid.

From previous studies, $LiNi_{1/3}Mn_{1/3}Co_{1/3}O_2$ has been reported as the common nickel manganese cobalt (NMC) compound in LIB cathodic material. In these studies, the same type of batteries was used, hence a uniform feed composition was obtained. In this work, XRD analysis identified $LiNi_{0.05}Mn_{0.05}Co_{0.9}O_2$ as the major NMC phase. Therefore, it will be used as an example to explain the mechanism through which H_2O_2 speeds up the leaching kinetics.

There is a strong ionic bond between Co^{3+} and oxygen in $LiNi_{0.05}Mn_{0.05}Co_{0.9}O_2$ and its dissolution involves the reduction of Co^{3+} in the solid state to the more soluble Co^{2+} (Golmohammadzadeh *et al.*, 2017).

According to Ferreira *et al.*, 2009, during leaching of $LiNi_{0.05}Mn_{0.05}Co_{0.9}O_2$, an intermediate oxide (Co_3O_4) is formed, which remains in the solid phase. Equations 60 and 61 represent the dissolution reactions of $LiNi_{0.05}Mn_{0.05}Co_{0.9}O_2$ in citric acid and DL-malic acid, respectively, without H_2O_2

$$20LiNi_{0.05}Mn_{0.05}Co_{0.9}O_{2(s)} + 10C_6H_8O_{7(aq)} \rightarrow 5Co_3O_{4(s)} + 20Li^{+}{}_{(aq)} + Ni^{2+}{}_{(aq)} + 3Co^{2+}{}_{(aq)} + Mn^{2+}{}_{(aq)} + 10C_6H_5O_7{}^{3-}{}_{(aq)} + 15H_2O_{(l)} + \frac{5}{2}O_{2\,(g)} \quad [60]$$

$$20LiNi_{0.05}Mn_{0.05}Co_{0.9}O_{2(s)} + 15C_4H_6O_{5(aq)} \rightarrow 5Co_3O_{4(s)} + 20Li^{+}{}_{(aq)} + Ni^{2+}{}_{(aq)} + 3Co^{2+}{}_{(aq)} + Mn^{2+}{}_{(aq)} + 15C_4H_4O_5{}^{2-}{}_{(aq)} + 15H_2O_{(l)} + \frac{5}{2}O_{2\,(g)} \quad [61]$$

In the absence of H_2O_2 the dissolution of Co_3O_4 is extremely difficult and requires excess amount of acid for it to be converted into the more soluble $Co_3(C_6H_5O_7)_2$. This makes the leaching process without H_2O_2 relatively slower. The proposed reactions for Co_3O_4 dissolution in citric acid and DL-malic acid, without H_2O_2 are represented by Equation 62 and 63.

$$Co_3O_{4(s)} + 2C_6H_8O_{7(aq)} \rightarrow Co_3(C_6H_5O_7)_{2(aq)} + 3H_2O_{(l)} + \frac{1}{2}O_{2\,(g)} \quad [62]$$

$$Co_3O_{4(s)} + 3C_4H_6O_{5(aq)} \rightarrow 3CoC_4H_4O_{5(aq)} + 3H_2O_{(l)} + \frac{1}{2}O_{2\,(g)} \quad [63]$$

H_2O_2 acts as a reductant and reduces Co^{3+} to Co^{2+} according to the half reactions represented by Equations 64 and 65. Equation 64 shows H_2O_2 acting as a reductant in an acid solution and Equation 65 represents the reaction for the reduction of Co^{3+} to Co^{2+}. According to the Equations 64 and 65, the potential for the reduction of Co^{3+} to Co^{2+} is supplied to the system. (Skoog *et al*., 2013).

$$H_2O_{2\,(l)} + 2H^{+}{}_{(aq)} + 2e^{-} \leftrightarrow 2H_2O_{(l)} \qquad E^{\theta} = +1.78\ V \quad [64]$$

$$Co^{3+}{}_{(aq)} + e^{-} \leftrightarrow Co^{2+}{}_{(aq)} \qquad E^{\theta} = +1.80\ V \quad [65]$$

This breaks the Co and oxygen bond in Co_3O_4 and as a result, the dissolution process progresses faster. The H_2O_2 assisted Co_3O_4 dissolution reactions in citric acid and DL-malic acid are shown by Equations 66 and 67, respectively.

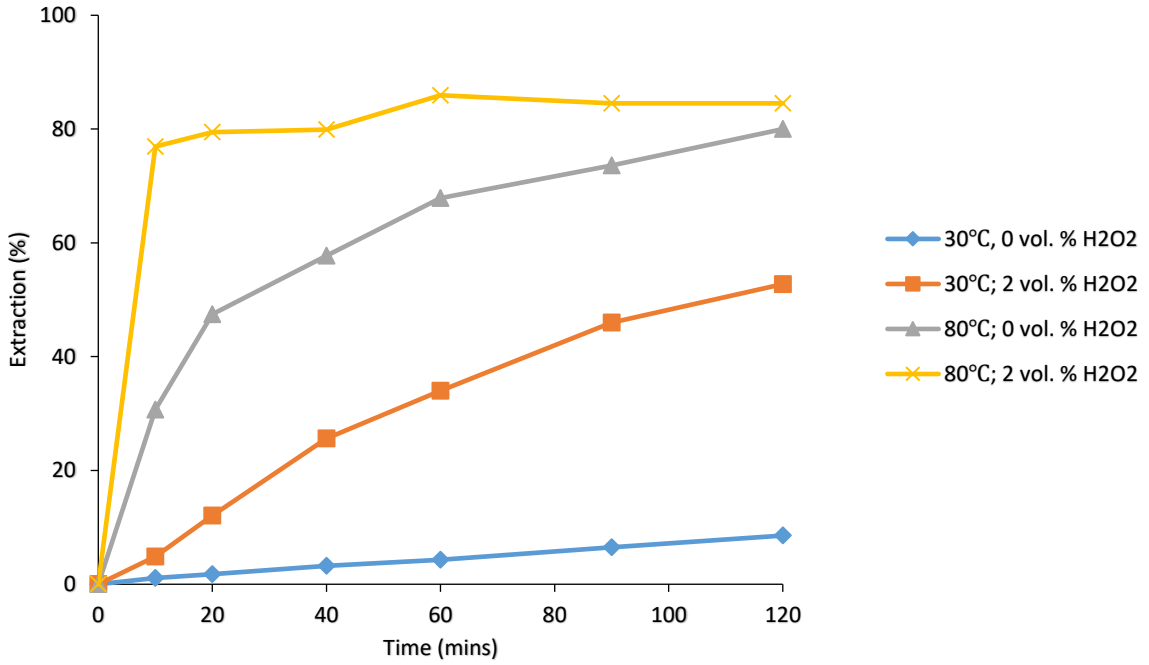

Figure 16: Effect of H_2O_2 addition on Co leaching with 1M citric acid at 20 g/L pulp density.

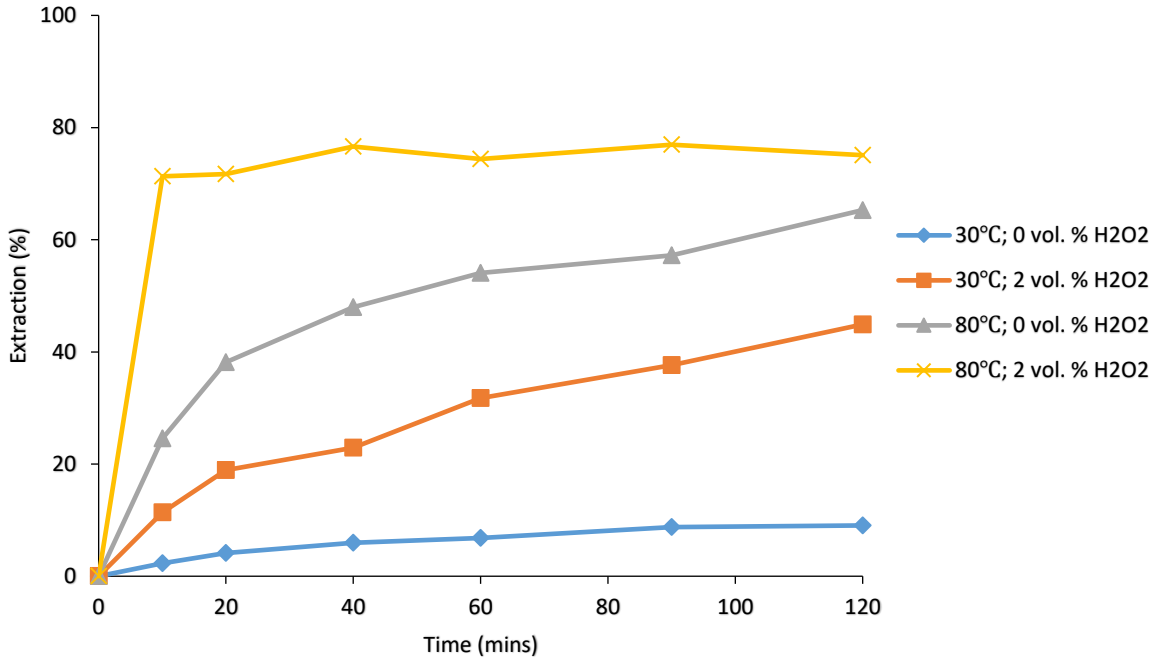

Figure 17: Effect of H_2O_2 addition on Co leaching with 1M DL-malic acid at 20 g/L pulp density.

$$Co_3O_{4(s)} + 2C_6H_8O_{7(aq)} + 3H_2O_{2(l)} \rightarrow Co_3(C_6H_5O_7)_{2(aq)} + 3H_2O_{(l)} + \frac{3}{2}O_{2(g)} \quad [66]$$

$$Co_3O_{4(s)} + 3C_4H_6O_{5(aq)} + H_2O_{2(l)} \rightarrow 3CoC_4H_4O_{5(aq)} + 3H_2O_{(l)} + \frac{1}{2}O_{2(g)} \quad [67]$$

Equations 68 and 69 show the reactions for the H_2O_2 assisted leaching of $LiNi_{0.05}Mn_{0.05}Co_{0.9}O_2$ in citric acid and DL-malic acid, respectively.

$$20LiNi_{0.05}Mn_{0.05}Co_{0.9}O_{2(s)} + 20C_6H_8O_{7(aq)} + 20H_2O_{2(l)} \rightarrow 5Co_3O_{4(s)} + 20Li^{+}{}_{(aq)} + Ni^{2+}{}_{(aq)} + 3Co^{2+}{}_{(aq)} + Mn^{2+}{}_{(aq)} + 20C_6H_5O_7{}^{3-}{}_{(aq)} + 50H_2O_{(l)} + 10O_{2(g)} \quad [68]$$

$$20LiNi_{0.05}Mn_{0.05}Co_{0.9}O_{2(s)} + 20C_4H_6O_{5(aq)} + 20H_2O_{2(l)} \rightarrow 5Co_3O_{4(s)} + 20Li^{+}{}_{(aq)} + Ni^{2+}{}_{(aq)} + 3Co^{2+}{}_{(aq)} + Mn^{2+}{}_{(aq)} + 20C_4H_4O_5{}^{2-}{}_{(aq)} + 50H_2O_{(l)} + 10O_{2(g)} \quad [69]$$

In some studies it has been reported that the reduction rate of Co^{3+} to Co^{2+} increases with an increase in temperature (Golmohammadzadeh *et al.*, 2017; Li *et al.*, 2010, 2009). However, H_2O_2 rapidly decomposes at high temperatures according to Equation 28, from section 2.7.2.3, and the decomposition rate increases with an increase in temperature (Li *et al.*, 2010, 2009).

Li and Ni also follow the Co leaching trends, with both organic acids. While H_2O_2 facilitates the dissolution of Co, Li and Ni leaching is also promoted since the metals are contained in the same oxide compound ($LiNi_{0.05}Mn_{0.05}Co_{0.9}O_2$). This is in agreement with the results reported by Li *et al.*, 2010.

4.2.2 Effect of temperature

Figures 18 shows the effect of temperature on metal dissolution with 1M citric acid and DL-malic acid, while Figures 19 and 20 show the effect of temperature on metal dissolution at 1.25M and 1.5M acid concentrations, respectively. For both citric acid and DL-malic acid, Co, Li and Ni behave just as one would expect. A comparison of the metal dissolution rates at different temperatures shows that increasing the temperature speeds up the leaching kinetics as evidenced by the higher recoveries after 30 minutes, at the higher temperatures (Figures 18, 19 and 20). The fastest leaching kinetics are obtained at the highest temperature (95°C).

This agrees well with what was reported from literature (Li *et al*., 2009; Li *et al*., 2010; Po *et al*., 2016; Li *et al*., 2014; Churl *et al*., 2002).

Temperature plays a key role in these leaching processes. Generally, increase in temperature supplies more kinetic energy to the reacting species, which increases the frequency of collisions and the fraction of species that have sufficient energy to react, which increases the rate constant. Therefore, higher temperatures cause faster leaching kinetics. How the leaching rate responds to temperature change is dependent on the rate limiting mechanism of the process. For chemical reaction controlled systems, rate constant (k) increases exponentially with increase in temperature, according to the Arrhenius' equation. This relationship is represented by Equation 70:

$$k = \mathrm{A}e^{\frac{-\mathrm{E_a}}{\mathrm{RT}}} \qquad [70]$$

Where T is the absolute temperature, R is the ideal gas constant, E_a is the specific activation energy and A is the pre-exponential factor.

Leaching rate can also be limited by diffusion of dissolved acid reactant from the bulk solution to the reaction surface through the boundary and product layer, or by the diffusion of dissolved product from the reaction surface, through the product and boundary layer to the bulk solution. In both cases, if either of these mechanisms or a combination of both is the rate limiting mechanism, the diffusion coefficient (D) increases linearly with increase in temperature, according to Stokes-Einstein's equation, represented by Equation 10, in section 2.5.4.2. From the Equation 10, it can be seen that D is directly proportional to the temperature. Since the diffusion coefficient (D) is directly proportional to diffusion rate of reactants from the bulk solution to the reaction surface (Equation 11) and products from the reaction surface to the bulk solution (Equation 12), an increase in temperature results in an increase in the leaching rate.

From the tests carried out with 1M and 1.5M citric and DL-malic acid, there is an increase in the Co, Li and Ni leaching extent with an increase in temperature from 60℃ to 95℃, as shown in Figures 18 and 20. Figure 19 shows the effect of temperature on leaching at 1.25M acid concentration. With 1.25M citric acid, metal leaching extent also witnesses an increase when the temperature is increased from 60℃ to 95℃ as shown in Figures 19 (a), (b) and (c).

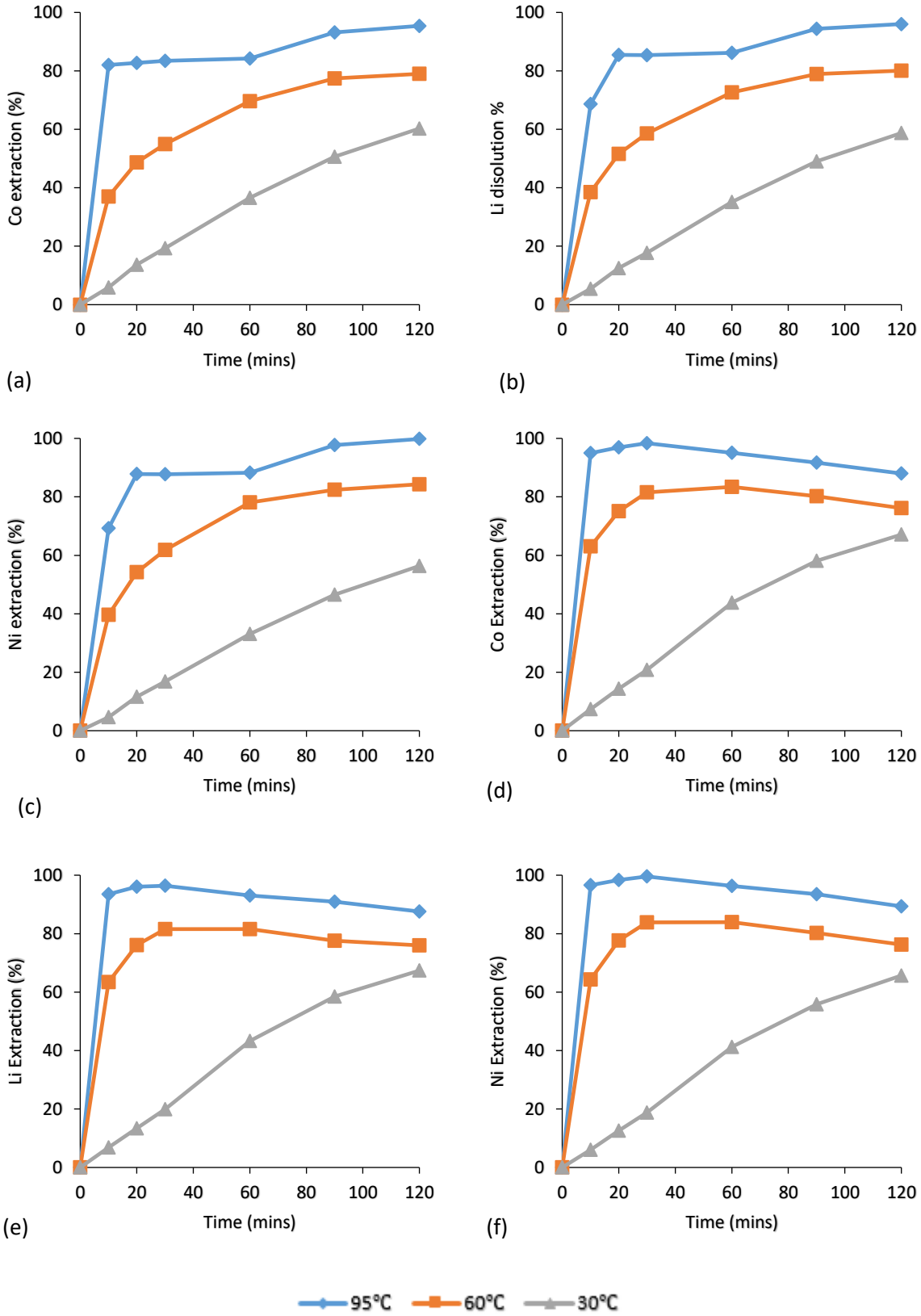

Figure 18: Effect of temperature on cobalt, lithium and nickel leaching with 1M citric acid [(a), (b) and (c)] and 1M DL-malic acid [(d), (e) and (f)].

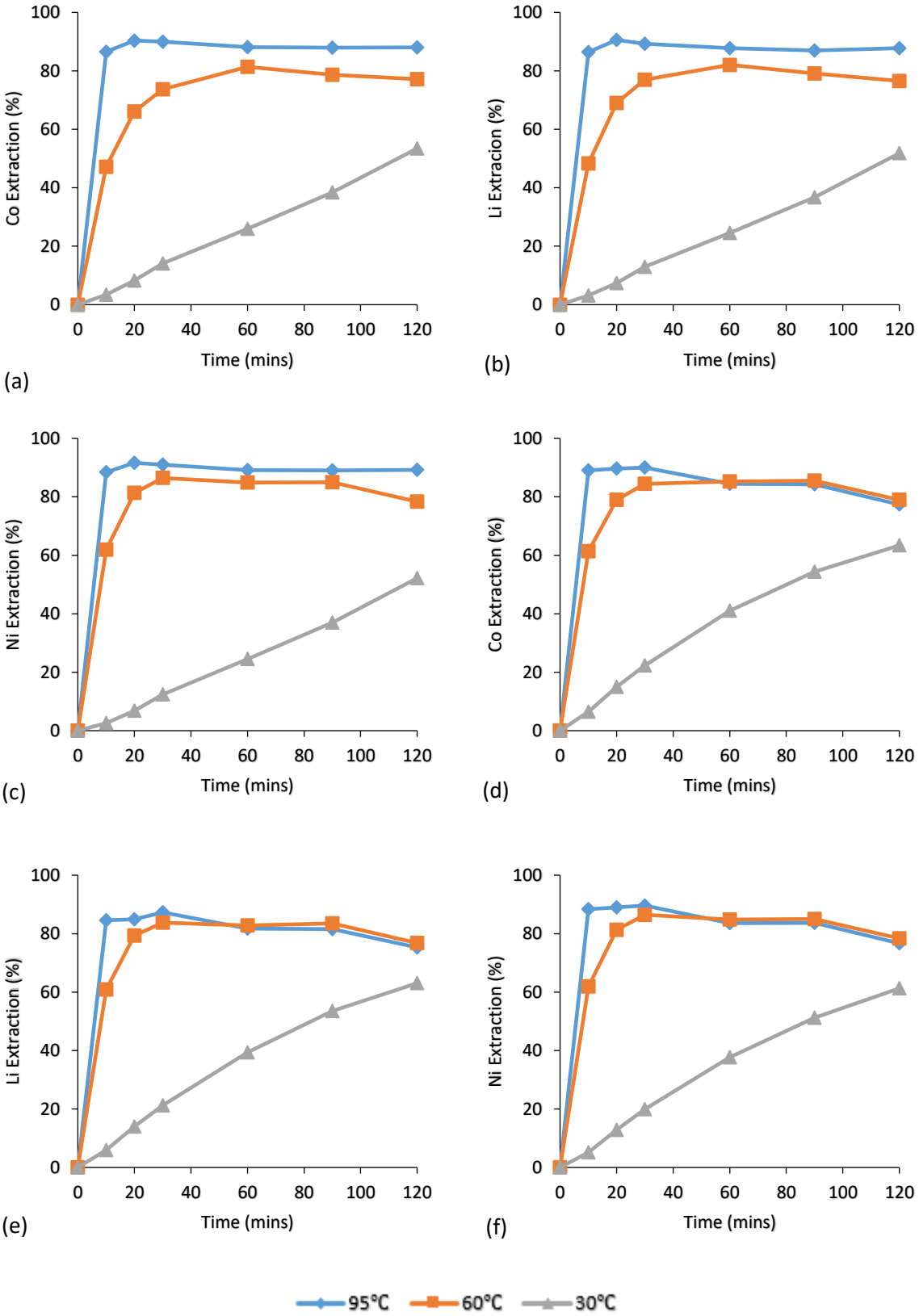

Figure 19: Effect of temperature on cobalt, lithium and nickel leaching with 1.25M citric acid [(a), (b) and (c)] and 1.25M DL-malic acid [(d), (e) and (f)].

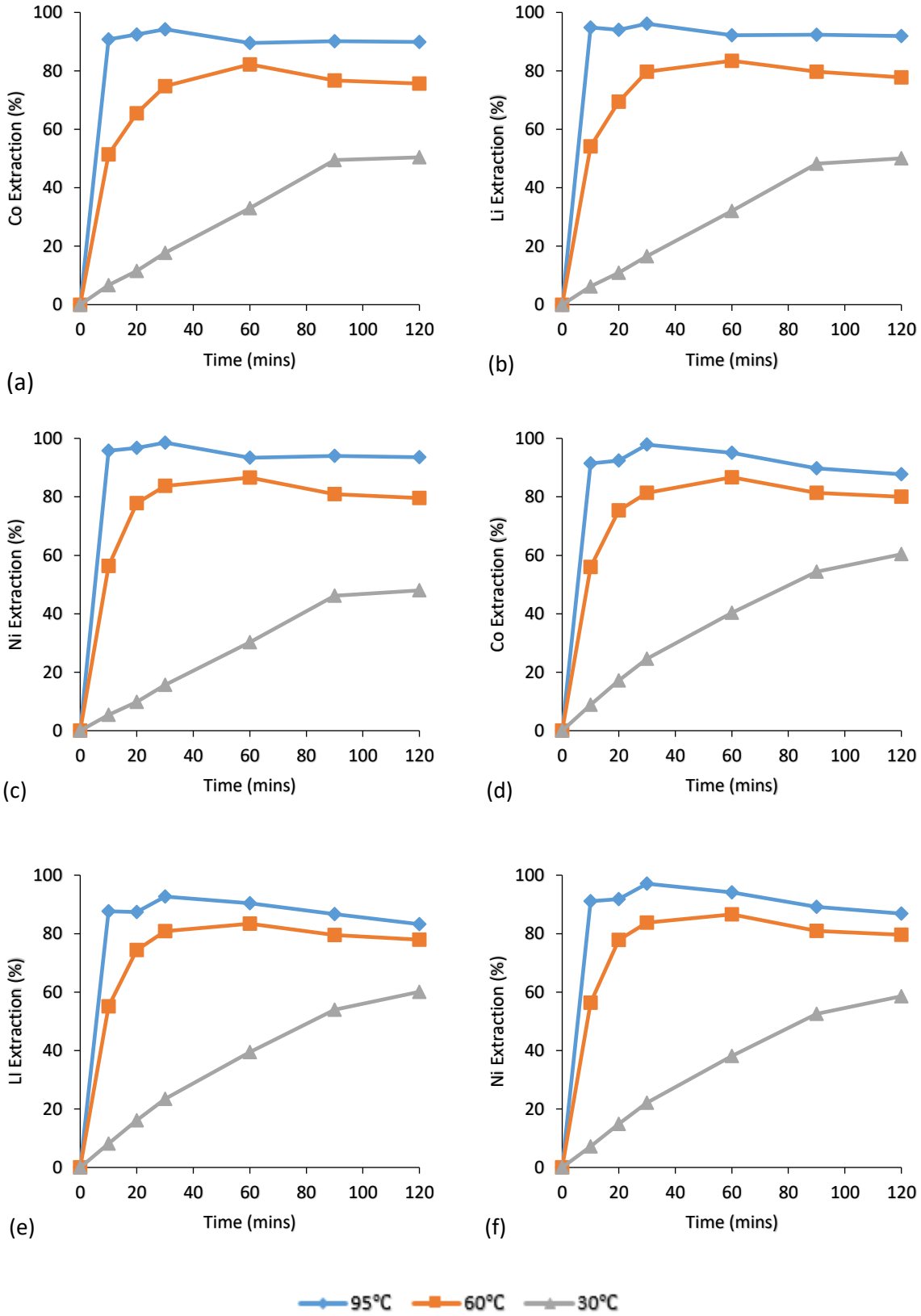

Figure 20: Effect of temperature on cobalt, lithium and nickel leaching with 1.5M citric acid [(a), (b) and (c)] and 1.5M DL-malic acid [(d), (e) and (f)].

Generally, the leaching data seems to indicate that there is an increase in the leaching extent with increase in temperature. There is no comprehensive data from literature on the effect of temperature on solubility of these metal organic acid complexes, but, the leaching data suggests that the solubility of the metal citrate and malate complexes increases with increase in temperature.

With 1.25M DL-malic acid, an increase in temperature from 60℃ to 95℃ does not, however, seem to have an effect on the leaching extent, with the increase in temperature resulting in no difference in leaching extent, as shown in Figures 19 (d), (e) and (f). A conclusion regarding why this was observed could not be made. It seems most reasonable to operate at a temperature of 95℃ since it causes the fastest leaching kinetics, for both citric and DL-malic acid leaching.

4.2.3 Effect of acid concentration

Figures 21 (a), (b) and (c) show the effect of citric acid concentration on Co, Li and Ni leaching, respectively, at 30℃. Figures 21 (d), (e) and (f) show the effect of DL-malic acid concentration on Co, Li and Ni leaching, respectively, at 30℃. From Figures 21 (a), (b) and (c), the metal dissolution rates with 1M and 1.5M citric acid are similar. It seems as if slightly slower leaching rates are exhibited at 1.25M citric acid concentration and it is not clear why. For the leaching tests with DL-malic acid, almost similar leaching rates are exhibited at all three acid concentrations, as shown in Figures 21 (d), (e) and (f). Generally, citric and DL-malic acid concentration appears not to have a significant effect on metal dissolution rate at 30℃.

This may be due to the fact that there is high enough percentage excess acid for the leaching rate at 30℃ to be modelled as having a pseudo zeroth order dependence on acid concentration. At 1M acid concentrations, the % excess acid is 615% for citric acid and 376% for DL-malic acid (sample calculations shown in Appendix B, section 8.2.1). After leaching for 120 minutes, at 30℃, about 50% metal dissolution has taken place, as shown in Figures 21 (a)-(f). This means that at every point within the 120 minute data capturing period, the % excess acid is actually more than 615% and 376% in the citric acid and DL-malic acid systems, respectively, hence, increasing the acid concentration from 1M-1.5M may not have a heavy impact on the leaching rate.

Figures 22 (a), (b) and (c) show the effect of citric acid concentration on Co, Li and Ni leaching at 60°C, respectively. From Figures 22 (a), (b) and (c), there is an increase in metal dissolution rate when citric acid concentration is increased from 1M to 1.25M and 1.5M. At 1M, 80% Co leaching was achieved after 120 minutes. When citric acid concentration was increased to 1.25M, 81% Co leaching was achieved within 60 minutes. The same observations were also made for citric acid leaching at 95°C. The effect of citric acid concentration on leaching at 95°C is shown in Figures 23 (a), (b) and (c). It can be seen that an increase in acid concentration results in an increase in metal dissolution rate.

This may potentially be explained using the Nerst model represented by Equation 9, from section 2.5.4.2. For leaching processes controlled by diffusion through the boundary layer, rate of reaction is directly proportional to the difference in leaching reagent concentration between the mineral reaction surface and the bulk solution. These processes may be controlled by diffusion through the boundary layer at 60°C and 95°C. Increasing citric acid concentration results in an increase in that acid concentration difference, generating a steeper diffusion gradient, which results in faster diffusion rate of dissolved acid reactant to the mineral surface. Consequently, this speeds up the leaching kinetics. This is in agreement with what was reported from literature (Li *et al.*, 2013, 2014; Li *et al.*, 2010).

From Figures 22 (a), (b) and (c), at 60°C, there is no change in Co, Li and Ni leaching rate when citric acid concentration is further increased from 1.25M to 1.5M. Since increase in citric acid concentration from 1M to 1.25M results in faster leaching kinetics, it would also be expected for the leaching kinetics to speed up when the acid concentration is increased from 1.25M to 1.5M. No conclusion could be made regarding why this was observed.

The effects of citric acid concentration on leaching at 95°C can be seen in Figures 23 (a), (b) and (c). The highest metal leaching extents were obtained with 1M citric acid (95% Co, 96% Li and 99% Ni dissolution after 120 minutes) and 1.5M citric acid (95% Co, 96% Li and 99% Ni dissolution within 30 minutes). The leaching extents achieved at these two acid concentrations are similar, but at 1M it appears as if equilibrium has not been reached and leaching is still taking place. This may be due to the solubility of metal citrate complexes in 1M acid being higher than that in 1.5M acid, suggesting that there is a decrease in the solubility of the complexes with an increase in citric acid concentration.

However, there is no data from literature on the solubility of these complexes in citric acid. A conclusion could not be made why 1.25M citric acid yields a leaching extent lower than the ones from 1M and 1.5M acid concentrations. The fastest leaching kinetics are obtained with 1.5M citric acid. Considering the additional energy costs that will be incurred by agitating and heating for longer periods of time with 1M citric acid, operating at 1.5M acid concentration seems most reasonable.

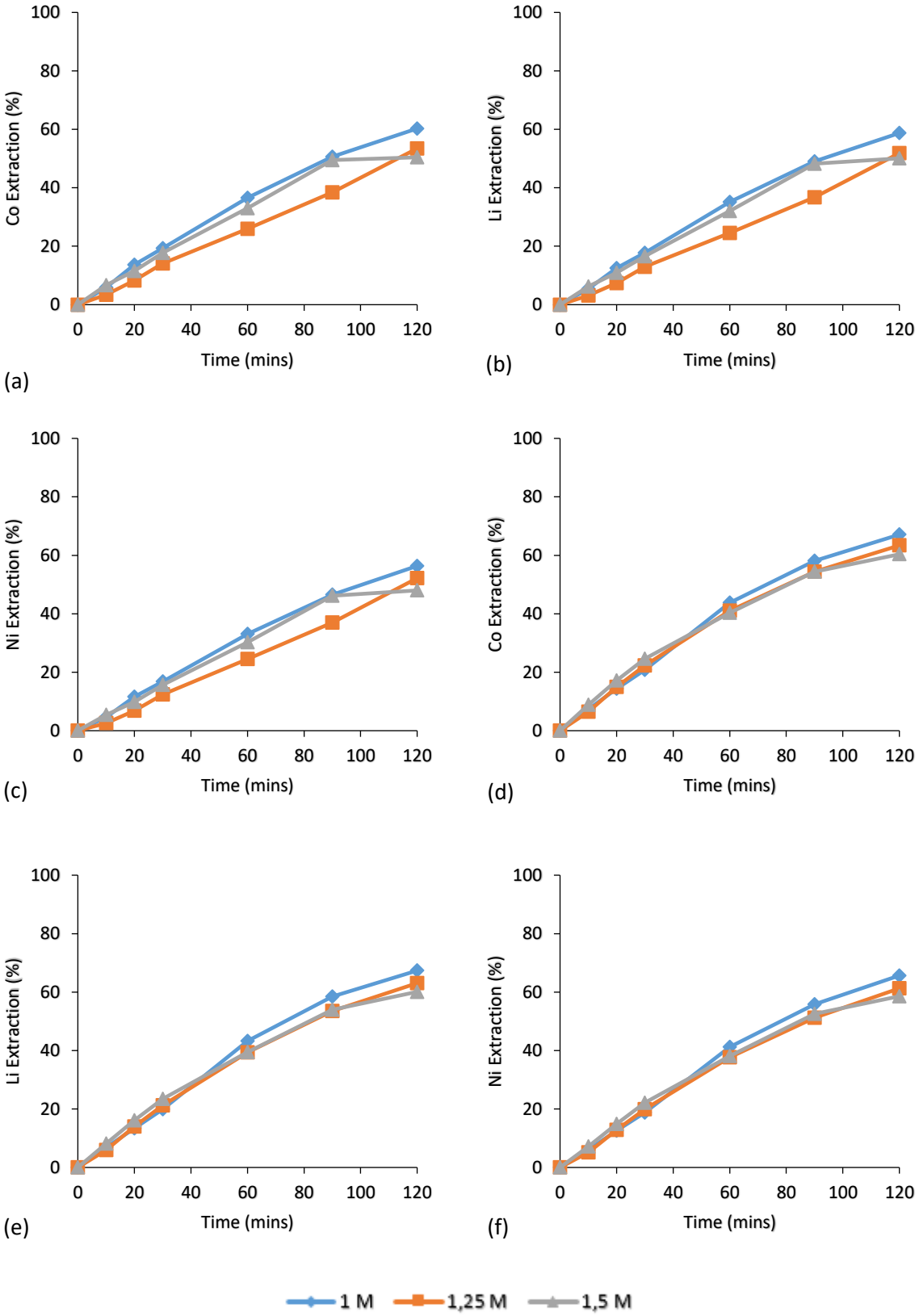

Figure 21: Effect of citric acid [(a), (b) and (c)] and DL-malic acid [(d), (e) and (f)] concentration on cobalt, lithium and nickel leaching at 30℃

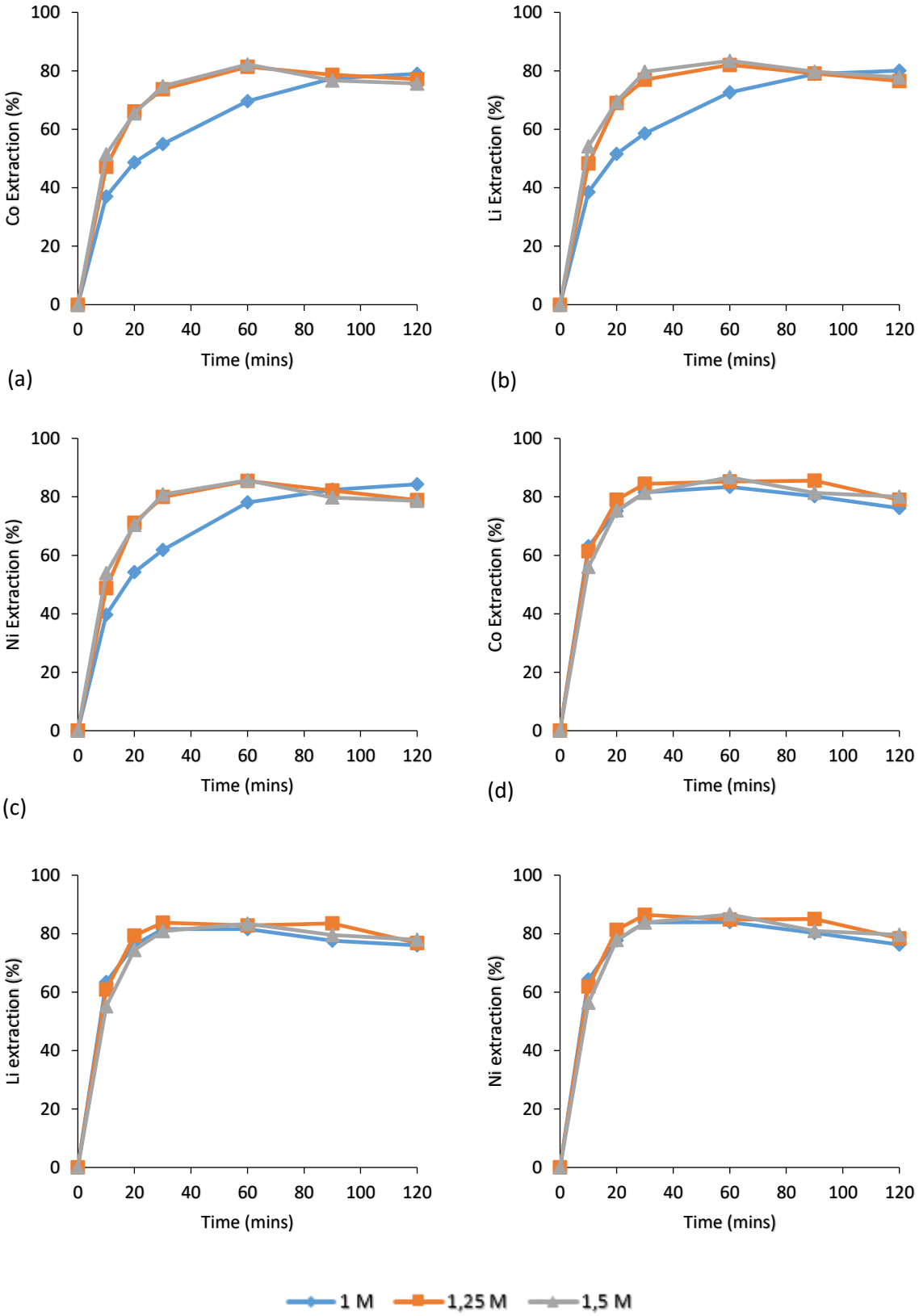

Figure 22: Effect of citric acid [(a), (b) and (c)] and DL-malic acid [(d), (e) and (f)] concentration on cobalt, lithium and nickel leaching at 60℃

Figures 22 (d), (e) and (f) show the effect of DL-malic acid concentration on Co, Li and Ni dissolution, respectively, at 60℃. DL-malic acid concentration appears to have no effect at all on leaching at 60℃, as evidenced by the similar leaching rates and extents at all three acid concentrations.

Figures 23 (d), (e) and (f) show the effect of DL-malic acid concentration on Co, Li and Ni leaching, respectively, at 95℃. It seems as if DL-malic concentration does not heavily impact the leaching kinetics as evidenced by the similar metal dissolution rates at all three acid concentrations.

The leaching extent does not, however, present a clear trend with changing DL-malic acid concentration, but, what can be noted is that the increase in acid concentration from 1M to 1.25M and 1.5M seems to result in a decrease in the leaching extent. This agrees with the results that were reported from a study by Li, *et al.*, 2010. This may be attributed to a decrease in metal solubility in DL-malic acid as the amount acid in the system is increased. However, there is no data from literature on the solubility of these metal malate complexes in DL-malic acid. It is not clear why leaching extent was higher with 1.5M DL-malic acid than it was with 1.25M DL-malic acid and a conclusion could not be made regarding this observation.

1M DL-malic acid yielded higher metal recoveries (99% Co, 96% Li, 99% Ni) than 1.5M DL-malic acid (97% Co, 92% Li, 97% Ni), after 30 minutes. Generally, these recoveries can be considered as being comparable, but, considering the higher recoveries yielded by 1M DL-malic acid and the additional costs that will be incurred in increasing the acid concentration, it would be best to operate at 1M acid concentration.

From Figures 18, 19, and 20, there is a decrease in metal concentration in solution with time for the leaching tests that were carried out at 60℃ and 95℃. This may be attributed to precipitation of metal complexes from solution. However, comparing Figures 18 (a), (b) and (c) against 18 (d), (e) and (f), at 1M acid concentrations, precipitation is observed with DL-malic acid but not with citric acid.

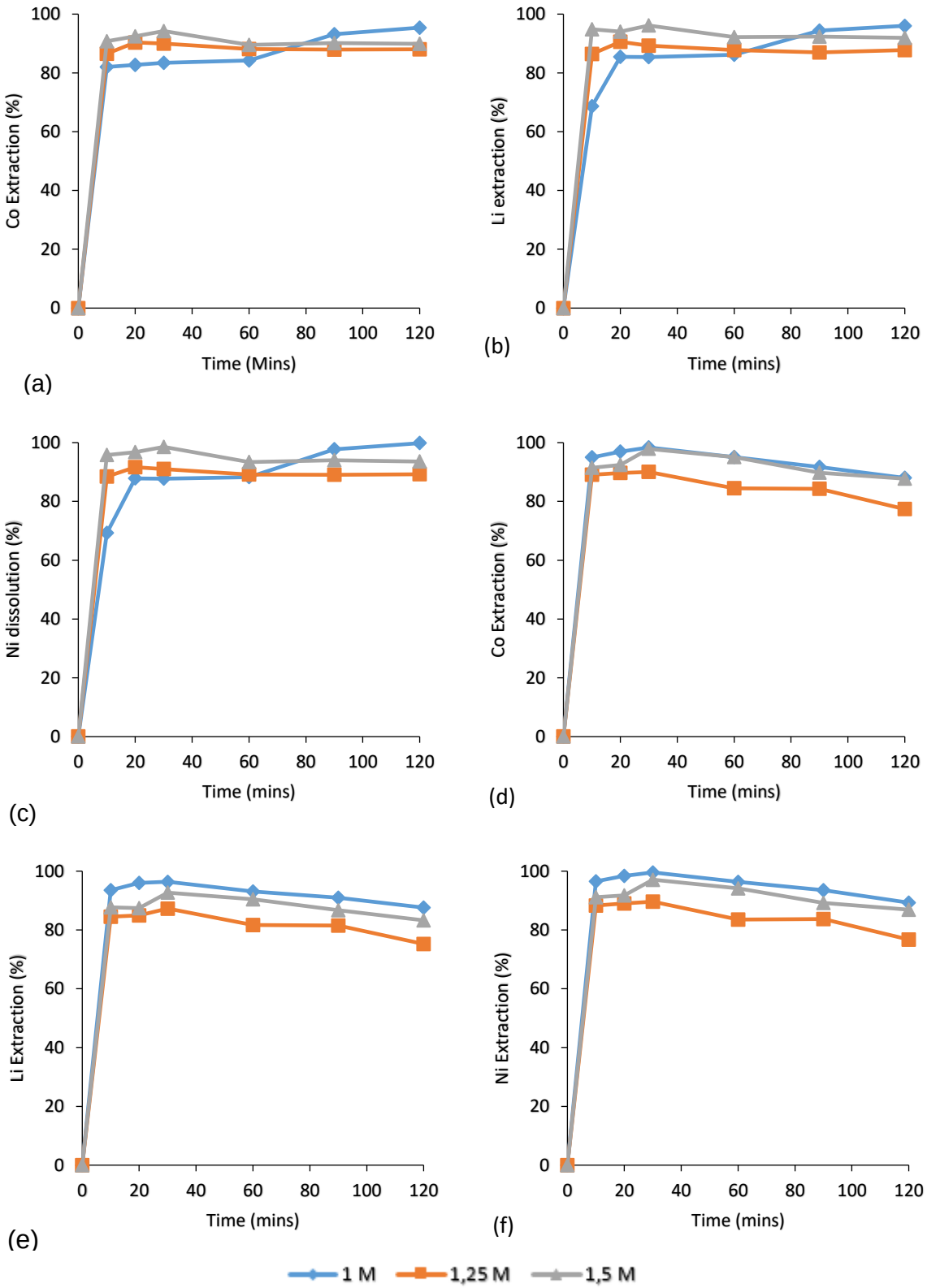

Figure 23: Effect of citric acid [(a), (b) and (c)] and DL-malic acid [(d), (e) and (f)] concentration on cobalt, lithium and nickel leaching at 95 ℃

This may be because with 1M citric acid, equilibrium has not been attained after 120 minutes, the solubility limit has not been reached yet and metal dissolution is still taking place. This is evidenced by Figures 18 (a), (b) and (c), which show that after 120 minutes, equilibrium has not been reached yet and the forward reaction is still being favoured; hence, no notable precipitation.

4.2.4 Reaction kinetics

In order to determine the rate-limiting step at the different conditions, Co leaching data from citric acid and DL-malic acid leaching were fitted to three kinetic models that were described by Levenspiel, 1999. Since Li and Ni follow the same trends as Co leaching, the data from Co leaching were considered as being representative of the Li and Ni extraction behavior. The three rate limiting steps are; diffusion through the boundary layer, chemical reaction and diffusion through the product layer. Equation 71 is the suitable model if the rate is limited by chemical reaction, while Equations 72 and 73 represent diffusion through the boundary layer and diffusion through the product layer limiting mechanisms, respectively.

$$1-(1-X)^{1/3}=kt \qquad [71]$$

$$1-(1-X)^{2/3}=kt \qquad [72]$$

$$1-\frac{2}{3}X-(1-X)^{2/3}=kt \qquad [73]$$

Table 16 shows a comparison of the three kinetic models applied to citric acid leaching. It appears as if the citric acid leaching process is controlled by diffusion in the boundary layer at 30℃ , since the R^2 values from the diffusion in boundary layer model are higher than the other two. Although the diffusion in boundary layer kinetic model seems to have the best fit, its R^2 values are almost similar to those from the chemical reaction model. In this scenario, the leaching rate can be considered as having a mixed control mechanism (boundary layer diffusion and chemical reaction) at 30℃.

Table 17 shows the kinetic models applied to DL-malic acid leaching tests. It appears as if chemical reaction is the rate-limiting mechanism at 30℃, at all three acid concentrations. This is evidenced by the chemical reaction model R^2 values, which are higher than the other two, as shown in Table 17.

For both citric acid and DL-malic acid, the leaching rate seems to be limited by diffusion through a product layer at 60℃, as evidenced by the R^2 values which are higher than the chemical reaction and diffusion in boundary layer ones (Tables 16 and 17). This suggests that there is a residue that develops around the mineral surfaces as the leaching progresses. As mentioned earlier in section 3.2, no calcination was done on the sample and organic PVDF and PTFE binder may still be on the cathodic material particles. During leaching, the binder and acetylene black electrolyte do not dissolve. They remain behind to form a black residue with a loose structure. As the leaching reaction progresses, there is build-up of this inert residue around the shrinking particles, and acid molecules must diffuse through this layer of ash to the reaction surface. The product layer is essentially carbon and fluorine.

Table 16: Comparison of the three kinetic models for citric acid leaching.

Boundary layer		**Chemical reaction**		**Product layer**		**Acid**	**Temp**
R^2	**k (min^{-1})**	**R^2**	**k (min^{-1})**	**R^2**	**k (min^{-1})**	**Concentration**	
0.9982	0.0042	0.996	0.0023	0.9439	0.0004	1M	30℃
0.9979	0.0031	0.9966	0.0016	0.8719	0.0002	1.25M	
0.999	0.004	0.9963	0.0022	0.86	0.0003	1.5M	
0.8305	0.0159	0.86	0.0089	0.9869	0.0016	1M	60℃
0.874	0.0225	0.9166	0.0134	0.9926	0.0034	1.25M	
0.8412	0.0229	0.8915	0.0137	0.9954	0.0035	1.5M	
0.7116	0.0412	0.7161	0.0264	0.7253	0.0082	1M	95℃
0.7602	0.0463	0.7897	0.034	0.8277	0.0107	1.25M	
0.7275	0.0487	0.7446	0.034	0.7617	0.012	1.5M	

At 95℃, the reaction rate is too fast for the kinetic models to be applied and the data does not fit well to the models, as indicated by the low R^2 values. But, since the leaching temperature is high (95℃), it may be assumed that the process is diffusion controlled, and given that there is a product layer that forms, at 95℃ the leaching process might also be limited by diffusion through a product layer. This analysis seems to be suggesting that at low temperatures, the leaching process is limited by chemical reaction. As temperature is

increased, the leaching process shifts from being chemical reaction controlled to being diffusion through a product layer controlled. This strongly agrees with the findings that were reported by Golmohammadzadeh *et al.*, 2017.

Table 17: Comparison of the three kinetic models for DL-malic acid leaching

Boundary layer		**Chemical reaction**		**Porous product layer**		**Acid Concentration**	**Temp**
R^2	**k (min^{-1})**	**R^2**	**k (min^{-1})**	**R^2**	**k (min^{-1})**		
0.9866	0.0047	0.9943	0.0027	0.9348	0.0006	1M	30℃
0.9941	0.0047	0.9983	0.0026	0.9123	0.0004	1.25M	
0.9583	0.0043	0.9767	0.0024	0.9595	0.0005	1.5M	
0.7544	0.0266	0.8196	0.016	0.9512	0.0048	1M	60℃
0.8055	0.0278	0.8714	0.0176	0.971	0.0053	1.25M	
0.8376	0.0261	0.8937	0.0162	0.9803	0.0047	1.5M	
0.7373	0.0533	0.7714	0.04	0.7859	0.0148	1M	95℃
0.7091	0.0466	0.7141	0.0317	0.7205	0.0108	1.25M	
0.717	0.049	0.728	0.0343	0.7387	0.0121	1.5M	

4.2.5 Comparison of citric and DL-malic acid

Slightly higher recoveries were obtained using DL-malic acid as a lixiviant. Table 18 shows bulk prices of industrial grade citric acid and DL-malic acid. It can be seen from Table 18 that the price of DL-malic acid is about twice as much as that of citric acid. Citric acid was selected as the more suitable leaching agent since it is cheaper.

Table 18: Bulk prices of industrial grade organic acids.

Acid	**Price**
Citric acid	USD 700-900/Metric Ton
DL-malic acid	USD 1800-2500/Metric Ton

4.2.6 Statistical analysis

4.2.6.1 ANOVA

Analysis of variance was carried out on the full factorial experimental design that was used during the leaching tests. For both acids, Co, Li and Ni extraction were used as the response variables. The ANOVA data that were generated are presented in Tables 30-35, in Appendix B. The p-values in Tables 30-35 suggest that temperature has a statistically significant effect on Co, Li and Ni extraction at 95% confidence level (the values are < 0.05). Acid concentration does not have a statistically significant effect on metal extraction, as evidenced by the p-values > 0.05. This further supports what has already been discussed in sections 4.2.2 and 4.2.3, namely, that temperature has a significant impact on the leaching process, while acid concentration does not.

4.2.6.2 Repeatability

To check for the repeatability of the leaching tests, three repeat runs were carried out for each acid at the optimum conditions. Repeat runs were carried out using 1.5M citric acid and 1M DL-malic acid with 2% v/v H_2O_2 at 20 g/L pulp density and 95℃. A data table for the repeatability tests is presented in Appendix B, Table 36.

For citric acid leaching, the maximum recoveries are obtained after 30 minutes, with 92±1.07% Co, 92±0.63% Li and 95±1.23% Ni extraction. Based on the error limits, Li dissolution has the highest repeatability followed by Co and then Ni. For DL-malic acid leaching repeats, the maximum recoveries were also obtained after 30 minutes for all three repeats, with averages of 95±2.70% Co, 95±2.21% Li and 97±1.86% Ni dissolution. Ni dissolution has the highest repeatability followed by Li and then Co.

Overall, the repeatability of the leaching tests with both acids can be considered as being high. The recoveries for citric acid and DL-malic acid leaching are within ±2% and ±3% error limits, respectively. Figure 24 shows the extraction behavior of Co, Li and Ni in citric acid and DL-malic acid during the repeat runs. From Figure 24, it can be seen that the replicated extraction curves have similar trends, for both citric acid and DL-malic acid, which is also an indication of good repeatability.

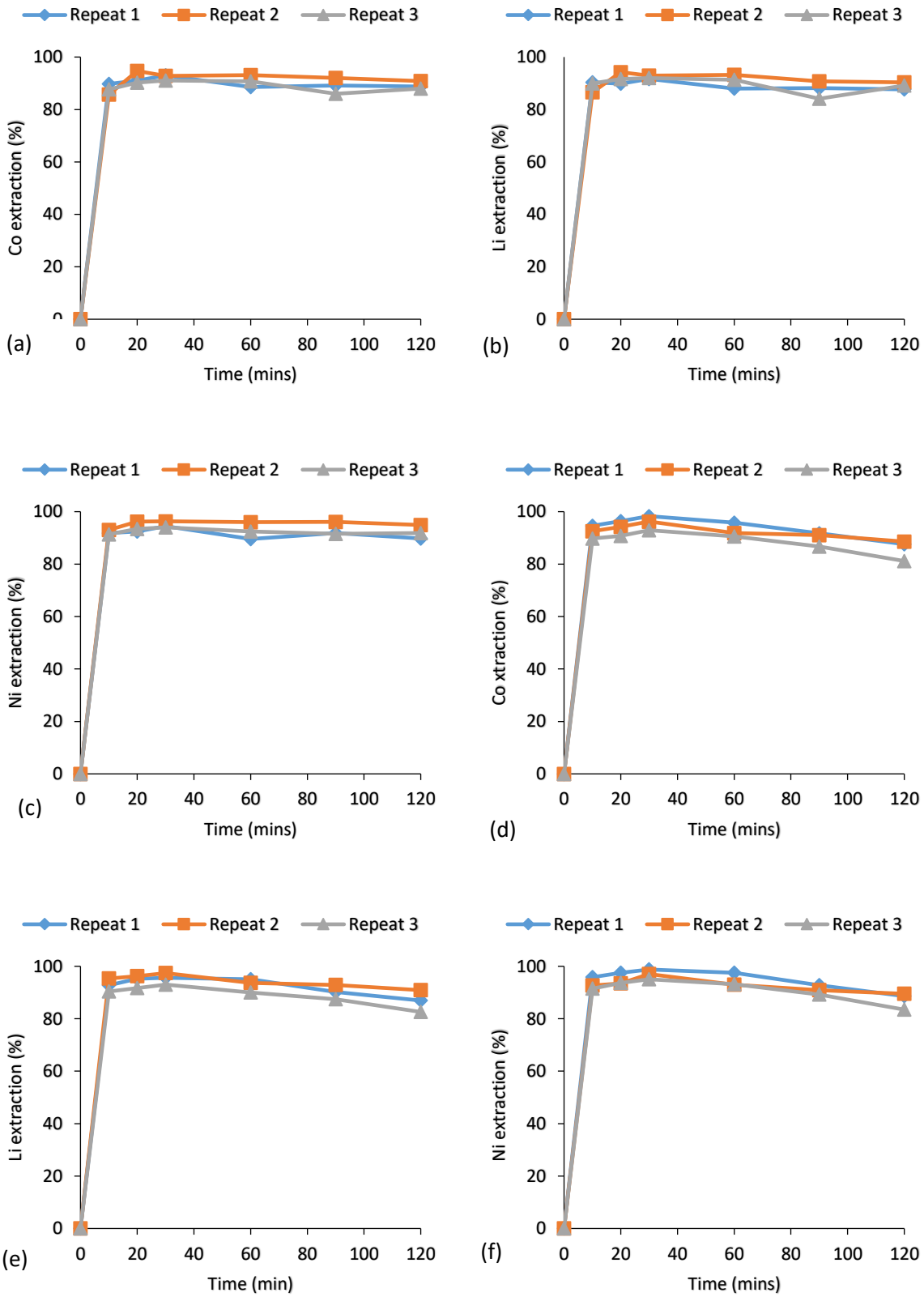

Figure 24: Extraction behavior in citric acid {(a) Co, (b) Li, and (c) Ni} and in DL-malic acid {(d) Co, (e) Li and (f) Ni} during repeat runs.

4.3 Solvent extraction

4.3.1 Mn extraction

The aim of the solvent extraction step was to investigate the extraction of Mn and Al and separate them from the rest of the elements in solution. Results on the effects of pH, O/A ratio and D2EHPA concentration on the separation process are presented in this section. Percent extraction, distribution coefficients and separation factors of Mn relative to each metal were used to evaluate the effectiveness of the solvent extraction tests. A decision on the most suitable conditions for the separation process was made based on these results.

Figure 25 (a) shows the effect of O/A ratio and pH on Mn extraction with 10% v/v D2EHPA, while Figure 25 (b) shows the effect of O/A ratio and pH on the Mn distribution coefficient, with 10% v/v D2EHPA. Figure 25 (c) illustrates the effect of O/A ratio and pH on Mn extraction, while Figure 25 (d) shows the effect of O/A ratio and pH on the Mn distribution coefficient, using 20% v/v D2EHPA.

From Figures 25 (a) - (d), it can be seen that metal extraction increases when there is more extractant in the system (either due to higher O/A ratio or due to higher % extractant in the organic phase). This can be attributed to the presence of more D2EHPA in the system available to complex with the metal species from the aqueous phase. This also agrees with the reports from literature (Chen & Ho, 2018; Chen & Zhou, 2014; Chen *et al.*, 2015).

From Figure 25 (a) - (d), increase in pH results in higher metal extraction. This can be explained using Equation 38 which represents the general solvent extraction reaction. When pH is increased, there is a decrease in the concentration of H^+ ions in the aqueous solution and the system responds in a way that counters this effect, that is the generation of more H^+ ions. This means that the equilibrium shifts to the right and the forward reaction is favored, which results in increased metal extraction. This also agrees with reports by Chen *et al.*, 2015 and Chen & Ho, 2018.

Comparing Figures 25 (a) and (c), at the higher D2EHPA concentration (20% v/v) the increase in Mn extraction with pH increase becomes less remarkable. The use of a higher extractant

concentration lowers the pH at which extraction occurs. This is because of the extra protons being introduced to the system, coming from the D2EHPA.

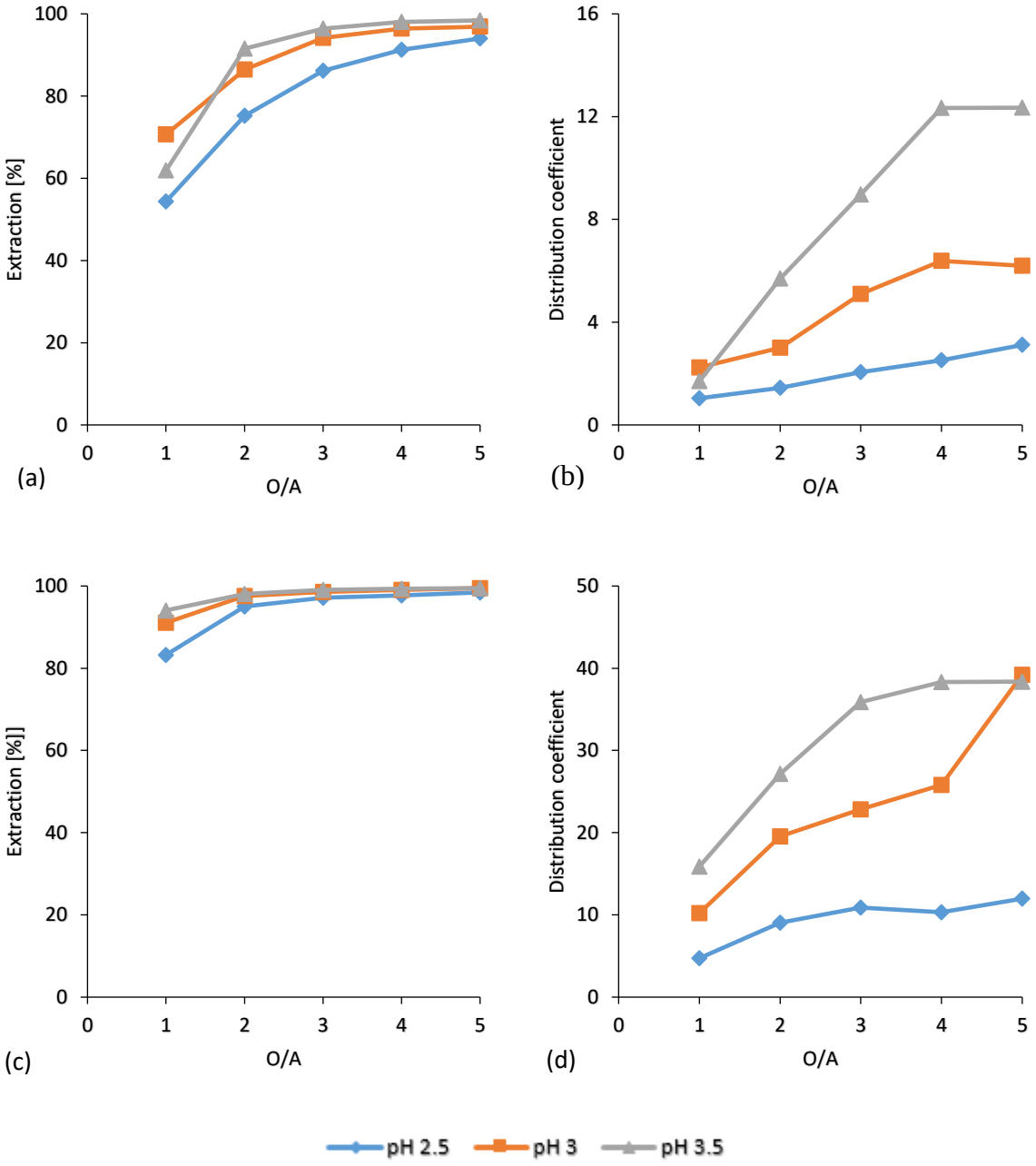

Figure 25: (a) Mn % extraction and (b) Distribution coefficient using 10% v/v D2EHPA; (c) Mn % extraction and (d) Distribution coefficient using 20% v/v D2EHPA

4.3.2 Co-extraction of other elements

Figure 26 (a) shows metal extraction at pH 2.5 with 10% v/v D2EHPA. Co, Li and Ni extraction is generally constant, not exceeding 10%, as the O/A is increased from 1 to 5. Although the ratio at which the organic phase and aqueous phase are fed to the system is increased, there

is no appreciable extraction. The selectivity in this solvent extraction process may possibly be driven by the strength of the bonds between the metal cations and citrate anion. Mn, Co and Ni ionic radii are almost similar. However, Co and Ni have a higher nuclear charge than Mn and they form stronger bonds with the citrate anions than those formed by Mn. Therefore, it is easier to break the bonds between Mn and citrate anions, allowing for cation exchange. Al and Li have smaller ionic radii than Mn and their cations also form stronger bonds with the citrate anions than Mn. This makes D2EHPA selective towards Mn.

Al extraction witnesses a steady increase from about 16% to 46% as the O/A ratio is increased from 1 to 5. It appears as if there is more Al extraction than Co, Li and Ni at pH 2.5. This suggests that D2EHPA has a higher affinity for Al than the other metals, hence an increase in Al extraction when more D2EHPA is added to the system.

Figure 26 (d) shows metal extraction with 20% v/v D2EHPA at pH 2.5. There is increase in metal extraction with an increase in O/A ratio. Co and Li extraction increase by about 20%, while Ni extraction increases by just over 10%. From O/A ratio 3 to 5, around 65% Al is extracted. Effectively, increase in % extractant and O/A ratio increases Al, Co, Li and Ni co-extraction. This can be explained using the general extraction reaction (Equation 38). An increase in the amount of D2EHPA results in the system reacting in a way that uses up the extractant to counter the effect. This shifts the equilibrium to the right and the forward reaction is favored, resulting in more metal extraction.

Figure 26 (b) shows extraction results with 10% v/v D2EHPA at pH 3. Comparing the extraction at pH 2.5 with extraction at pH 3, both with 10% v/v D2EHPA, it is observed that there is relatively higher Co Li and Ni co-extraction at pH 3 (16% Co, 19% Li and 12%Ni at O/A ratio 5). This would be expected since increase in pH favors the forward extraction reaction (Equation 38). There is extensive literature on how the extraction of these metals from sulphate solutions with D2EHPA and Cyanex 272 increases with an increase in pH. Some work was also done by Chen & Zhou, 2014 and Chen *et al.*, 2015, from which it was reported that their co-extraction metals during Mn extraction from citrate solution with D2EHPA increases with an increase in pH.

However, Al extraction witnesses a drop when pH is increased from 2.5 to 3. For example, about 36% Al is extracted at O/A ratio 5 and pH 3, which is lower than the 47% extraction

obtained at pH 2.5 and O/A ration 5 (at 10% v/v D2EHPA). It appears as if Al extraction decreases with an increase in pH. This may be because of more competition for the extractant offered by the other metals in solution when pH is raised. When pH is increased, Co, Li, Mn and Ni extraction increases, which increases competition for the extractant. The extractant that is supposed to be used for Al extraction at a lower pH will be used for Co, Li, Mn and Ni extraction, resulting in an overall decrease in Al extraction when pH is increased. The increase in Co, Li and Ni extraction with increase in O/A ratio is not remarkable.

Figure 26 (e) shows extraction with 20% v/v D2EHPA at pH 3. There is higher Co, Li and Ni co-extraction with 20% v/v D2EHPA than with 10% v/v D2EHPA, at pH 3 due to the greater amount of extractant in 20% v/v D2EHPA, which increases extraction. The co-extraction of these metals also witnesses an increase when the O/A ratio is increased from 1-5.

From Figure 26 (e), it can be seen that Mn extraction reaches near completion at O/A ratio 3 and when the O/A ratio is further increased, Co, Li and Ni co-extraction increases drastically. This may be because all the extra D2EHPA that is added to the system at O/A ratios 4 and 5 is used for Al, Co, Li and Ni extraction since the amount of extractant at O/A ratio 3 is enough for complete Mn extraction.

This increase in co-extraction is also illustrated by the separation factors. Figure 28 shows the Mn/Al, Mn/Co, Mn/Li and Mn/Ni separation factors for extraction with 20% v/v D2EHPA. At pH 3, the Mn/Al, Mn/Co, Mn/Li and Mn/Ni separation factors start dropping from O/A ratio 3 up to 5, showing that there is an increase in co-extraction of these metals when the O/A ratio is increased from 3 to 5.

Comparing Figures 26 (b) and (c), it can be observed that there is higher Co, Li and Ni co-extraction at pH 3.5 than at pH 3, with 10% v/v D2EHPA and O/A ratios 3 and 4, especially Li. Al extraction witnesses a decrease when the pH is raised from 3 to 3.5, further supporting what was suggested earlier in the discussion that Al extraction decreases with an increase in pH. Figure 26 (f) shows extraction behavior with 20% D2EHPA at pH 3.5. At pH 3.5, 20% v/v D2EHPA causes higher Co, Li and Ni co-extraction than 10% v/v D2EHPA. This can be seen by comparing Figures 26 (c) and (f).

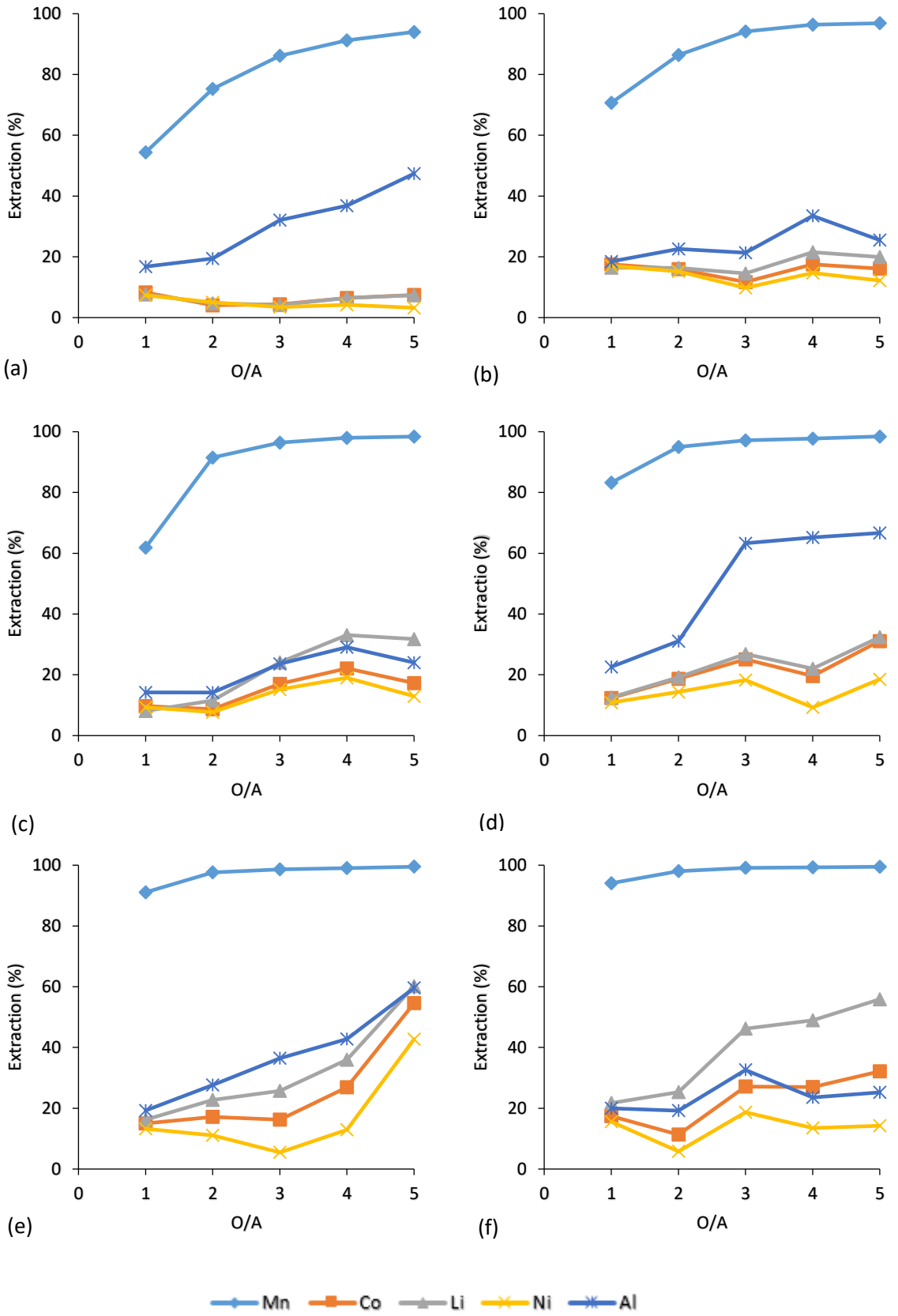

Figure 26: Solvent extraction at (a) pH 2.5, (b) pH 3, (c) pH 3.5, with 10% v/v D2EHPA; Extraction at (d) pH 2.5, (e) pH 3, (f) pH 3.5, with 20% v/v D2EHPA.

The results that have been discussed so far seem to indicate that there is greater selectivity at low extractant concentration and pH; and an increase in one or both of these factors results in loss of selectivity.

4.3.3 Separation factors

The aim of the solvent extraction tests was to determine the optimum conditions for Mn and Al separation from the rest of the metals in the PLS. Therefore, the Mn/Al, Mn/Co, Mn/Li and Mn/Ni separation factors, as well as the percentage extractions at different conditions were considered in the selection of the most suitable conditions.

Figures 27 and 28 show the separation factors with 10% v/v D2EHPA and 20% v/v D2EHPA, respectively. Since it was desired for as much Al as possible to be extracted along with Mn, conditions that yielded low Mn/Al separation factors were required. The lowest Mn/Al separation factors were obtained with 10% v/v D2EHPA at pH 2.5, ranging from 9 to 18 when O/A ratio was increased from 1 to 5, as shown in Figure 27 (a). With 20% v/v D2EHPA at pH 2.5, the Mn/Al separation factors increased from 20 to 33 when O/A ratio was varied from 1 to 5, as shown in Figure 28 (a).

The Mn/ Co separation factors will be discussed next. The highest separation factor (405) was obtained with 20% v/v D2EHPA at pH 3.5 and O/A ratio 5, as shown in Figure 28 (b). However, pH 3.5 yielded higher Mn/Al separation factors, which was not desired since it would result in a higher Al content in the product solution. The second highest (376) was at pH 3 and O/A ratio 3 with 20% v/v D2EHPA. Under these conditions the Mn/Al separation factor was 123, and it was relatively higher that the ones at pH 2.5, which were all below 50. The Mn/Co separation factor at pH 3.5 and O/A ratio 5 with 10% v/v D2EHPA then followed with a value of 295, as shown in Figure 27 (b). However, under these conditions, the Mn/Al separation factor was 195 and this would also result in undesirably high Al content in the product solution. A pH of 2.5 at O/A ratio 5 and 10% v/v D2EHPA were selected as the most suitable conditions for Mn-Co separation, since the separation factor (266) was reasonably high, with 94% Mn, 47% Al extraction and less than 8% Co co-extraction in one stage. The Mn/Al separation factor was also low (19).

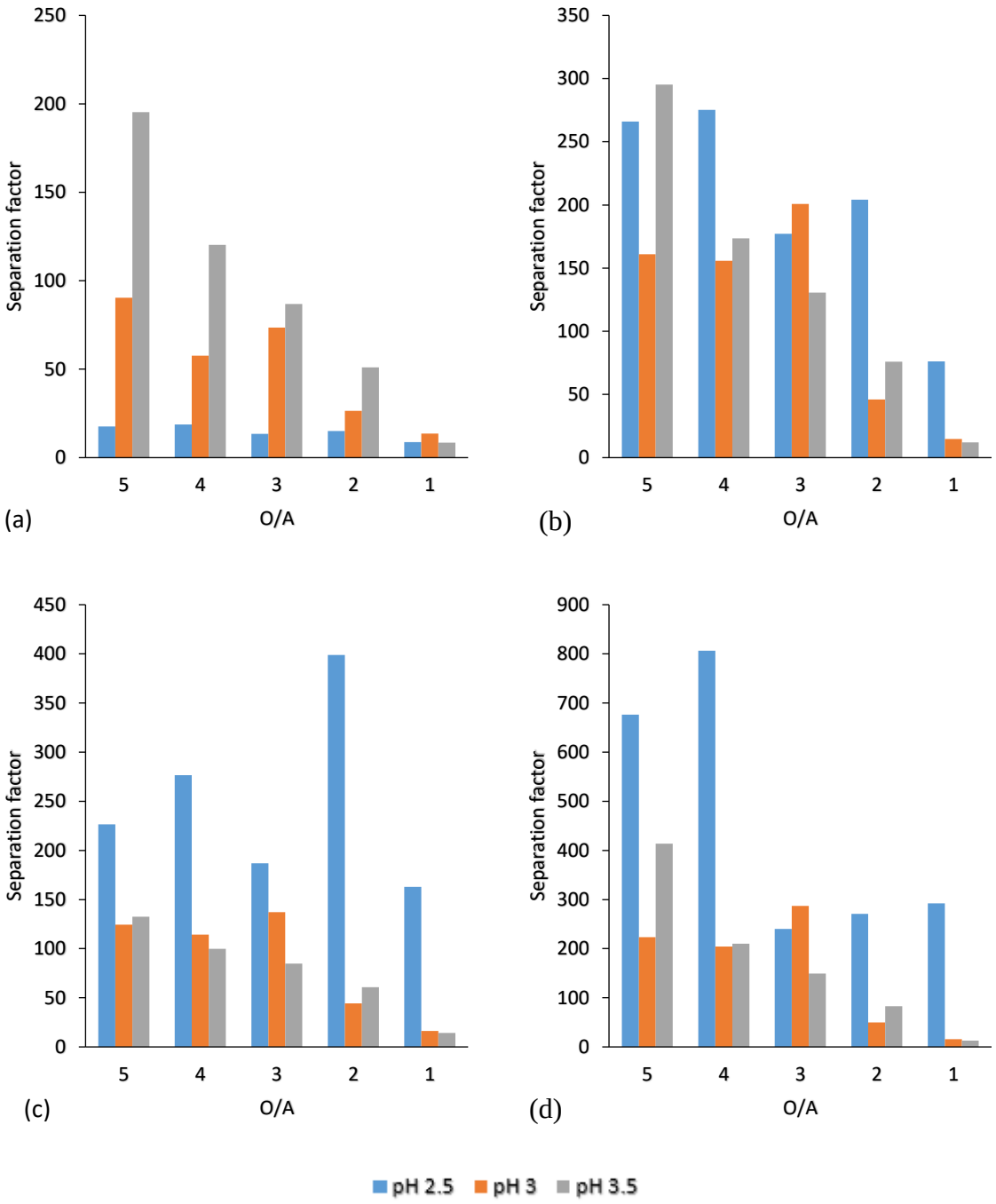

Figure 27: (a) Mn/Al, (b) Mn/Co, (c) Mn/Li and (d) Mn/Ni separation factors with 10% v/v D2EHPA

Mn/Li separation factors are considered next. Comparing the Mn/Li separation factors from Figures 27 (c) and 28 (c), it can be seen that the highest separation factors were obtained with 10% v/v D2EHPA at pH 2.5. The highest separation was at O/A ratio 2, but the disadvantage of this O/A ratio was that it yielded lower Mn/Co (204) and Mn/Ni (271) separation factors.

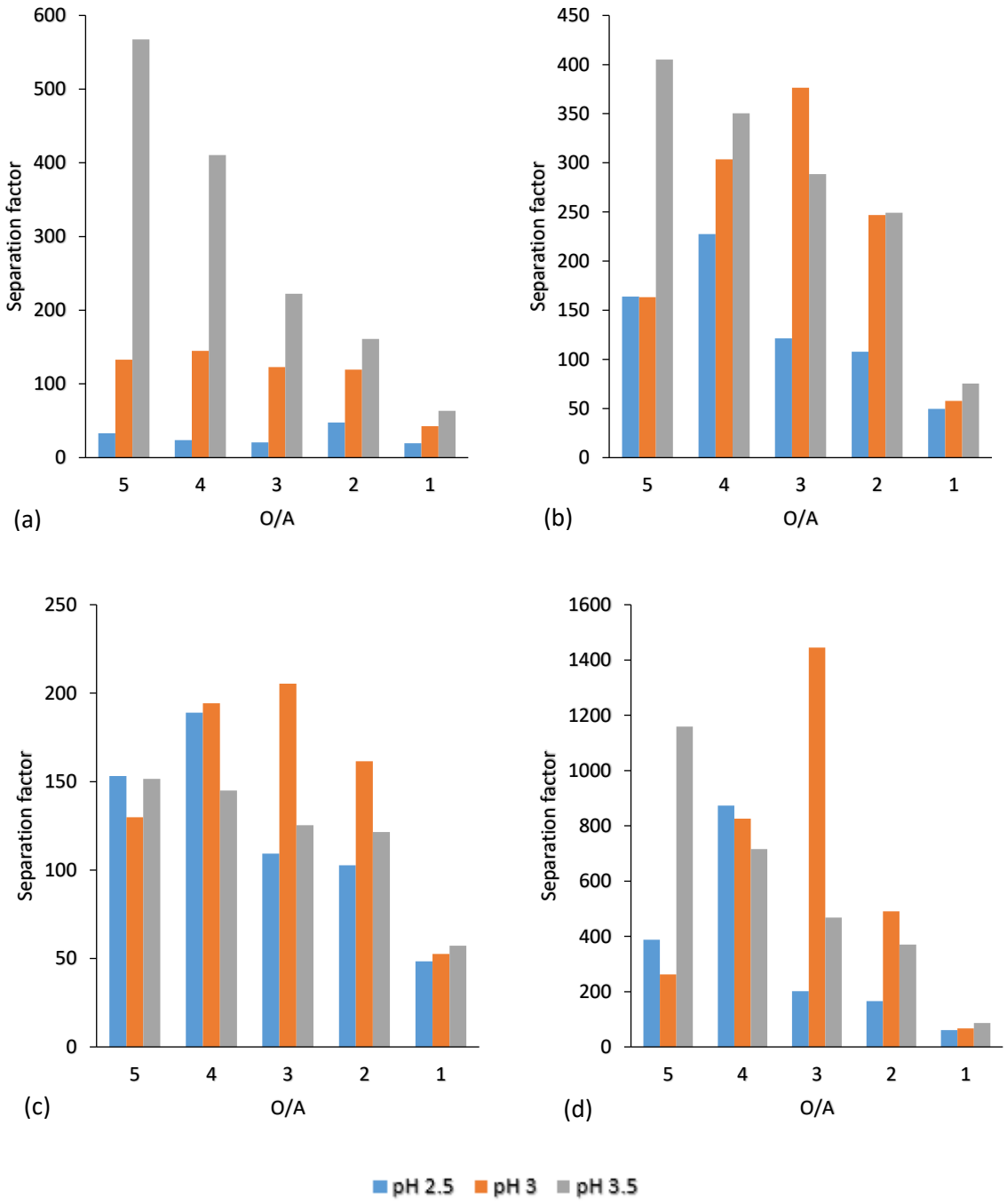

Figure 28: (a) Mn/Al, (b) Mn/Co, (c) Mn/Li and (d) Mn/Ni separation factors with 20% v/v D2EHPA

The second highest Mn/Li separation factor was 276, at O/A ratio 4 with 91% Mn extraction in one stage. This was followed by 227 at O/A ratio 5, with 94% Mn extraction in one stage. 10% v/v D2EHPA, at pH 2.5 and O/A ratio 4 and 5 were considered as potential suitable conditions for Mn-Li separation since they yielded the best results

Figure 28 (d) shows the Mn/Ni separation factors with 20% v/v D2EHPA. For Mn-Ni separation, the highest separation factors were obtained with 20% v/v D2EHPA. The highest one (1445) was at pH 3 and O/A ratio 3, while the second highest (1159) was at pH 3.5 and O/A ratio 5, as shown in Figure 28 (d). However, under these conditions, the Mn/Li separation factors were lower than those at pH 2.5 and 10% v/v D2EHPA. For example, at pH 3 and O/A ratio 3, the Mn/Li separation factor was 205 and at pH 3.5 and O/A ratio 5, it was 150. These are lower than the 276 and 227 separation factors at O/A ratio 4 and 5, respectively, at pH 2.5, with 10% v/v D2EHPA.

10% v/v D2EHPA yielded higher Mn/Co and Mn/Li separation factors than 20% v/v D2EHPA at pH 2.5 and O/A ratio 4. The Mn/Ni separation factor was 676 with 10% v/v D2EHPA at O/A ratio 5 and pH 2.5. From this, it was concluded that 10% v/v D2EHPA, at pH 2.5 and O/A ratio 4 and 5 were suitable conditions for Mn and Al extraction from solution since they gave good Mn/Ni, Mn/Co and Mn/Li separation with reasonably high Al extraction. A data table for the separation factors is provided in Appendix C (Table 40).

For these reasons the most suitable conditions for the separation of Mn and Al from the rest of the metals in solution were selected as: pH 2.5 with 10% v/v D2EHPA at O/A ratio 5. An O/A ratio of 5 was selected since it yielded relatively higher Mn (94%) and Al (47%) extraction in one stage.

4.3.4 Graphical analysis

The McCabe-Thiele method was used to estimate the theoretical number of equilibrium stages required for complete Mn extraction from the solution. It was applied to data from the optimum conditions that were selected from the previous section (pH 2.5, O/A ratio 5, 10% v/v D2EHPA), where there was 94% Mn and 47% Al extraction, with 7% Co, 9% Li, 3% Ni and 4% Cu co-extraction. The McCabe-Thiele graph for Mn extraction at these conditions is shown in Figure 29. From the McCabe-Thiele diagram, it can be seen that 2 equilibrium stages are required to extract more than 99% Mn.

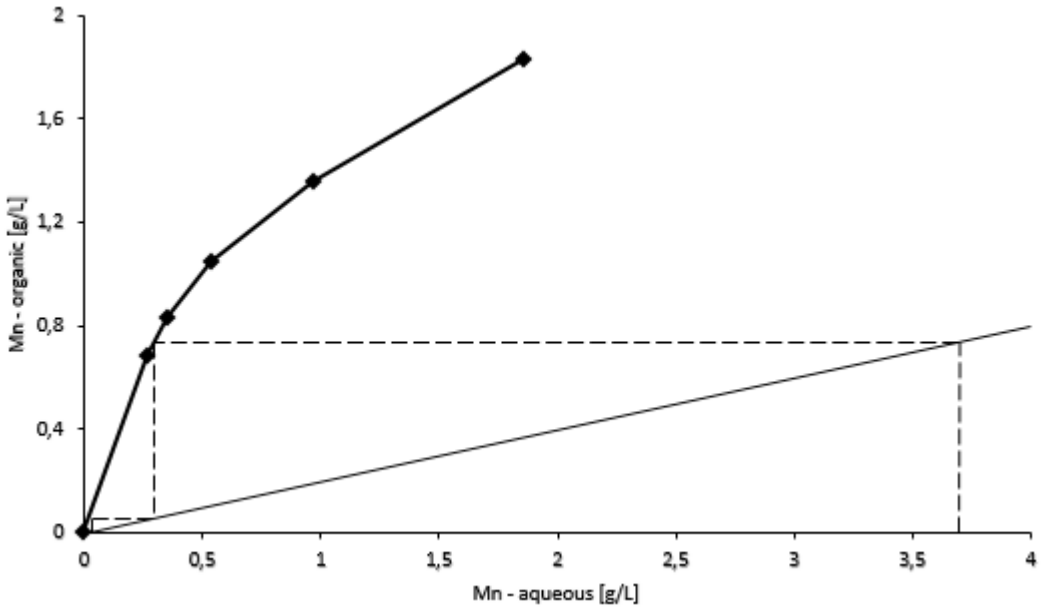

Figure 29: McCabe-Thiele for Mn extraction with 20% v/v D2EHPA at pH 2.5 and O/A ratio 5

4.3.5 Repeatability

Equation 74, adapted from Measey *et al.*, 2003 was used to quantify the repeatability of the solvent extraction tests.

$$r = \frac{MS_{between} - MS_{within}}{MS_{between} + (n-1)MS_{within}} \quad [74]$$

Where $MS_{between}$ is the mean square between groups (the 5 runs carried out at pH 2.5 and 10% v/v D2EHPA), MS_{within} is the mean square within groups (within each run/3 replicates), n is the number of replicates and r is the repeatability.

The repeatability is a fraction between 0 and 1, which expresses the variation that arises from the differences between groups and not from within groups. If there is consistency in the average group, the variation within the group will be low, this means that the ratio of variation between groups to variation within groups, which is the repeatability, will be high (Measey *et al.*, 2003).

To test for repeatability of the solvent extraction tests, the tests with 10% v/v D2EHPA at pH 2.5 were carried out in triplicates. Table 19 shows data on the concentration of metals in aqueous solution after extraction, from the triplicate tests.

Table 19: Data on the concentration of metals in aqueous solution after extraction with 10% v/v D2EHPA at pH 2.5

		Concentration in aqueous solution after extraction (g/L)				
	O/A ratio	**Original**	**Repeat 1**	**Repeat 2**	**Average**	**Standard deviation**
Al	1	0.1917	0.1948	0.1933	0.1933	0.0016
	2	0.1798	0.1836	0.1832	0.1822	0.0021
	3	0.1470	0.1476	0.1473	0.1473	0.0003
	4	0.1395	0.1458	0.1445	0.1433	0.0033
	5	0.1139	0.1151	0.1155	0.1148	0.0009
Co	1	4.1587	4.1619	4.1529	4.1578	0.0046
	2	4.1568	4.1592	4.1573	4.1578	0.0012
	3	4.0737	4.0835	4.0837	4.0803	0.0057
	4	4.0667	4.0701	4.0069	4.0479	0.0356
	5	3.9824	3.9799	3.9155	3.9593	0.0379
Li	1	1.4149	1.4191	1.4137	1.4159	0.0028
	2	1.4137	1.4040	1.4041	1.4073	0.0056
	3	1.3785	1.3881	1.3732	1.3800	0.0076
	4	1.3739	1.3769	1.3572	1.3694	0.0106
	5	1.3324	1.3325	1.3118	1.3256	0.0120
Mn	1	1.8602	1.8577	1.8123	1.8434	0.0270
	2	0.9724	0.9715	0.9531	0.9657	0.0109
	3	0.5362	0.5159	0.5160	0.5227	0.0117
	4	0.3542	0.3339	0.3340	0.3407	0.0117
	5	0.2638	0.2136	0.2230	0.2335	0.0267
Ni	1	4.9738	4.9625	4.9695	4.9686	0.0057
	2	4.9390	4.9419	4.9359	4.9389	0.0030
	3	4.8668	4.8717	4.8626	4.8670	0.0046
	4	4.9300	4.9286	4.9200	4.9262	0.0054
	5	4.8792	4.8803	4.8887	4.8827	0.0052

For each metal, single factor ANOVA was done on the data (metal concentration in aqueous phase after extraction) displayed in Table 19 and it generated the means square values that were used for calculating the repeatability. The repeatability values, as calculated by equation 74, are shown in Table 20. According to Table 20, Mn (0.998) extraction has the highest repeatability, followed by Al (0.996), Ni (0.986), Li (0.947) and then Co (0.924). In all five instances, the repeatability can be considered as being very high.

Table 20: Repeatability values for extraction with 10% v/v D2EHPA at pH 2.5

		Between groups	**Within groups**
Al	Mean square	0.003	3.8×10^{-6}
	n	3	
	r	0.996	
Co	Mean square	0.021	0.00055
	n	3	
	r	0.924	
Li	Mean square	0.0038	7×10^{-5}
	n	3	
	r	0.947	
Mn	Mean square	1.3	0.0004
	n	3	
	r	0.998	
Ni	Mean square	0.0052	2.4×10^{-5}
	n	3	
	r	0.986	

To further demonstrate the repeatability of the solvent extraction tests, the isotherms for Mn extraction at pH 2.5 and 10% v/v D2EHPA were reconstructed. Figure 30 shows the replicated isotherms for Mn extraction at the aforementioned conditions. The Mn extraction isotherms are almost identical, which shows high repeatability of the solvent extraction tests.

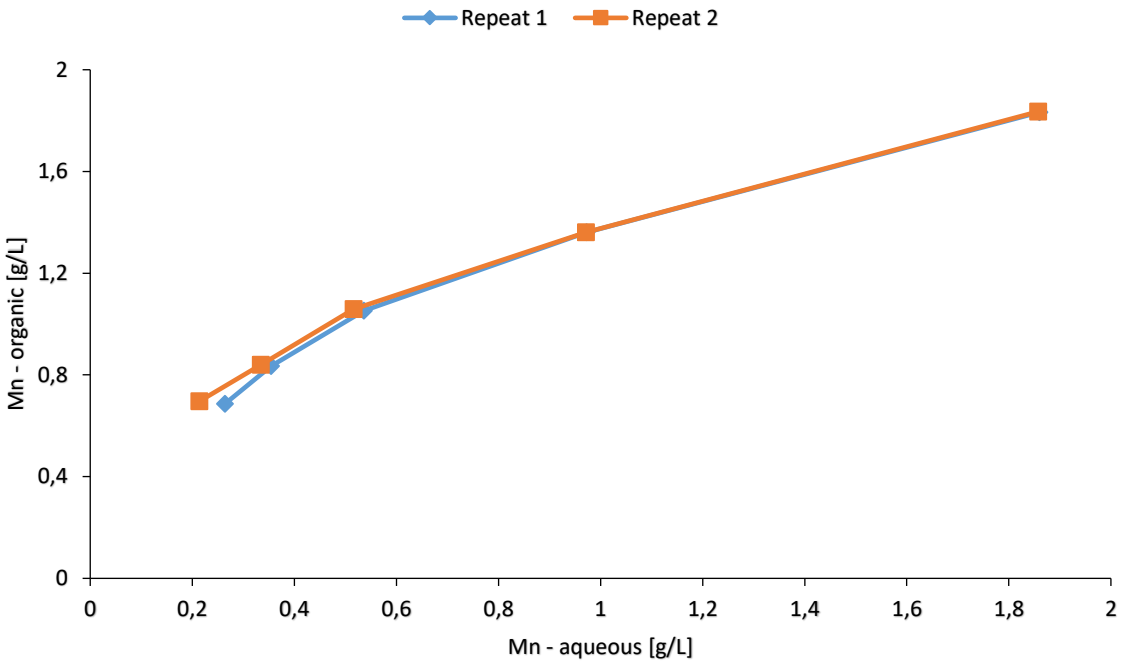

Figure 30: Replicated isotherm for Mn extraction at pH 2.5 with 10% v/v D2EHPA

4.3.6 Stripping

Stripping tests were carried out to investigate the effect of A/O ratio and H_2SO_4 concentration on stripping and the best stripping results were obtained using 0.5M H_2SO_4 at A/O ratio 3. Figure 31 shows the stripping results with 0.5M H_2SO_4. More data on the stripping tests is presented in Appendix D, Tables 41 and 42. At 0.5M acid concentration and A/O ratio 3, 99 $\pm$ 0.21% Mn stripping was achieved, while 99 $\pm$ 0.46% Li, 98 $\pm$ 1.60% Co, 4 $\pm$ 2.67% Al and 14 $\pm$ 1.68% Ni were also stripped. A 93% pure Mn solution was produced, whose concentration was as follows: Al (0.05 mg/L), Co (3.57 mg/L), Cu (0.03 mg/L), Li (1.79 mg/L), Mn (78.35 mg/L) and Ni (0.63 mg/L).

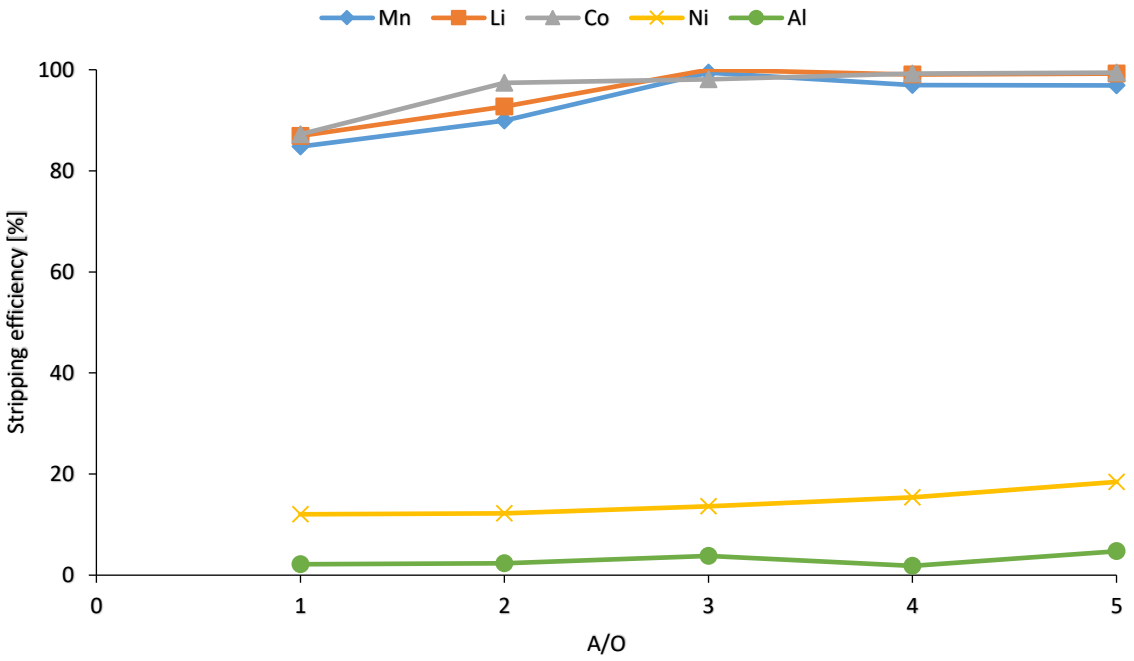

Figure 31: Stripping tests with 0.5M Sulphuric acid

4.5 Chemical precipitation

The aim of the first set of phosphate precipitation tests was to investigate the effect of temperature on solubility of phosphates of the metals in the pregnant leach solution. Figure 32 shows metal recovery through precipitation as phosphates, at different temperatures. The solubilities of $Co_3(PO_4)_2$, $Mn_3(PO_4)_2$ and $Ni_3(PO_4)_2$ are not affected by temperature changes, in the range 50℃-80℃. This is to be expected since these phosphates are classified as being insoluble in aqueous solutions. The solubility constants of $Co_3(PO_4)_2$, Li_3PO_4, $Mn_3(PO_4)_2$ and $Ni_3(PO_4)_2$ in aqueous solutions at 25℃ are 2.05×10^{-35}, 2.37×10^{-4}, 3.57×10^{-36} and 4.74×10^{-32}, respectively (HSU, 1968). It should be noted that in this context, metal extraction refers to precipitation as metal carbonate or phosphate. Over 97% Co, 99% Mn and 98% Ni are recovered as phosphate precipitates at all four temperatures. Although $AlPO_4$ is classified as being water insoluble (Ksp at 25℃ = 9.84×10^{-21}) (HSU, 1968), the results seem to indicate that its solubility increases with an increase in temperature.

Li_3PO_4 precipitation increases with an increase in temperature. About 4% Li is recovered at 50℃, 8% at 60℃, 26% at 70℃ and at 80℃, about 72% Li is precipitated. There is no data from

literature on the solubility of Li_3PO_4 at different temperatures, except at 20°C, where it is 0.039 g/100 m/L, according to Chen & Zhou, 2014.

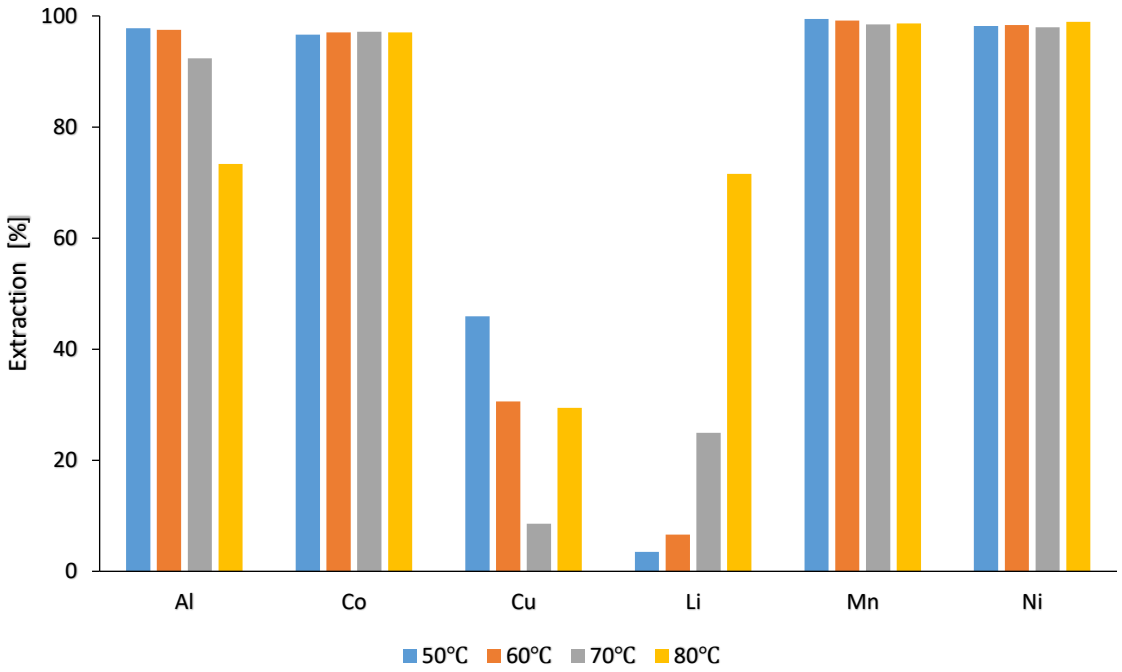

Figure 32: Metal phosphate precipitation tests on PLS at different temperatures

From Figure 32, it appears as if the solubility of Li_3PO_4 decreases with an increase in temperature. It is known that the solubility of Li_2CO_4 in aqueous solutions decreases with an increase in temperature (1.54 g/100mL at 0°C; 1.43 g/100mL at 10°C; 1.29 g/100mL at 25°C; 1.08 g/100mL at 40°C and 0.69 g/100mL at 100°C) (Nguyen *et al.*, 2014). Since Li_3PO_4 and Li_2CO_4 are both Li salts, it can be expected that Li_3PO_4 exhibits the same trend as Li_2CO_4 solubility in aqueous solution. This means that Li can be separated from the rest of the metals in the pregnant leach solution using these differences in the solubilities of their phosphate salts at different temperatures. If Mn and Al can be extracted by solvent extraction, Co and Ni can be precipitated as phosphates at a lower temperature (50°C), and the Li can be recovered using a second precipitation stage at a higher temperature (80°C).

To investigate this proposed separation order, Mn and Al extraction with D2EHPA was carried out using the optimum conditions determined by the solvent extraction tests, where after phosphate precipitation at 50°C was performed. The results are shown in Figure 33. Over 98% Co and Ni extraction is obtained, with less than 4% Li extraction.

This is quite similar to what is presented in Figure 32, at 50℃. Since 90% Al and 99% Mn are extracted in the solvent extraction step, the Co-Ni product contains small amounts of Al Li, Mn and Cu. The purity and composition of this product will be discussed in the mass balance section. In Figures 33-37, the amounts of metal recovered are expressed as a percentage of the amount of metal in solution after Mn and Al extraction with D2EHPA.

Subsequent phosphate precipitation at 80℃ was performed and the results are shown in Figure 34. About 75% Li is extracted and this is comparable to the recoveries obtained from precipitation at 80℃, from Figure 32. Only about 2% Co, 1% Mn and less than 1% Ni and Al are extracted. Most of the Al, Co and Ni is extracted in the preceding stages and what is extracted at this stage are the remaining small quantities. Although it is indicated that about 22% of Cu was extracted, it can be neglected since Cu is present in the solution in very low concentrations, and about 75% of it has already been extracted in the previous precipitation stage. This results in a high purity lithium product, the composition of which will be discussed in the mass balance section.

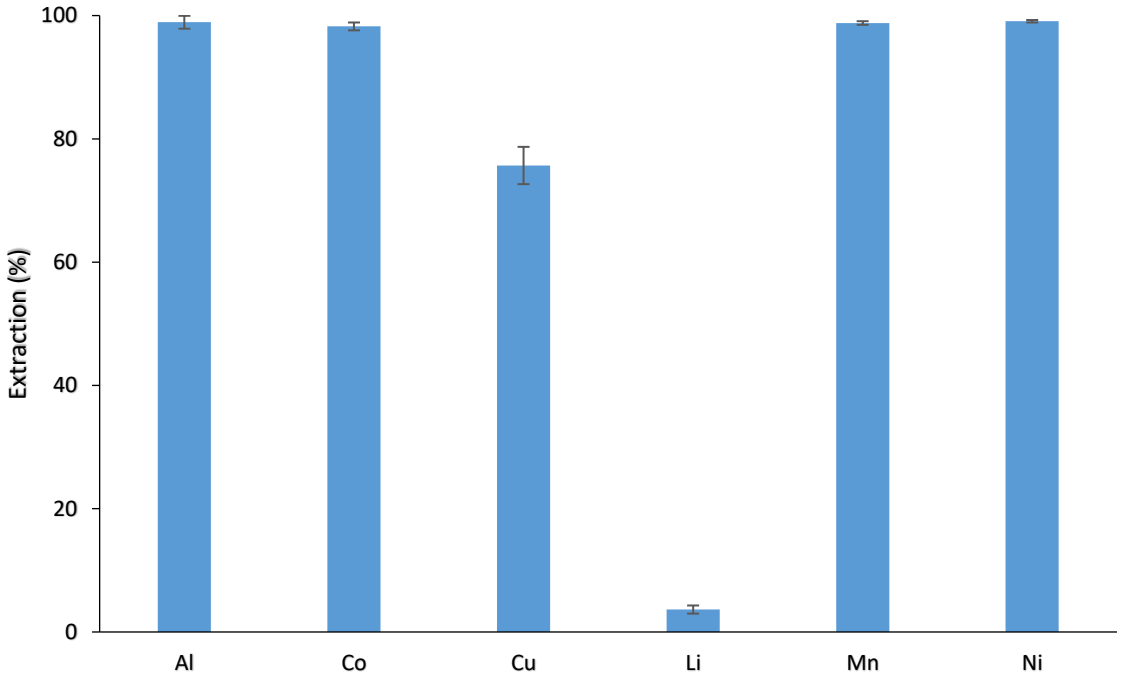

Figure 33: Phosphate precipitation at 50℃ after solvent extraction with D2EHPA

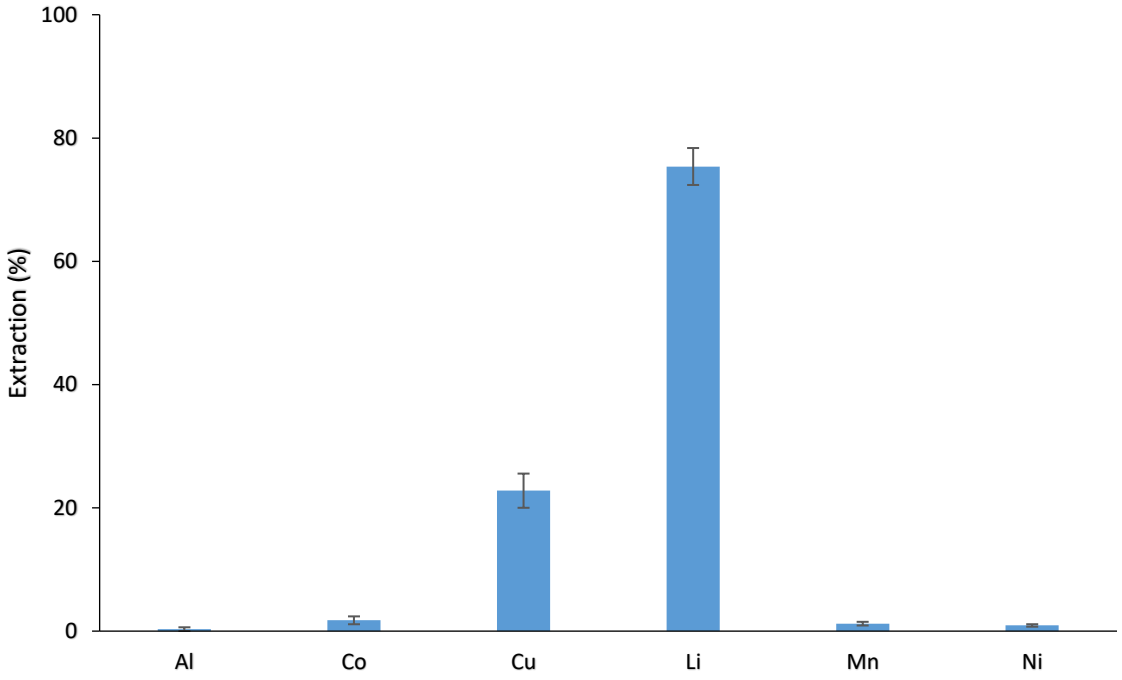

Figure 34: Subsequent phosphate precipitation at 80 ℃ after solvent extraction with D2EHPA and phosphate precipitation at 50 ℃

Na_2CO_3 was also considered as an alternative precipitating agent in this separation process. After Mn and Al extraction with D2EHPA, subsequent carbonate precipitation tests were carried out at room temperature and the results are shown in Figure 35. About 76% Al, 48% Co, 80% Mn and 70% Ni recoveries are obtained. Less than 2% Li is extracted, as shown in Figure 35.

The low Li recoveries may be attributed to the higher Li_2CO_4 solubility in aqueous solution at low temperatures, which decrease with increase in temperature (1.54 g/100mL at 0℃, 1.43 g/100mL at 10℃, 1.29 g/100mL at 25℃, 1.08 g/100mL at 40℃ and 0.69 g/100mL at 100℃). If the solubility is high at low temperatures, then the degree of precipitation is low.

This was followed by phosphate precipitation at 80℃, and the results are shown in Figure 36. Over 97% Co, Ni and nearly 100% Al are recovered as phosphate precipitates. This product is a mixture of Li, Ni and Co, with a relatively higher Co and Ni content, since their recoveries from the preceding carbonate precipitation stage are low.

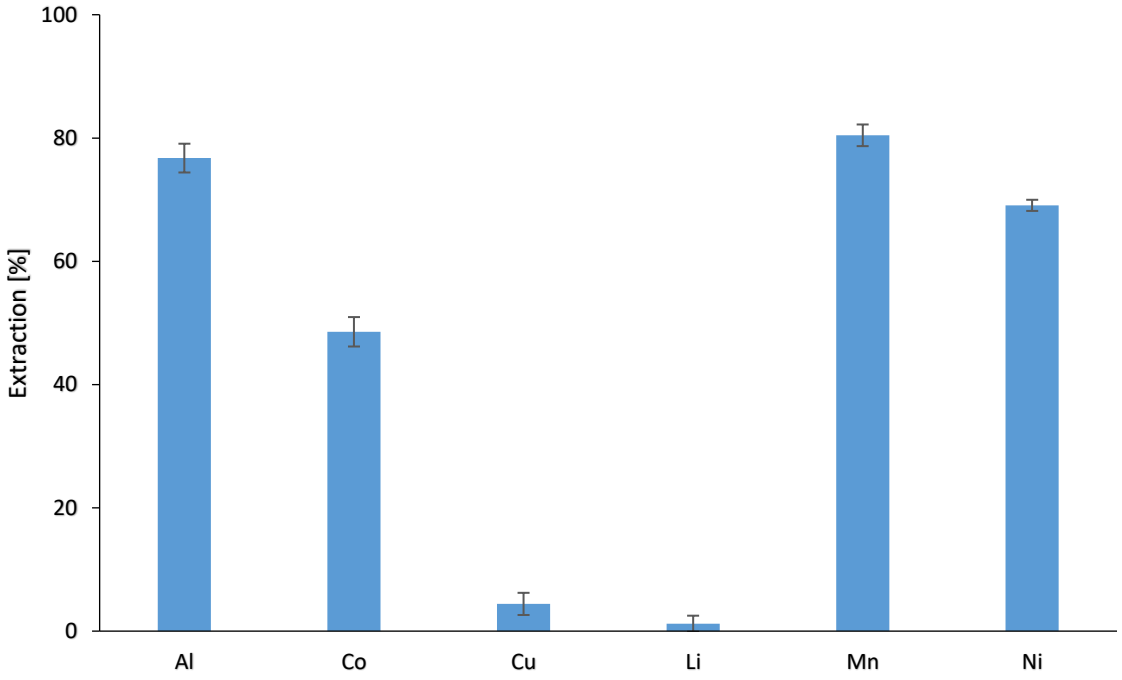

Figure 35: Carbonate precipitation after solvent extraction with D2EHPA

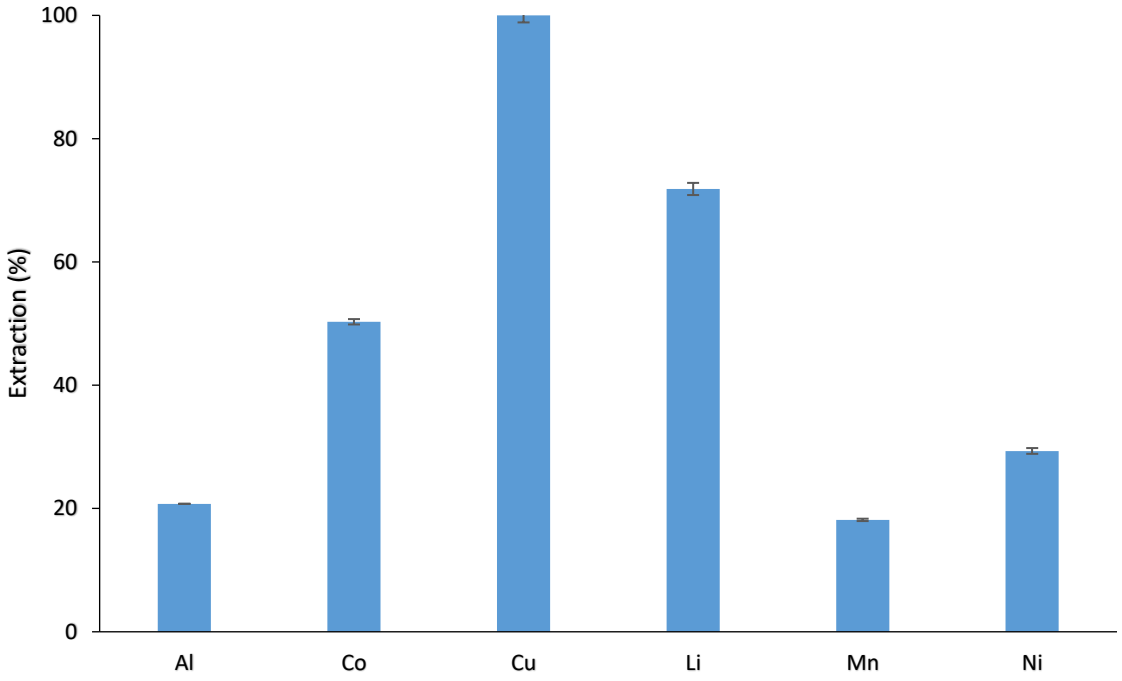

Figure 36: Phosphate precipitation at 80 after solvent extraction with D2EHPA and carbonate precipitation at room temperature

Carbonate precipitation at room temperature and phosphate precipitation at 50℃, were meant to serve the same purpose, which is to selectively precipitate out all the metals in solution and leave behind Li. The Li was to be recovered in a second precipitation stage to get a cleaner Li product. Comparing the recoveries from Figures 33 and 35, phosphate precipitation yields over 98% Al, Co, Mn and Ni recoveries, while 76% Al, 48% Co and 70% Ni recoveries are obtained from carbonate precipitation. This suggests that it is more efficient to recover metals as phosphates than as carbonates from citrate solutions. Chen & Zhou, 2014 reported that if carbonate is used to precipitate metals from citrate solutions, about 70-80% metal recoveries are obtained, but when phosphate is used, 90% metal recoveries are obtained. The first equilibrium dissociation constant (k_1) of phosphoric acid (7.5×10^{-3}) is higher than those of both citric acid (7.4×10^{-4}) and carbonic acid (4.2×10^{-7}), but the k_1 for citric acid is greater than the one for carbonic acid, therefore metal carbonate precipitation from a citrate solution is less efficient than phosphate precipitation, hence NaH_2PO_4 is the more suitable precipitating agent than Na_2CO_3 (Chen & Zhou, 2014).

Phosphate precipitation at 80℃ after Mn and Al extraction with D2EHPA was also investigated. Mn and Al extraction with D2EHPA was carried, followed by phosphate precipitation at 80℃. Figure 37 shows the results of metal precipitation at 80℃ after Mn and Al extraction with D2EHPA. Over 99% Al, Co, Mn and Ni recoveries are achieved, while 75% Li is extracted. Li extraction is significantly high due to the lower solubility of Li_3PO_4 at the high precipitation temperature. Although the results indicate that over 99% Al and Mn are extracted, it should be noted that their concentrations are very low in the feed solution to this particular precipitation step, since most of it is recovered during solvent extraction. This results in a more defined Co, Li and Ni product, whose composition is discussed in the mass balance.

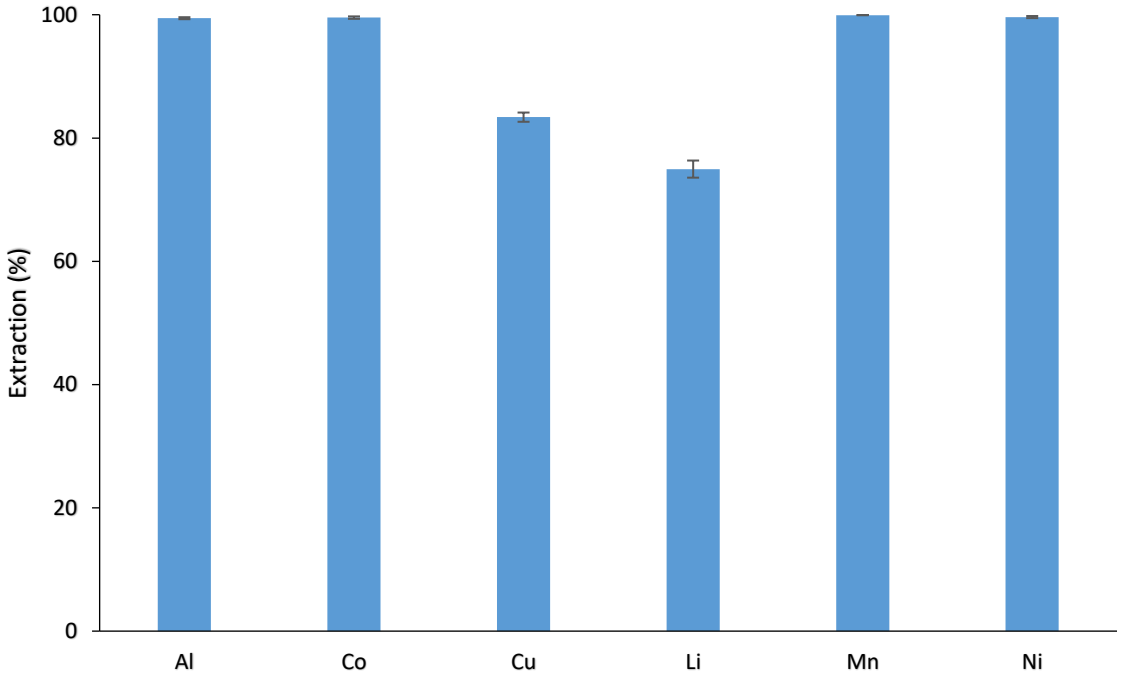

Figure 37: Phosphate precipitation at 80℃ after solvent extraction with D2EHPA

Chapter 5: Mass balance

Process routes from 5 scenarios were experimentally investigated. In order to compare the different routes and select the most suitable flowsheet, a theoretical mass balance for each scenario was constructed using the results from the experimental tests.

The leaching of all metals was based on the optimum leaching conditions obtained from the leaching tests (Temperature = 95℃, citric acid concentration = 1.5M, H_2O_2 concentration = 2% v/v and pulp density = 20 g/L). The separation of Mn and Al from the rest of the elements in the pregnant leach solution was also based on optimum conditions from the solvent extraction tests (O/A ratio = 5, D2EHPA concentration = 10% v/v, pH = 2.5, agitation speed = 300 rpm and at room temperature). Leaching of Al and Cu and Mn was not discussed in Chapter 4 but it was quantified during the leaching experiments.

Listed below are the assumptions that were made when the mass balance was performed:

1. The composition of the cathodic material/feed to the leaching process remained constant.
2. The composition of the pregnant leach solution fed to the metal recovery circuit remained constant.
3. Recovery of all the elements from leaching, solvent extraction and chemical precipitation was based on experimental results.
4. An overall run time of 95% was assumed for the theoretical plant.
5. A dry feed throughput of 20 t/h was assigned to the theoretical plant.

To construct the mass balance, for each scenario, the cathodic material feed mass was input together with the feed composition. The elemental masses in the feed were then calculated using the feed composition and total mass. The masses of metals that report to each product stream were then calculated using the feed elemental masses and recoveries from the experiments. Determination of the mass of tailings was based on a balance of the entire system for each scenario.

$$\text{Mass}_{(\text{Tailings})} = \text{Mass}_{(\text{Solid feed})} - \text{Total mass}_{(\text{ metal mass that reports to all product streams})}$$

Table 21 summarizes the products from each flowsheet, together with the compositions of these products. Table 22 shows the total metal recoveries in each product stream for all the scenarios, in terms of the initial solid feed.

Table 21: Summary of the products from all scenarios and their compositions

Scenario	Product description	Al	Co	Cu	Li	Mn	Ni
1	Al, Co, Li, Mn, Ni phosphate (wt. %)	1.06	29.38	0.04	7.47	25.19	36.87
2	Al, Co, Mn, Ni phosphates (wt. %)	1.53	31.59	0.07	0.33	26.94	39.54
	Li phosphate (wt. %)	0.31	10.39	0.21	76.15	6.17	6.75
3	Mn solution (mg/L)	0.05	3.71	0.02	1.83	80.01	0.64
	Co, Li, Ni phosphates (wt. %)	0.22	38.42	0.11	9.54	0.17	51.54
4	Mn solution (mg/L)	0.05	3.71	0.02	1.83	80.01	0.64
	Co, Ni phosphates (wt. %)	0.24	42.07	0.11	0.51	0.18	56.87
	Li phosphate (wt. %)	0.01	6.29	0.29	88.98	0.02	4.42
5	Mn solution (mg/L)	0.05	3.71	0.02	1.83	80.01	0.64
	Co, Ni phosphates (wt. %)	0.31	34.11	0.01	0.28	0.25	65.04
	Li phosphate (wt. %)	0.10	44.17	0.32	20.80	0.07	34.54

Scenario 1 involves direct phosphate precipitation of metals from the pregnant leach solution. The process route is simple and has relatively lower costs. The main disadvantage is that there is no metal separation, Co, Li, Mn and Ni are recovered as phosphates in one compound. Co (29 wt. %), Mn (25 wt. %) and Ni (37 wt. %) are the main constituents of the product, with about 7 wt. % Li and 1 wt. % Al, as shown in Table 21. It can be sold to battery manufacturers to be used as raw material for further battery manufacturing. The flowsheet and stream table for scenario 1 are presented in Figure 42 and Table 46, respectively, in Appendix F.

Table 22: Total metal recoveries in each stream from all scenarios

		Recovery (%)					
Scenario	**Product description**	**Al**	**Co**	**Cu**	**Li**	**Mn**	**Ni**
1	Al, Co, Li, Mn, Ni phosphate	64.25	91.44	28.79	68.82	92.63	97.51
2	Al, Co, Mn, Ni phosphates	85.69	90.91	50.28	2.85	91.63	96.73
	Li phosphate	1.90	3.24	17.55	70.30	2.27	1.79
3	Mn solution	3.00	12.80	9.20	16.65	92.77	0.79
	Co, Li, Ni phosphates	9.07	81.01	63.10	59.57	0.42	92.37
4	Mn solution	3.00	12.80	9.20	16.65	92.77	0.79
	Co, Ni phosphates	9.02	79.96	57.27	2.89	0.41	91.87
	Li phosphate	0.03	1.43	17.24	59.91	0.01	0.85
5	Mn solution	3.00	12.80	9.20	16.65	92.77	0.79
	Co, Ni phosphates	7.00	39.53	3.34	0.97	0.34	64.05
	Li phosphate	1.89	40.93	77.20	57.09	0.08	27.20

In scenario 2, there are two stages of metal phosphate precipitation, one at 50°C followed by another one at 80°C. There are two product streams, the first is a Co, Mn and Ni compound (32 wt. % Co, 27 wt. % Mn and 40 wt. % Ni), while the second one is a Li compound (76% purity) with 10 wt. %, 6 wt. % and 7 wt. % Co, Mn and Ni, respectively, as shown in Table 21. This is also a simple and relatively low cost process, as evidenced by the flowsheet in Figure 43, Appendix F. Co, Mn and Ni are recovered as one compound, which can be sold to battery manufacturers. The advantage that it has over scenario 1 is the production of a separate and cleaner Li product, with lower Al content (0.31 wt. %), as shown in Table 21 and it fetches a

higher price on the market. The Li product can also be sold to battery manufacturers. The mass balance for this scenario is shown in Table 47, Appendix F.

In scenario 3, there is extraction of Mn and Al with D2EHPA, followed by phosphate precipitation of the remaining metals at 80℃. It has more complexity compared to scenarios 1 and 2, due to the solvent extraction and stripping steps. There are two valuable product streams, a Mn strip solution of 93% purity and a Co, Li and Ni phosphate compound with 38 wt. % Co, 10 wt. % Li and 52 wt. % Ni, as shown in Table 21. The Co-Li-Ni phosphate compound can also be sold to battery manufacturers. It has an appreciably lower Al content (0.22 wt. %), which makes it ideal for use as raw material in battery manufacturing. A Mn solution is generated, and the Mn can be recovered by phosphate precipitation to produce a Mn product with 93% purity. Comparing scenarios 2 and 3, scenario 2 is a better option than 3 because it produces a separate Li product with a considerably high purity (76 wt. % Li), and also due to its simplicity and lower cost. The flowsheet and stream table for scenario 3 are presented in Figure 44 and Table 48, respectively, in Appendix F.

In scenario 4 there is Mn and Al extraction with D2EHPA, followed by phosphate precipitation at 50℃ (targeting Co and Ni), then subsequent phosphate precipitation at 80℃ (targeting Li). The process route has more complexity since it has three valuable product streams. Scenario 5 involves Mn and Al extraction with D2EHPA followed by carbonate precipitation at room temperature (targeting Co and Ni), then subsequent phosphate precipitation at 80 ℃ (targeting Li).

Comparing scenarios 4 and 5, it can be seen that they are similar and have the same level of sophistication. This is shown by their associated flowsheets and mass balances, presented in Appendix F. Figure 45 and Table 49 show the flowsheet and mass balance, respectively, for scenario 4. Figure 46 and Table 50 show the flowsheet and mass balance, respectively, for scenario 5. However, in scenario 5 there is poor precipitation of Co and Ni in the carbonate precipitation stage. Although less than 1% Li is extracted in the carbonate precipitation stage, there is low Co and Ni extraction (48% Co and 70% Ni). This results in undesirably high Co and Ni contents and the remaining solution, which is carried forward to the phosphate precipitation at 80℃ stage. This results in a low purity Li product with a composition of 44 wt. % Co, 21 wt. % Li and 35 wt. % Ni, as shown in Table 21.

From Table 21, the flowsheet in scenario 4 is the most efficient one and produces the best results. What makes it the best choice are its unique metal separation capabilities, with three clearly defined valuable product streams: a Mn solution (93% purity), a Co-Ni product (0.24 wt. % Al, 42 wt. % Co, 0.11 wt. % Cu, 0.51 wt. % Li, 0.2 wt. % Mn and 57 wt. % Ni), and a Li product with 89 wt. % Li and other elements (0.01 wt. % Al, 6 wt. % Co, 0.3 wt. % Cu, 0.2 wt. % Mn and 4 wt. % Ni).

Chapter 6: Conclusions and recommendations

6.1 Conclusions

From the experimental results it was concluded that organic acids are effective leaching reagents for Co, Li and Ni recovery from LIB cathodic active material. Using 1.5M citric acid with 2% v/v H_2O_2 at 95℃ and 20 g/L pulp density, 95% Co, 96% Li and 99% Ni were recovered after 30 minutes. With 1M DL-Malic acid in the presence of 2% v/v H_2O_2 at 95℃ and 20 g/L pulp density, 99% Co, 96% Li and 99% Ni were recovered within 30 minutes.

Both citric acid and DL-malic acid leaching processes were affected by H_2O_2 addition. There was significant increase in leaching rate when H_2O_2 was added. This was due to the reduction of Co^{3+} to the more soluble Co^{2+} by H_2O_2, during $LiNi_{0.05}Mn_{0.05}Co_{0.9}O_2$ dissolution, which speeded up the leaching kinetics. It was concluded that H_2O_2 plays a key role and should be included in the leaching process. An increase in the leaching rate was observed when temperature was increased from 30℃ to 95℃, for both citric acid and DL-malic acid, with the fastest leaching kinetics being obtained at 95℃ (over 95% metal recoveries within 30 minutes). Increase in temperature also caused an increase in the leaching extent because the solubility of the metal citrate and malate complexes increases with an increase in temperature. It was therefore concluded that 95℃ was the most suitable leaching temperature.

With citric acid, there was an increase in leaching rate when the acid content was increased from 1M to 1.5M, and the fastest leaching kinetics were obtained with 1.5M citric acid. On the other hand, DL-malic acid concentration did not appear to have to have an effect on leaching kinetics in the range 1-1.5M. An increase in both citric acid and DL-malic acid concentration resulted in a slight decrease in the leaching extent and it could have been due to solubility loss. ANOVA was carried out and from the analysis it was determined that only temperature had a statistically significant effect on metal extraction.

Data from the leaching tests were fitted to three different kinetic models to determine the rate controlling mechanisms under different conditions. The results indicated that, for both acids, the leaching process is chemical reaction controlled at low temperatures (30℃). As the temperature is increased there is a shift in the rate limiting step and diffusion through a

product layer becomes rate limiting at higher temperatures (60°C). This is due to PTFE and PVDF binders coating the particle surfaces. They do not dissolve in acid, but remain behind to form an inert residue around the shrinking cathodic particles. The product layer is essentially carbon and fluorine.

The leaching performances of citric and DL-malic acid with regard to Li and Ni recoveries were similar, both achieving 96% Li and 99% Ni recoveries under optimum conditions. However, with regard to Co leaching, DL-malic acid was the superior leaching reagent, yielding 99% Co recovery (4% higher than citric acid). Industrial grade DL-malic acid costs almost twice as much as citric acid. Since citric acid is cheaper, it was concluded that it would be a better option for this process.

From the solvent extraction results it was concluded that separation of Mn and Al from a Co, Li and Ni citrate solution was possible. Using 10% v/v D2EHPA at pH 2.5, O/A ratio 5 and room temperature, 47% Al, 7% Co, 9% Li, 94% Mn and 3% Ni were extracted in one stage. The McCabe-Thiele method determined that two equilibrium stages are required to extract over 99% Mn. This was verified experimentally and 99% Mn and 89% Al were extracted, with 13% Co, 17% Li and 6% Ni co-extraction in two stages. This agreed with what had been predicted by the McCabe-Thiele method.

Phosphate precipitation tests revealed that the solubility of Li_3PO_4 decreases with an increase in temperature. When the temperature was varied from 50°C to 80°C, precipitation of Li as Li_3PO_4 increased from around 3% to 72%. However, solubility of the rest of the metal phosphates appeared not to be affected by temperature as there was consistent phosphate precipitation from 50°C to 80°C. It was therefore concluded that Li can be separated from the rest of the elements in two phosphate precipitation stages. The first stage at 50°C which targets all the metals except Li, followed by the second one at 80°C which targets Li.

Metal recovery from LIB citrate leach solutions is possible (flowsheet shown in Figure 45). The process flowsheet incorporates leaching with citric acid, Mn and Al extraction with D2EHPA from PLS after leaching, followed by phosphate precipitation at 50°C and subsequent phosphate precipitation at 80°C. This results in three valuable product streams, a Co-Ni product with composition :0.24 wt. % Al, 42 wt. % Co, 0.11 wt. % Cu, 0.51 wt. % Li, 0.2 wt. %

Mn and 57 wt. % Ni, an 89% pure Li product with composition: 0.01 wt. % Al, 6 wt. % Co, 0.3 wt. % Cu, 0.2 wt. % Mn and 4 wt. % Ni and a 93% pure Mn solution.

6.2 Recommendations

There is need for careful monitoring of the amount of Al in the feed to the leaching process. Al interferes with metal separation in downstream processes, due to the high co-extraction of Al during Co, Li and Ni extraction. In order to get high purity products in the final streams, Al content in the feed to the leaching circuit should be lowered as much as possible. Since the Al in the solid feed is residual Al from the NaOH leaching of cathodes step, increasing the residence time during the NaOH leaching step could possibly increase Al dissolution. This might slightly increases Co, Li and Ni losses to the NaOH leaching process, but it may be justified by the high purity products that will be obtained in downstream processes.

The potential use of higher pulp densities during leaching should also be considered as this will increase the economic feasibility of the process. An investigation should be done in order to understand metal behavior during leaching at higher solid contents.

Mn and Al extraction with D2EHPA needs to be optimized. Extraction at lower pH and extractant concentration should be investigated, with the aim of further lowering Co, Li and Ni co-extraction. At lower pH, total Mn and Al extraction could be achieved with minimal Co, Li and Ni co-extraction, using multistage extraction.

The precipitation of metals from solution as phosphates needs to be optimized. Since the experimental results have shown that the solubility of Li_3PO_4 decreases as temperature is increased from 50℃ to 80℃, the trend could possibly hold over a much wider temperature range. The amount of Li that is co-precipitated in the first precipitation stage in scenario 4 could be lowered if precipitation temperatures lower than 50℃ are used. Li recovery in the second precipitation stage could possibly be improved if the precipitation is carried out at higher temperature (>80℃).

Further study should also be done to investigate the effect of pH on Al, Co, Cu, Mn and Ni phosphate precipitation at different temperatures and understand the interactions between temperature and pH in metal phosphate precipitation.

7. References

Al-Thyabat, S., Nakamura, T., Shibata, E. & Iizuka, A. 2013. Adaptation of minerals processing operations for lithium-ion (LiBs) and nickel metal hydride (NiMH) batteries recycling: Critical review. *Minerals Engineering*. 45:4–17.

Bernardes, A.M., Espinosa, D.C.R. & Tenório, J.A.S. 2004. Recycling of batteries: A review of current processes and technologies. *Journal of Power Sources*. 130(1–2):291–298.

Bhattacharyya, A., Mohapatra, P.K. & Manchanda, V.K. 2007. Solvent extraction and extraction chromatographic separation of Am3+ and Eu3+ from nitrate medium using cyanexw® 301. *Solvent Extraction and Ion Exchange*. 25(1):27–39.

Brandl, H. & Faramarzi, M.A. 2006. Microbe-metal-interactions for the biotechnological treatment of metal-containing solid waste. *China Particuology*. 4(2):93–97.

Brisk, M.L. & McManamey, W. 1969. Liquid extraction of metals from sulphate solutions by alkylphosphoric acids. I. Equilibrium distributions of copper, cobalt and nickel with di-(2-ethyl hexyl) phosphoric acid. *Journal of Applied Chemistry*. 19:109.

Castillo, S., Ansart, F., Laberty-Robert, C. & Portal, J. 2002. Advances in the recovering of spent lithium battery compounds. *Journal of Power Sources*. 112(1):247–254.

Chen, W.-S. & Ho, H.-J. 2018. Recovery of Valuable Metals from Lithium-Ion Batteries NMC Cathode Waste Materials by Hydrometallurgical Methods. *Metals*. 8(5):321.

Chen, X. & Zhou, T. 2014. Hydrometallurgical process for the recovery of metal values from spent lithium-ion batteries in citric acid media. *Waste Management and Research*. 32(11):1083–1093.

Chen, X., Chen, Y., Zhou, T., Liu, D., Hu, H. & Fan, S. 2015. Hydrometallurgical recovery of metal values from sulfuric acid leaching liquor of spent lithium-ion batteries. *Waste Management*. 38(1):349–356.

Chen, X., Zhou, T., Kong, J., Fang, H. & Chen, Y. 2015. Separation and recovery of metal values from leach liquor of waste lithium nickel cobalt manganese oxide based

cathodes. *Separation and Purification Technology*. 141(February 2015):76–83.

Cheret, D. & Santen, S. 2011. *Patent No. US 7,169,206 B2*. United States Patent.

Conard, B.R. 1992. The role of hydrometallurgy in achieving sustainable development. *Hydrometallurgy*. 30(1–3):1–28.

Darvishi, D., Haghshenas, D.F., Alamdari, E.K., Sadrnezhaad, S.K. & Halali, M. 2005. Synergistic effect of Cyanex 272 and Cyanex 302 on separation of cobalt and nickel by D2EHPA. *Hydrometallurgy*. 77(3–4):227–238.

Devi, N.., Nathsarma, K.. & Chakravortty, V. 1998. Separation and recovery of cobalt(II) and nickel(II) from sulphate solutions using sodium salts of D2EHPA, PC 88A and Cyanex 272. *Hydrometallurgy*. 49(1–2):47–61.

European Li-Ion Battery Advanced Manufacturing for Electric Vehicles. 2014. *Li-ion Bateries Recycling. The batteries end of life*.

Ferreira, D.A., Martins, L., Prados, Z., Majuste, D. & Mansur, M.B. 2009. Hydrometallurgical separation of aluminium , cobalt , copper and lithium from spent Li-ion batteries. 187:238–246.

Flett, D.S. 2005. Solvent extraction in hydrometallurgy: The role of organophosphorus extractants. *Journal of Organometallic Chemistry*. 690(10):2426–2438.

Flett, D.S. & Spink, D.R. 1976. Solvent extraction of non-ferrous metals: A review 1972-1974. *Hydrometallurgy*. 1(3):207–240.

Foust, A., Wenzel, L., Maus, L., Clump, C. & Andersen, L. 2008. Sol. *Solvent extraction*.

Gaines, L. 2014. The future of automotive lithium-ion battery recycling: Charting a sustainable course. *Sustainable Materials and Technologies*. 1:2–7.

Gandhi, M.N., Deorkar, N. V. & Khopkar, S.M. 1993. Solvent extraction separation of cobalt(II) from nickel and other metals with cyanex 272. *Talanta*. 40(10):1535–1539.

Gao, W., Zhang, X., Zheng, X., Lin, X., Cao, H., Zhang, Y. & Sun, Z. 2017. Lithium Carbonate Recovery from Cathode Scrap of Spent Lithium- Ion Battery : A Closed-Loop Process.

Georgi-Maschler, T., Friedrich, B., Weyhe, R., Heegn, H. & Rutz, M. 2012. Development of a recycling process for Li-ion batteries. *Journal of Power Sources*. 207:173–182.

Golmohammadzadeh, R., Rashchi, F. & Vahidi, E. 2017. Recovery of lithium and cobalt from spent lithium-ion batteries using organic acids: Process optimization and kinetic aspects. *Waste Management*. 64:244–254.

Grimes, S.M., Donaldson, J.D., Chaudhary, A.J. & Ul Hassan, M. 2000. Simultaneous recovery of metals and destruction of organic species: Cobalt and phthalic acid. *Environmental Science and Technology*. 34(19):4128–4132.

Habashi, F. 1999. *a Textbook of Hydrometallurgy*. Second ed. Vol. 1. Québec, Canada: Métallurgie Extractive Québec.

Havlík, T. 2008. *Hydrometallurgy - Principles and applications*. Vol. 61. Cambridge, England: Woodhead Publishing Limited.

Hayashi, M., Takahashi, M. & Shodai, T. 2009. Preparation and electrochemical properties of pure lithium cobalt oxide films by electron cyclotron resonance sputtering. *Journal of Power Sources*. 189(1):416–422.

He, L.P., Sun, S.Y., Mu, Y.Y., Song, X.F. & Yu, J.G. 2017. Recovery of Lithium, Nickel, Cobalt, and Manganese from Spent Lithium-Ion Batteries Using l -Tartaric Acid as a Leachant. *ACS Sustainable Chemistry and Engineering*. 5(1):714–721.

HSU, P.H. 1968. Interaction Between Aluminum and Phosphate in Aqueous Solution. 115–127.

Jackson, E. 1986. *Hydrometallurgical Extraction and Reclamation*. West Sussex: Ellis Horwood Limited.

Jha, M.K., Kumari, A., Jha, A.K., Kumar, V., Hait, J. & Pandey, B.D. 2013. Recovery of lithium and cobalt from waste lithium ion batteries of mobile phone. *Waste Management*. 33(9):1890–1897.

Jun SONG, Y. 2017. *Patent No. US 2017/0084965 A1*. United States Patent.

Kang, J., Senanayake, G., Sohn, J. & Shin, S.M. 2010. Recovery of cobalt sulfate from spent

lithium ion batteries by reductive leaching and solvent extraction with Cyanex 272. *Hydrometallurgy*. 100(3–4):168–171.

Karnchanawong, S. & Limpiteeprakan, P. 2009. Evaluation of heavy metal leaching from spent household batteries disposed in municipal solid waste. *Waste Management*. 29(2):550–558.

Kislik, V.S. 2012. *Solvent Extraction: Classical and Novel Approaches*. First ed. Amsterdam, The Netherlands: Elsevier.

Knights, B.D.H. & Sallojee, F. 2015. *Lithium Battery Recycling Process-keeping the future fully charged*.

Kushnir, D. 2015. Lithium Ion Battery Recycling Technology 2015: Current State and Future Prospects. 1–56.

Lee, C.K. & Rhee, K.I. 2002. Preparation of LiCoO2from spent lithium-ion batteries. *Journal of Power Sources*. 109(1):17–21.

Lee, C.K. & Rhee, K.I. 2003. Reductive leaching of cathodic active materials from lithium ion battery wastes. *Hydrometallurgy*. 68(1–3):5–10.

Levenspiel, O. 1999. *Chemical reaction engineering*. Vol. 38.

Li, L., Ge, J., Wu, F., Chen, R., Chen, S. & Wu, B. 2009. Recovery of cobalt and lithium from spent lithium ion batteries using organic citric acid as leachant. *Journal of Hazardous Materials*. 176(1–3):288–293.

Li, L., Ge, J., Chen, R., Wu, F., Chen, S. & Zhang, X. 2010. Environmental friendly leaching reagent for cobalt and lithium recovery from spent lithium-ion batteries. *Waste Management*. 30(12):2615–2621.

Li, L., Lu, J., Ren, Y., Zhang, X.X., Chen, R.J., Wu, F. & Amine, K. 2012. Ascorbic-acid-assisted recovery of cobalt and lithium from spent Li-ion batteries. *Journal of Power Sources*. 218:21–27.

Li, L., Dunn, J.B., Zhang, X.X., Gaines, L., Chen, R.J., Wu, F. & Amine, K. 2013. Recovery of metals from spent lithium-ion batteries with organic acids as leaching reagents and

environmental assessment. *Journal of Power Sources*. 233:180–189.

Li, L., Zhai, L., Zhang, X., Lu, J., Chen, R., Wu, F. & Amine, K. 2014. Recovery of valuable metals from spent lithium-ion batteries by ultrasonic-assisted leaching process. *Journal of Power Sources*. 262:380–385.

Li, L., Qu, W., Zhang, X., Lu, J., Chen, R., Wu, F. & Amine, K. 2015. Succinic acid-based leaching system : A sustainable process for recovery of valuable metals from spent Li-ion batteries. 282:544–551.

Li, L., Fan, E., Guan, Y., Zhang, X., Xue, Q., Wei, L., Wu, F. & Chen, R. 2017. Sustainable Recovery of Cathode Materials from Spent Lithium-Ion Batteries Using Lactic Acid Leaching System.

Liley, P.E., Thomson, G.H., Friend, D.G., Daubert, T.E. & Buck, E. 1997. *Physical and Chemical Data*.

Measey, G.J., Silva, J.B. & Di-Bernardo, M. 2003. Testing for repeatability in measurements of length and mass in Chthonerpeton indistinctum (Amphibia: Gymnophiona), including a novel method of calculating total length of live caecilians. *Herpetological Review*. 34(1):35–39.

Mishra, D., Kim, D.J., Ralph, D.E., Ahn, J.G. & Rhee, Y.H. 2008. Bioleaching of metals from spent lithium ion secondary batteries using Acidithiobacillus ferrooxidans. *Waste Management*. 28(2):333–338.

Mubarok, M.Z. & Hanif, L.I. 2016. Cobalt and Nickel Separation in Nitric Acid Solution by Solvent Extraction Using Cyanex 272 and Versatic 10. *Procedia Chemistry*. 19:743–750.

Nayaka, G.P., Manjanna, J., Pai, K. V., Vadavi, R., Keny, S.J. & Tripathi, V.S. 2015. Recovery of valuable metal ions from the spent lithium-ion battery using aqueous mixture of mild organic acids as alternative to mineral acids. *Hydrometallurgy*. 151:73–77.

Nguyen, V.T., Lee, J.C., Jeong, J., Kim, B.S. & Pandey, B.D. 2014. Selective recovery of cobalt, nickel and lithium from sulfate leachate of cathode scrap of Li-ion batteries using liquid-liquid extraction. *Metals and Materials International*. 20(2):357–365.

Nogueira, C.A., Oliveira, P.C. & Pedrosa, F.M. 2009. Separation of cadmium, cobalt, and nickel by solvent extraction using the nickel salts of the extractants. *Solvent Extraction and Ion Exchange*. 27(2):295–311.

Olivier, M.C., Dorfling, C. & Eksteen, J.J. 2011. Developing a solvent extraction process for the separation of cobalt and iron from nickel sulfate solutions. Stellenbosch University.

Pecina, T., Franco, T., Castillo, P. & Orrantia, E. 2008. Leaching of a zinc concentrate in sulphuric acid solutions containing hydrogen peroxide and complexing agents. *Minerals Engineering*. 21:23–30.

Pérez, M. & Hillier, F.S. 2003. *Leaching and Adsorption Resourcebook*. Vol. 18.

Preston, J.S. 1982. Solvent extraction of cobalt and nickel by organophosphorus acids I. Comparison of phosphoric, phosphonic and phosphonic acid systems. *Hydrometallurgy*. 9(2):115–133.

Reddy, B.R., Priya, D.N. & Park, K.H. 2006. Separation and recovery of cadmium(II), cobalt(II) and nickel(II) from sulphate leach liquors of spent Ni-Cd batteries using phosphorus based extractants. *Separation and Purification Technology*. 50(2):161–166.

Rickelton, W.A., Flett, D.S. & West, D.W. 1984. COBALT-NICKEL SEPARATION BY SOLVENT EXTRACTION WITH BIS(2,4,4 TRIMETHYLPENTYL)PHOSPHINIC ACID. *Solvent Extraction and Ion Exchange*. 2(6):815–838.

Rodrigues, L.E.O.C. & Mansur, M.B. 2010. Hydrometallurgical separation of rare earth elements, cobalt and nickel from spent nickel-metal-hydride batteries. *Journal of Power Sources*. 195(11):3735–3741.

Rydberg, J., Cox, M., Musikas, C. & Choppin, G.R. 2004. *Solvent Extraction Principles and Practice*. Second ed. New York: Marcel Dekker.

Sahu, S.K., Agrawal, A., Pandey, B.D. & Kumar, V. 2004. Recovery of copper, nickel and cobalt from the leach liquor of a sulphide concentrate by solvent extraction. *Minerals Engineering*. 17(7–8):949–951.

Sarangi, K., Reddy, B.R. & Das, R.P. 1999. Extraction studies of cobalt (II) and nickel (II) from

chloride solutions using Na-Cyanex 272. Separation of Co(II)/Ni(II) by the sodium salts of D2EHPA, PC88A and Cyanex 272 and their mixtures. *Hydrometallurgy*. 52(3):253–265.

Serjeant, E.B. & Dempsey, B. 1979. *Ionisation Constants of Organic Acids in Aqueous Solutions*. Pergamon.

Shin, S.M., Kim, N.H., Sohn, J.S., Yang, D.H. & Kim, Y.H. 2005. Development of a metal recovery process from Li-ion battery wastes. *Hydrometallurgy*. 79(3–4):172–181.

Skoog, D.A., West, D.M., Holler, F.J. & Crouch, S. 2013. *Fundamentals of analytical chemistry*. Nelson Education.

SNAM, 2017. n.d. [Online], Available: http://www.snam.com/activites/marketting-alloys-next.php [2017, July 24].

Sonoc, A., Jeswiet, J. & Soo, V.K. 2015. Opportunities to improve recycling of automotive lithium ion batteries. *Procedia CIRP*. 29(December):752–757.

Sun, L. & Qiu, K. 2012. Organic oxalate as leachant and precipitant for the recovery of valuable metals from spent lithium-ion batteries. *Waste Management*. 32(8):1575–1582.

Tsakiridis, P.E. & Agatzini, S.L. 2004. Simultaneous solvent extraction of cobalt and nickel in the presence of manganese and magnesium from sulfate solutions by Cyanex 301. 72:269–278.

Wang, H. & Friedrich, B. 2015. Development of a Highly Efficient Hydrometallurgical Recycling Process for Automotive Li – Ion Batteries. *Journal of Sustainable Metallurgy*. 168–178.

Wang, R.C., Lin, Y.C. & Wu, S.H. 2009. A novel recovery process of metal values from the cathode active materials of the lithium-ion secondary batteries. *Hydrometallurgy*. 99(3–4):194–201.

Xie, F., Zhang, T.A., Dreisinger, D. & Doyle, F. 2014. A critical review on solvent extraction of rare earths from aqueous solutions. *Minerals Engineering*. 56:10–28.

Zeng, X., Li, J. & Singh, N. 2014. Recycling of spent lithium-ion battery: A critical review. *Critical Reviews in Environmental Science and Technology*. 44(10):1129–1165.

Zou, H. 2012. Development of a Recycling Process for Li-Ion Batteries. 1:27–28.

8. Appendices

8.1 Appendix A: LIB Cathodic material characterization

8.1.1 Aqua regia digestion

Table 23 shows the mass of metal that dissolved during aqua regia tests on 20 g samples of LIB cathodic active material.

Table 23: Mass of metal dissolved during aqua regia digestions

Test	Mass leached (mg)					
	Al	Co	Cu	Li	Mn	Ni
1	117.30	2672.80	8.85	812.17	2158.30	3115.97
2	155.80	2835.24	11.13	947.69	2518.97	3391.10
3	137.87	2712.76	10.57	918.76	2322.89	3243.44
4	142.24	2646.68	10.41	907.44	2377.75	3074.65
5	134.89	2573.89	9.55	826.98	2079.16	2922.68
6	139.79	2676.70	10.26	979.33	2237.29	3191.09
7	139.44	2657.32	9.80	918.86	2227.25	3109.35
8	132.59	2723.05	9.26	950.64	2271.54	3173.23
9	140.66	2719.86	9.64	922.78	2274.15	3217.01
10	143.13	2728.35	9.75	919.08	2348.72	3274.54
Average	138.37	2694.67	9.92	910.37	2281.60	3171.30

8.1.2 Estimation of oxygen fraction from XRD

Estimating the fraction of oxygen in the cathodic material using $Li_{1.2}Mn_{0.49}Ni_{0.16}Fe_{0.16}O_2$ and $LiNi_{0.05}Mn_{0.05}Co_{0.9}O_2$ phases from figure 10 was as follows:

Molar mass of $Li_{1.2}Mn_{0.49}Ni_{0.16}Fe_{0.16}O_2$ = 85.2 g/mol

Molar mass of $LiNi_{0.05}Mn_{0.05}Co_{0.9}O_2$ = 97.9 g/mol

% of oxygen in $Li_{1.2}Mn_{0.49}Ni_{0.16}Fe_{0.16}O_2$ = $32\ g/mol / 85.2\ g/mol \times 100\%$ = 37.56%

% of oxygen in $LiNi_{0.05}Mn_{0.05}Co_{0.9}O_2$ = $32\ g/mo/97.9\ g/mol \times 100\%$ = 32.69%

Average %O in the oxide phase = (37.56% + 32.69%)/2 = 35.12%

Fraction of oxide phase in the cathodic material = 100% - carbon fraction = 100% - 30.73% = 69.28%, 35.12% of which is oxygen.

Therefore fraction of oxygen in the cathodic material = $35.12/100 \times 69.28\%$ = 24.33%

Fraction of the metallic phase = 100% - carbon fraction – oxygen fraction

= 100% - 30.73% - 24.33%

=44.95%

8.1.3 SEM analysis

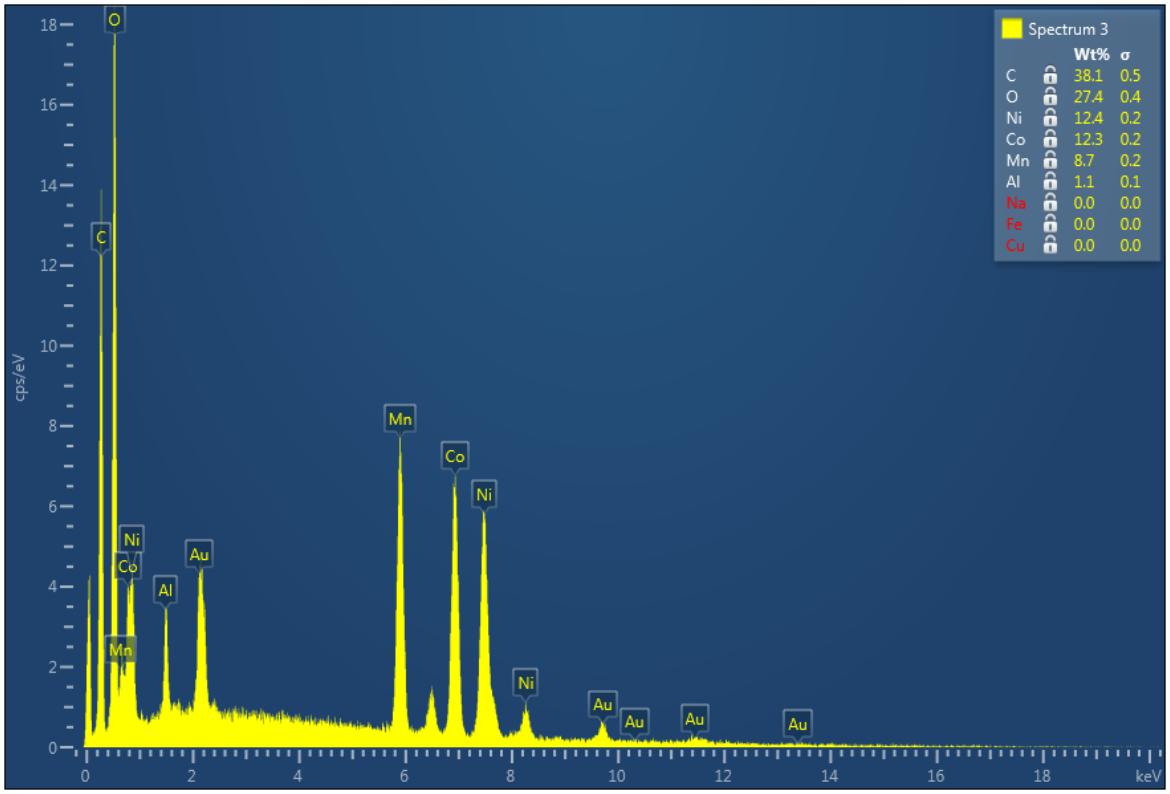

Figure 38: SEM - Spectrum for analysis 2

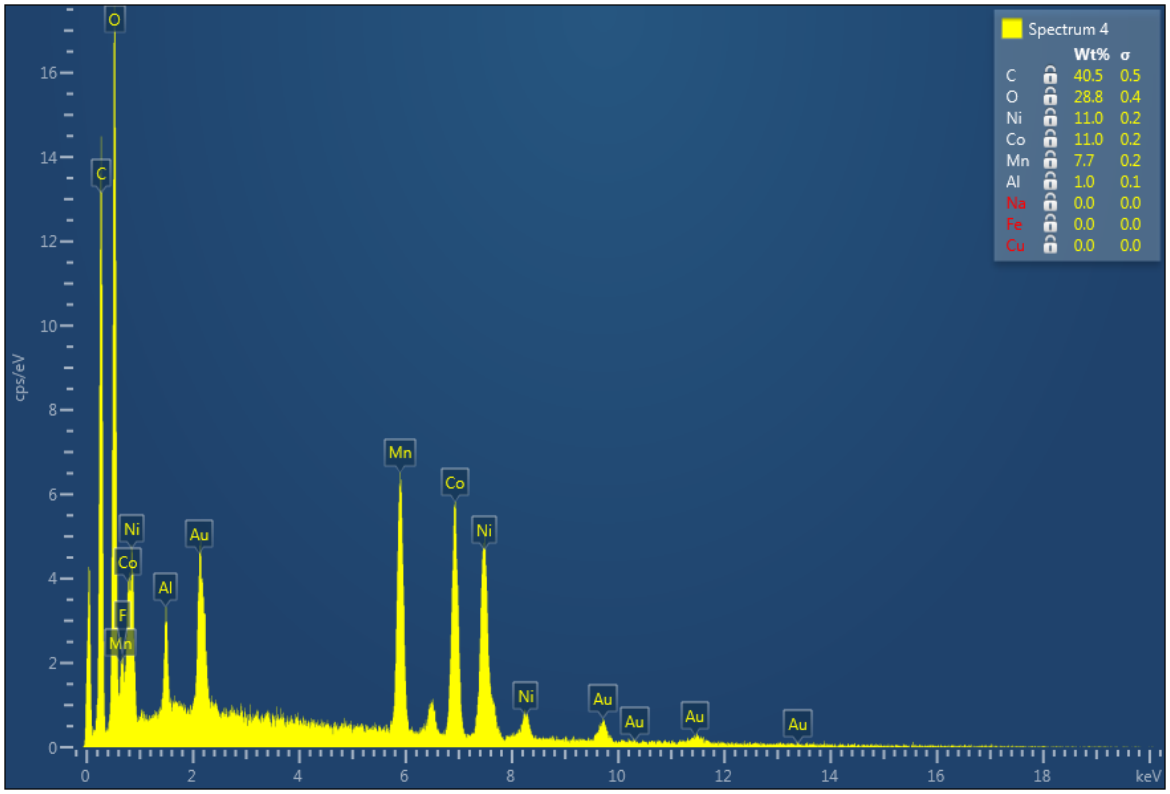

Figure 39: SEM - Spectrum for analysis 3

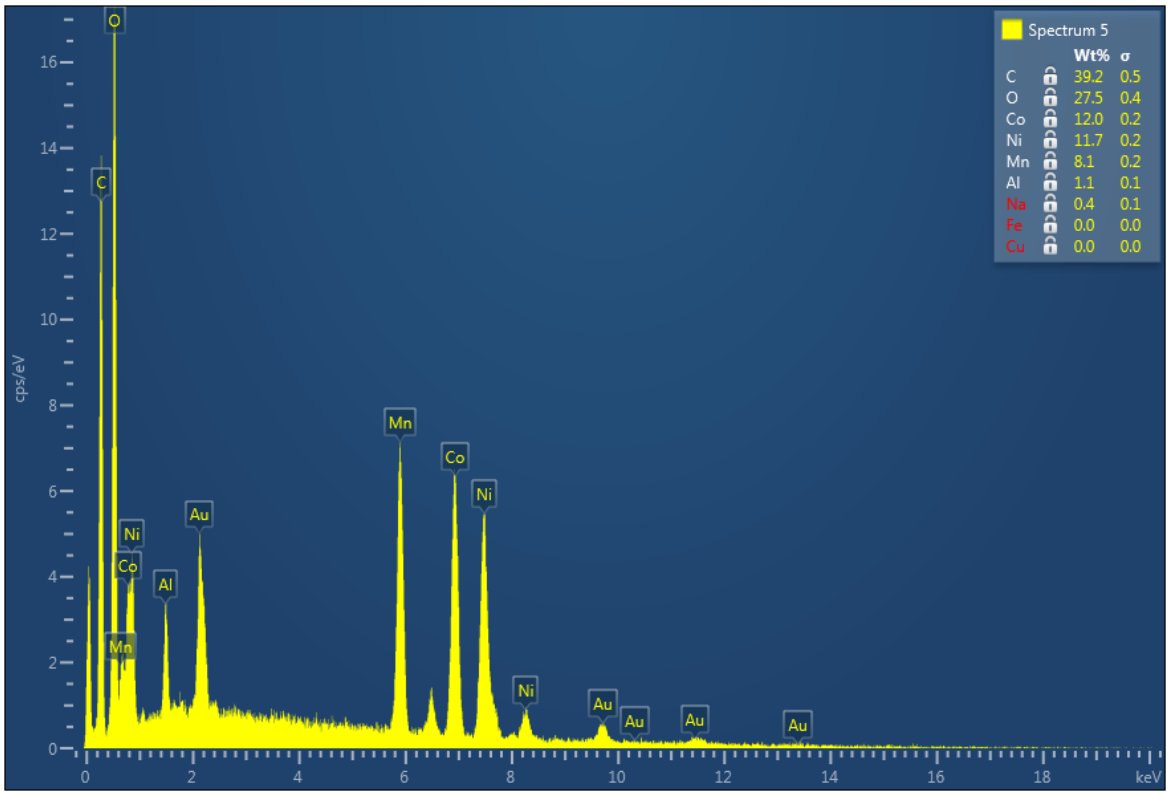

Figure 40: SEM - Spectrum for analysis 4

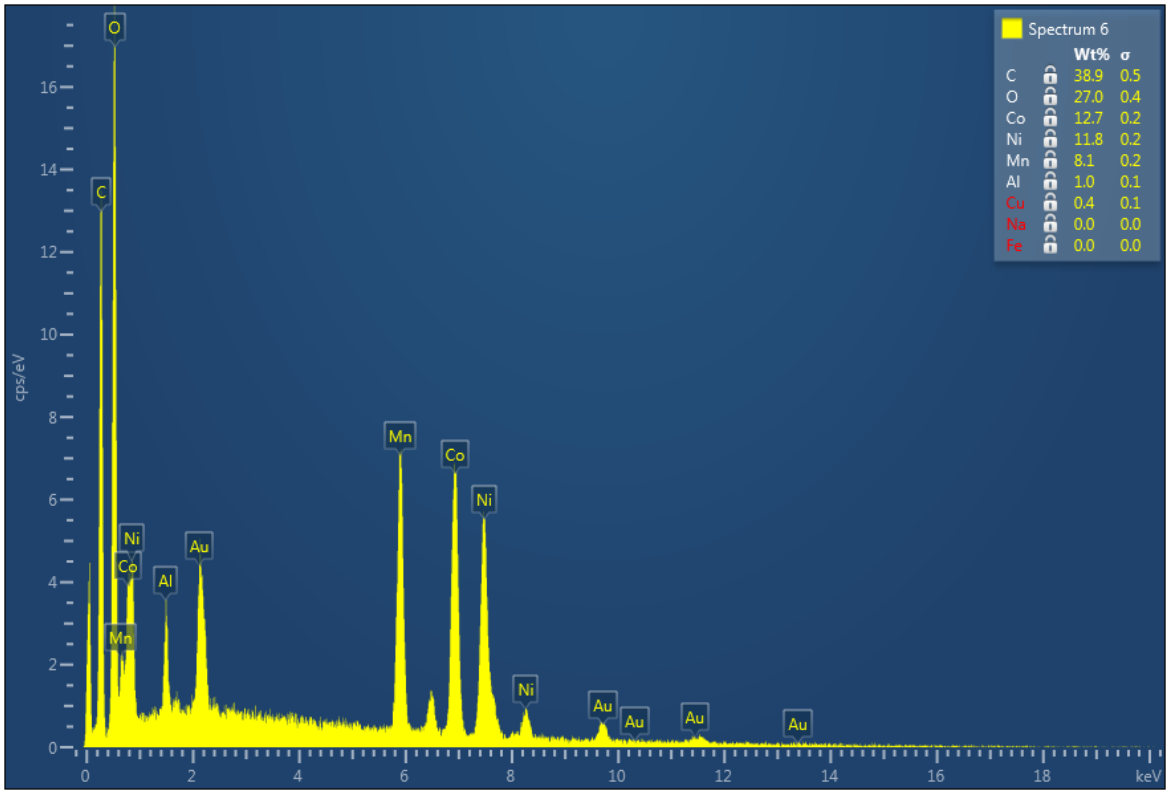

Figure 41: SEM - Spectrum for analysis 5

8.2. Appendix B: Acid Leaching

8.2.1 Sample calculations of acid requirements

Shown below is a demonstration of how the theoretical amount of acid required for total dissolution of metals in the cathodic material was calculated:

A pulp density of 20 g/L was used for the leaching tests. From Table 14, there is 0.14g Al, 2.63g Co, 0.01g Cu, 0.89g Li, 2.23g Mn and 3.1g Ni in 20g of feed. Which means 0.01M Al, 0.04M Co, 0.0002M Cu, 0.13M Li, 0.04M Mn and 0.05M Ni reacts, assuming total dissolution.

From stoichiometry of the dissolution reactions of these metals in citric acid, the ratios of the number of moles of citric acid/number of metal are as follows; citric acid/Al = 1, citric acid/Co, Cu, Mn, Ni = 2/3, citric acid/Li = 1/3.

Therefore, the total amount of acid required for total dissolution of metals = 1 × 0.01M + 2/3 × (0.04M + 0.0002M + 0.04M + 0.05M) + 1/3 × 0.13M = 0.14M.

The theoretical amount of citric acid required for total dissolution of all metals at a pulp density of 20 g/L is 0.14M.

When 1M citric acid is used, excess amount of acid = 1M – 0.14M = 0.86M. Theoretical % excess citric acid = 0.86/0.14 × 100% = 615%. The % excess acid for 1.25M and 1.5M citric acid is 793% and 972%, respectively.

The same approach was used for calculating the theoretical amount of DL-malic acid required and % excess DL-malic acid.

The ratios of the number of moles of DL-malic acid/number of moles of metal are as follows; DL-malic acid/Al = 3/2, DL-malic acid/Co, Cu, Mn, Ni = 1, DL-malic acid/Li = 1/2.

Therefore, the total amount of acid required for total dissolution of metals = 3/2 × 0.01M + 1 × (0.04M + 0.0002M + 0.04M + 0.05M) + 1/2 × 0.13M = 0.21M.

The theoretical amount of DL-malic acid required for total dissolution of all metals at a pulp density of 20 g/L is 0.21M.

When 1M DL-malic acid is used, excess amount of acid = 1M – 0.21M = 0.79M. Theoretical % excess DL-malic acid = 0.79/0.21 × 100% = 376%. The % excess acid for 1.25M and 1.5M DL-malic acid is 496% and 615%, respectively.

8.2.2 Citric acid leaching data

Table 24: Citric acid leaching data at 30℃.

Acid concentration		Mass of metal leached from 5g feed (mg)						Metal Extraction (%)					
	Time (mins)	Al	Co	Cu	Li	Mn	Ni	Al	Co	Cu	Li	Mn	Ni
1M	10	20.16	39.61	1.83	12.44	35.38	36.65	58.30	5.88	73.40	5.46	6.20	4.62
	20	22.61	92.16	1.89	28.56	77.66	91.90	65.36	16.8	76.25	12.55	13.61	11.59
	30	22.55	130.04	1.79	40.46	107.84	133.29	65.21	13.0	71.87	17.78	18.91	16.81
	60	21.74	246.49	1.86	80.03	205.49	262.36	62.86	35.9	75.23	35.16	36.03	33.09
	90	21.74	340.85	1.85	111.69	282.73	369.14	62.83	56.0	74.49	49.07	49.57	46.56
	120	22.43	406.00	1.85	133.65	335.34	446.91	64.82	60.27	74.79	58.72	58.79	56.39
1.25M	10	17.34	22.73	1.59	7.23	22.51	20.13	50.09	3.37	64.06	3.17	3.95	2.54
	20	22.95	56.08	1.85	16.75	48.19	53.84	66.35	8.32	74.23	7.36	8.45	6.79
	30	23.09	95.30	1.78	29.60	81.31	98.05	66.72	14.15	71.56	13.00	14.25	12.37
	60	22.16	174.71	1.81	55.78	148.53	194.34	64.06	25.93	73.09	24.50	26.04	24.51
	90	22.36	259.01	1.74	83.69	219.29	292.81	64.65	38.45	70.01	36.77	38.44	36.93
	120	21.49	359.99	1.71	117.98	305.70	413.75	62.10	53.44	68.80	51.83	53.59	52.18
1.5M	10	22.15	45.19	1.94	14.21	39.59	42.75	64.01	6.71	78.16	6.24	6.94	5.39
	20	22.20	77.85	1.88	24.84	66.45	78.15	64.18	11.56	75.24	10.91	11.65	9.86
	30	22.00	119.25	1.90	37.78	99.19	124.00	63.58	17.70	76.34	16.60	17.39	15.64
	60	21.96	222.41	1.90	72.91	184.21	239.98	63.47	33.01	76.64	32.04	32.29	30.27
	90	22.49	333.59	1.93	109.78	272.94	365.73	65.00	49.52	77.38	48.23	47.85	46.13
	120	19.13	339.64	1.46	113.96	279.70	380.54	55.30	50.42	59.01	50.07	49.04	48.00

Table 25: Citric acid leaching data at 60℃

Acid concentration		Mass of metal leached from 5g feed (mg)						Metal Extraction (%)					
	Time (mins)	Al	Co	Cu	Li	Mn	Ni	Al	Co	Cu	Li	Mn	Ni
1M	10	23.61	249.08	1.95	87.69	220.40	314.18	68.26	36.97	78.24	38.53	38.64	39.63
	20	22.79	328.03	2.06	117.40	294.68	426.44	65.87	48.69	83.09	51.58	51.66	53.79
	30	22.45	370.28	2.03	133.35	334.28	483.54	64.90	54.96	81.39	58.59	58.60	60.99
	60	24.33	469.16	2.21	165.33	417.85	608.20	70.30	69.64	89.30	72.64	73.25	76.71
	90	25.25	521.60	2.19	179.56	445.21	648.86	72.97	77.43	88.19	78.89	78.05	81.84
	120	25.69	532.04	2.16	182.25	452.05	655.03	74.25	78.98	86.84	80.08	79.25	82.62
1.25M	10	23.91	317.69	2.00	109.98	282.30	386.60	69.10	47.16	80.30	48.32	49.49	48.76
	20	25.01	445.05	2.15	157.04	399.83	563.69	72.29	66.06	86.57	69.00	70.09	71.10
	30	25.63	496.83	2.09	175.25	442.34	633.93	74.07	73.75	83.83	77.00	77.55	79.96
	60	24.73	548.21	2.16	186.75	470.59	677.56	71.48	81.38	87.03	82.05	82.50	85.46
	90	24.99	529.91	2.03	180.13	453.29	651.56	72.23	78.66	81.64	79.14	79.47	82.18
	120	18.81	393.53	1.46	134.73	337.14	625.38	54.36	58.41	58.63	59.20	59.11	78.88
1.5M	10	25.55	346.29	2.10	123.38	305.83	427.21	73.85	51.40	84.60	54.20	53.62	53.88
	20	25.15	441.05	2.09	158.04	390.71	558.16	72.69	65.47	84.27	69.44	68.50	70.40
	30	25.90	503.89	2.23	181.38	447.26	640.76	74.87	74.80	89.60	79.69	78.41	80.82
	60	25.36	553.91	2.09	189.93	464.46	679.19	73.32	82.22	83.94	83.45	81.43	85.67
	90	23.46	517.11	2.04	181.43	439.88	632.76	67.83	76.76	82.05	79.72	77.12	79.81
	120	23.41	509.69	1.96	176.94	429.36	623.05	67.68	75.66	79.04	77.74	75.27	78.59

Table 26: Citric acid leaching data at 95℃

Acid concentration		Mass of metal leached from 5g feed (mg)						Metal Extraction (%)					
	Time (mins)	Al	Co	Cu	Li	Mn	Ni	Al	Co	Cu	Li	Mn	Ni
1M	10	27.45	552.39	2.41	156.20	478.50	696.28	79.33	82.00	97.14	68.63	83.89	87.82
	20	21.94	442.21	2.04	194.63	382.43	549.18	63.41	65.64	81.86	85.51	67.05	69.27
	30	27.68	562.26	2.43	194.40	479.28	695.31	79.99	83.46	97.84	85.41	84.02	87.70
	60	29.39	567.45	2.40	196.20	484.06	699.70	84.94	84.23	96.43	86.20	84.86	88.25
	90	33.03	642.73	2.44	218.56	543.44	791.35	95.45	95.41	98.25	96.03	95.27	99.81
	120	32.28	627.65	2.49	214.81	532.91	774.81	93.28	93.17	100.05	94.38	93.43	97.73
1.25M	10	28.16	582.74	2.31	196.84	498.19	716.53	81.42	86.50	93.26	86.48	87.34	90.38
	20	29.50	608.80	2.31	206.15	519.29	742.10	85.28	90.37	93.22	90.58	91.04	93.60
	30	29.61	606.33	2.36	203.26	514.46	737.18	85.60	90.00	95.10	89.31	90.19	92.98
	60	29.90	593.65	2.31	199.85	503.95	730.58	86.41	88.12	93.14	87.81	88.35	92.15
	90	29.94	592.36	2.20	197.86	501.00	723.00	86.54	87.93	88.32	86.93	87.83	91.19
	120	30.54	593.18	2.28	199.80	503.89	720.43	88.29	88.05	91.83	87.79	88.34	90.87
1.5M	10	29.09	611.46	2.34	215.90	526.26	759.26	84.07	90.77	93.91	94.86	92.26	95.77
	20	29.34	622.56	2.28	214.13	524.89	766.85	84.80	92.41	91.69	94.08	92.02	96.72
	30	30.30	634.83	2.44	218.79	535.60	781.33	87.59	94.23	97.91	96.13	93.90	98.55
	60	29.58	602.96	2.35	209.90	511.16	740.13	85.49	89.50	94.49	92.22	89.61	93.35
	90	29.84	607.49	2.28	210.21	513.51	745.25	86.25	90.18	91.63	92.36	90.03	94.00
	120	30.39	605.50	2.33	209.26	510.96	741.91	87.85	89.88	93.62	91.95	89.58	93.58

8.2.3 DL-malic acid leaching

Table 27: DL-malic acid leaching data at 30°C

Acid concentration		Mass of metal leached from 5g feed (mg)						Metal Extraction (%)					
	Time (mins)	Al	Co	Cu	Li	Mn	Ni	Al	Co	Cu	Li	Mn	Ni
1M	10	22.74	49.28	2.21	15.55	43.88	47.81	65.72	7.31	89.15	6.83	7.69	6.03
	20	24.26	96.59	2.23	30.51	81.43	99.48	70.13	14.34	89.39	13.41	14.27	12.55
	30	24.39	140.29	2.41	45.38	118.88	149.04	70.47	20.82	97.08	19.94	20.84	18.80
	60	24.29	295.10	2.38	98.53	249.28	327.19	70.20	43.80	95.79	43.29	43.70	41.27
	90	23.95	391.48	2.28	133.04	333.11	442.31	69.22	58.11	91.46	58.45	58.40	55.79
	120	24.16	452.00	2.26	153.33	387.43	520.65	69.83	67.09	90.87	67.37	67.92	65.67
1.25M	10	21.40	43.53	1.90	13.64	38.91	41.08	61.87	6.46	76.41	5.99	6.82	5.18
	20	23.50	100.58	2.10	31.80	86.33	102.14	67.92	14.93	84.36	13.97	15.13	12.88
	30	23.94	150.24	2.13	48.34	128.45	157.94	69.17	22.30	85.78	21.24	22.52	19.92
	60	23.13	276.21	2.09	89.55	233.13	299.08	66.83	41.00	84.14	39.34	40.87	37.72
	90	22.18	366.50	2.09	121.79	313.46	406.09	64.11	54.40	83.90	53.51	54.95	51.22
	120	22.44	427.08	1.99	143.53	363.04	485.90	64.87	63.40	79.86	63.06	63.64	61.29
1.5M	10	23.30	59.51	2.21	18.63	52.44	57.03	67.36	8.83	89.22	8.18	9.19	7.19
	20	24.03	115.43	2.14	36.69	98.81	118.01	69.46	17.13	86.00	16.12	17.32	14.89
	30	24.46	165.64	2.23	53.34	141.76	175.81	70.69	24.59	89.70	23.44	24.85	22.17
	60	25.06	271.83	2.26	89.83	234.83	302.21	72.43	40.35	91.29	39.46	41.17	38.12
	90	24.26	366.66	2.18	122.74	316.79	416.33	70.12	54.43	87.34	53.93	55.54	52.51
	120	23.40	406.65	2.13	136.79	350.99	464.48	67.65	60.36	85.46	60.10	61.53	58.58

Table 28: DL-malic acid leaching data at 60°C

Acid concentration		Mass of metal leached from 5g feed (mg)						Metal Extraction (%)					
	Time (mins)	Al	Co	Cu	Li	Mn	Ni	Al	Co	Cu	Li	Mn	Ni
1M	10	24.10	425.06	2.24	144.31	372.24	509.60	69.65	63.10	89.84	63.41	65.26	64.28
	20	24.61	505.83	2.28	173.13	443.46	616.03	71.16	75.08	91.71	76.06	77.75	77.70
	30	25.23	549.30	2.43	185.55	472.46	665.11	72.92	81.54	97.79	81.53	82.83	83.89
	60	24.93	561.96	2.30	185.65	468.66	665.38	72.06	83.42	92.72	81.57	82.16	83.92
	90	23.89	540.08	2.21	176.60	446.29	636.01	69.03	80.17	88.82	77.59	78.24	80.22
	120	23.21	513.20	2.11	172.88	434.14	604.45	67.11	76.18	84.82	75.96	76.11	76.24
1.25M	10	25.41	413.74	2.34	138.63	359.36	490.90	73.45	61.42	94.05	60.91	63.00	61.92
	20	25.78	532.20	2.34	180.65	464.13	644.78	74.52	79.00	94.09	79.37	81.37	81.33
	30	26.09	569.03	2.34	190.64	488.19	685.38	75.39	84.47	94.30	83.76	85.59	86.45
	60	25.08	574.10	2.25	188.43	477.41	672.89	72.49	85.22	90.51	82.79	83.70	84.87
	90	25.53	576.23	2.29	190.10	480.48	673.60	73.77	85.53	92.32	83.53	84.23	84.96
	120	23.78	532.11	2.16	174.83	440.71	621.46	68.71	78.99	87.00	76.81	77.26	78.38
1.5M	10	24.00	377.04	2.26	125.43	327.61	446.88	69.35	55.97	90.86	55.11	57.43	56.36
	20	24.93	507.89	2.31	169.24	438.26	616.86	72.03	75.39	92.96	74.36	76.83	77.80
	30	25.25	548.33	2.34	183.95	473.73	664.16	73.00	81.39	94.21	80.82	83.05	83.77
	60	25.69	583.99	2.38	189.81	483.93	686.49	74.25	86.69	95.42	83.40	84.83	86.59
	90	24.65	548.19	2.25	181.08	460.39	641.68	71.27	81.37	90.58	79.56	80.71	80.93
	120	24.45	539.23	2.19	177.31	450.61	631.28	70.68	80.04	88.15	77.91	79.00	79.62

Table 29: DL-malic acid leaching data at 95℃

Acid concentration		Mass of metal leached from 5g feed (mg)						Metal Extraction (%)					
	Time (mins)	Al	Co	Cu	Li	Mn	Ni	Al	Co	Cu	Li	Mn	Ni
1M	10	29.65	645.59	2.48	212.84	548.58	765.55	85.69	95.83	99.81	93.52	96.17	96.56
	20	30.88	656.49	2.43	218.58	559.03	779.73	89.23	97.45	97.53	96.04	98.01	98.35
	30	31.59	672.29	2.49	219.38	567.19	789.38	91.32	99.80	100.12	96.39	99.44	99.56
	60	31.20	645.11	2.50	211.81	548.20	763.73	90.18	95.76	100.53	93.07	96.12	96.33
	90	31.11	628.96	2.44	207.03	528.43	741.50	89.92	93.36	98.04	90.96	92.64	93.53
	120	30.35	597.30	2.43	199.35	507.25	708.01	87.74	88.66	97.83	87.59	88.93	89.30
1.25M	10	26.68	600.16	2.41	189.61	493.13	700.60	77.09	89.09	97.32	83.31	86.45	88.37
	20	27.29	603.93	2.38	188.34	493.23	691.74	78.88	89.65	95.46	82.75	86.47	87.25
	30	28.30	606.43	2.41	193.39	504.39	699.80	81.80	90.02	96.99	84.97	88.43	88.27
	60	27.43	568.99	2.34	182.54	474.25	669.33	79.26	84.46	93.96	80.20	83.14	84.42
	90	27.96	568.05	2.44	180.70	469.81	655.51	80.82	84.32	97.96	79.39	82.37	82.68
	120	25.74	521.09	2.14	166.71	433.40	602.13	74.38	77.35	86.01	73.25	75.98	75.95
1.5M	10	27.83	615.93	2.45	199.53	511.16	722.44	80.41	91.43	98.61	87.66	89.61	91.12
	20	28.61	622.71	2.45	198.89	510.34	727.73	82.69	92.44	98.52	87.38	89.47	91.79
	30	30.44	659.28	2.46	210.95	541.63	769.81	87.99	97.86	99.31	92.69	94.96	97.10
	60	30.68	640.61	2.45	205.78	527.14	746.46	88.66	95.09	98.86	90.41	92.41	94.15
	90	29.59	604.56	2.44	197.31	502.04	706.90	85.53	89.74	98.35	86.70	88.01	89.16
	120	28.99	590.83	2.36	189.44	484.20	688.74	83.80	87.70	95.13	83.20	84.89	86.87

8.2.4 ANOVA tables

8.2.4.1 Citric acid leaching

Table 30: Co extraction

Source of Variation	***SS***	***df***	***MS***	***F***	***P-value***	***F crit***
Acid concentration	17,02082	2	8,510411	0,636744	0,575339	6,944272
Temperature	2331,509	2	1165,755	87,2211	0,000502	6,944272
Error	53,46204	4	13,36551			
Total	2401,992	8				

Table 31: Li extraction

Source of Variation	***SS***	***df***	***MS***	***F***	***P-value***	***F crit***
Acid concentration	17,92282	2	8,961411	0,720098	0,540618	6,944272
Temperature	2612,485	2	1306,242	104,9637	0,00035	6,944272
Error	49,77884	4	12,44471			
Total	2680,186	8				

Table 32: Ni extraction

Source of Variation	***SS***	***df***	***MS***	***F***	***P-value***	***F crit***
Acid concentration	11,33076	2	5,665378	0,442427	0,670528	6,944272
Temperature	3248,268	2	1624,134	126,8337	0,000241	6,944272
Error	51,22091	4	12,80523			
Total	3310,819	8				

8.2.4.2 DL-malic acid leaching

Table 33: Co extraction

Source of Variation	***SS***	***df***	***MS***	***F***	***P-value***	***F crit***
Acid concentration	21,52569	2	10,76284	0,713789	0,543135	6,944272
Temperature	1622,262	2	811,1308	53,79395	0,001285	6,944272
Error	60,31391	4	15,07848			
Total	1704,101	8				

Table 34: Li extraction

Source of Variation	***SS***	***df***	***MS***	***F***	***P-value***	***F crit***
Acid concentration	32,73216	2	16,36608	1,018074	0,439137	6,944272
Temperature	1220,99	2	610,4952	37,97668	0,002503	6,944272
Error	64,30211	4	16,07553			
Total	1318,025	8				

Table 35: Ni extraction

Source of Variation	***SS***	***df***	***MS***	***F***	***P-value***	***F crit***
Acid concentration	35,71487	2	17,85743	1,116066	0,411952	6,944272
Temperature	1737,385	2	868,6927	54,29216	0,001262	6,944272
Error	64,00133	4	16,00033			
Total	1837,102	8				

8.2.5 Leaching tests repeatability data

Table 36: Citric acid and DL-malic acid leaching repeatability tests data

		Citric acid leaching						DL-malic acid leaching					
	Time [minutes]	**10**	**20**	**30**	**60**	**90**	**120**	**10**	**20**	**30**	**60**	**90**	**120**
Cobalt extraction [%]	Repeat 1	89.79	91.05	92.99	88.52	89.2	88.79	94.64	96.40	98.29	95.82	91.79	87.64
	Repeat 2	85.7	94.67	92.79	93.15	92.06	90.8	92.56	94.18	96.25	91.90	91.04	88.56
	Repeat 3	87.7	90.28	91.05	90.71	85.98	87.93	89.73	90.77	92.94	90.57	86.75	81.21
	Average	87.73	92	92.28	90.79	89.08	89.17	92.31	93.78	95.83	92.76	89.86	85.80
	Standard Deviation	2.04	2.34	1.07	2.31	3.04	1.47	2.47	2.83	2.70	2.73	2.72	4.00
Lithium extraction [%]	Repeat 1	90.39	89.84	91.64	87.94	88.13	87.66	92.78	95.27	95.62	95.08	90.24	86.90
	Repeat 2	86.57	94.23	92.86	93.19	90.76	90.36	95.34	96.27	97.41	93.72	92.84	90.89
	Repeat 3	89.96	91.6	91.98	91.37	84.12	89.16	90.42	91.73	93.02	90.02	87.46	82.61
	Average	88.97	91.89	92.16	90.83	87.67	89.06	92.85	94.42	95.35	92.94	90.18	86.80
	Standard Deviation	2.09	2.21	0.63	2.66	3.34	1.35	2.46	2.38	2.21	2.62	2.69	4.14
Nickel extraction [%]	Repeat 1	91.88	92.5	94.45	89.59	91.88	89.77	95.79	97.57	98.78	97.54	92.78	88.59
	Repeat 2	93.04	96.16	96.34	96.01	96.14	94.89	92.70	93.51	97.05	93.01	90.85	89.50
	Repeat 3	91.38	93.44	94.02	92.49	91.58	91.85	91.45	93.65	95.05	93.19	89.24	83.47
	Average	92.1	94.03	94.94	92.70	93.2	92.17	93.31	94.91	96.96	94.58	90.96	87.19
	Standard Deviation	0.85	1.9	1.23	3.21	4.35	2.58	2.24	2.3	1.86	2.57	1.77	3.26

8.3 Appendix C: Solvent extraction tests

Table 37: Solvent extraction tests with 10% v/v D2EHPA

		Aqueous solution concentration before extraction (g/L)						Aqueous solution concentration after extraction (g/L)						Extraction (%)					
pH	**O/A**	**Al**	**Co**	**Cu**	**Li**	**Mn**	**Ni**	**Al**	**Co**	**Cu**	**Li**	**Mn**	**Ni**	**Al**	**Co**	**Cu**	**Li**	**Mn**	**Ni**
2.5	5	0.10	2.06	0.01	0.69	1.80	2.44	0.05	1.95	0.01	0.65	0.11	2.39	47.37	6.47	4.62	7.36	94.02	3.23
	4	0.10	2.06	0.01	0.69	1.80	2.44	0.07	1.99	0.01	0.67	0.16	2.41	36.85	6.42	5.93	6.40	91.23	4.19
	3	0.10	2.06	0.01	0.69	1.80	2.44	0.07	1.99	0.01	0.67	0.25	2.38	32.04	4.33	6.35	4.16	86.17	3.47
	2	0.10	2.06	0.01	0.69	1.80	2.44	0.09	2.03	0.01	0.69	0.46	2.41	19.43	5.33	6.48	4.69	75.23	5.01
	1	0.10	2.06	0.01	0.69	1.80	2.44	0.09	2.03	0.01	0.69	0.88	2.43	16.79	8.25	8.03	7.59	54.36	7.33
3	5	0.10	2.06	0.01	0.69	1.80	2.44	0.08	1.73	0.01	0.56	0.06	2.14	25.49	16.12	18.07	19.91	96.87	12.16
	4	0.10	2.06	0.01	0.69	1.80	2.44	0.07	1.77	0.01	0.57	0.07	2.17	33.48	17.52	19.83	21.53	96.38	14.67
	3	0.10	2.06	0.01	0.69	1.80	2.44	0.09	1.92	0.01	0.63	0.11	2.32	21.35	11.72	16.18	14.52	94.16	9.80
	2	0.10	2.06	0.01	0.69	1.80	2.44	0.08	1.82	0.01	0.61	0.26	2.18	22.60	15.96	17.10	16.33	86.44	15.18
	1	0.10	2.06	0.01	0.69	1.80	2.44	0.09	1.79	0.01	0.61	0.56	2.13	18.47	17.48	18.80	16.45	70.67	17.01
3.5	5	0.10	2.06	0.01	0.69	1.80	2.44	0.08	1.71	0.00	0.47	0.03	2.12	24.02	17.29	20.65	31.80	98.41	12.98
	4	0.10	2.06	0.01	0.69	1.80	2.44	0.07	1.60	0.00	0.46	0.03	1.97	29.09	22.13	23.51	33.08	98.01	19.02
	3	0.10	2.06	0.01	0.69	1.80	2.44	0.08	1.71	0.01	0.53	0.06	2.07	23.64	17.08	18.66	24.10	96.41	15.24
	2	0.10	2.06	0.01	0.69	1.80	2.44	0.09	1.79	0.01	0.59	0.15	2.15	14.18	8.70	9.39	11.56	91.53	7.71
	1	0.10	2.06	0.01	0.69	1.80	2.44	0.09	1.80	0.01	0.62	0.67	2.15	14.25	9.75	10.99	8.11	61.91	9.28

Table 38: Solvent extraction tests with 20% v/v D2EHPA

		Aqueous solution concentration before extraction (g/L)						Aqueous solution concentration after extraction (g/L)						Extraction (%)					
pH	**O/A**	**Al**	**Co**	**Cu**	**Li**	**Mn**	**Ni**	**Al**	**Co**	**Cu**	**Li**	**Mn**	**Ni**	**Al**	**Co**	**Cu**	**Li**	**Mn**	**Ni**
2.5	5	0.10	2.06	0.01	0.69	1.80	2.44	0.04	1.51	0.00	0.50	0.03	2.11	66.68	31.14	30.90	32.41	98.46	18.57
	4	0.10	2.06	0.01	0.69	1.80	2.44	0.04	1.74	0.01	0.57	0.04	2.33	65.24	19.60	20.81	22.04	97.75	9.29
	3	0.10	2.06	0.01	0.69	1.80	2.44	0.04	1.62	0.00	0.54	0.05	2.10	63.34	25.15	26.53	26.85	97.18	18.26
	2	0.10	2.06	0.01	0.69	1.80	2.44	0.08	1.76	0.01	0.59	0.09	2.20	31.08	18.67	17.70	19.23	95.03	14.38
	1	0.10	2.06	0.01	0.69	1.80	2.44	0.08	1.88	0.01	0.64	0.31	2.26	22.62	12.35	14.51	12.56	83.26	10.88
3	5	0.10	2.06	0.01	0.69	1.80	2.44	0.04	0.93	0.00	0.28	0.01	1.40	59.58	54.58	47.10	60.17	99.49	42.72
	4	0.10	2.06	0.01	0.69	1.80	2.44	0.06	1.54	0.00	0.45	0.02	2.17	42.75	26.85	22.81	35.99	99.06	12.88
	3	0.10	2.06	0.01	0.69	1.80	2.44	0.07	1.74	0.01	0.52	0.02	2.33	36.46	16.25	13.66	25.77	98.58	5.48
	2	0.10	2.06	0.01	0.69	1.80	2.44	0.08	1.78	0.01	0.56	0.04	2.26	27.68	17.12	12.75	22.71	97.61	11.08
	1	0.10	2.06	0.01	0.69	1.80	2.44	0.08	1.75	0.01	0.58	0.16	2.12	19.28	15.02	15.88	16.25	91.08	13.27
3.5	5	0.10	2.06	0.01	0.69	1.80	2.44	0.08	1.40	0.00	0.31	0.01	2.09	25.27	32.15	23.48	55.88	99.48	14.21
	4	0.10	2.06	0.01	0.69	1.80	2.44	0.08	1.43	0.00	0.34	0.01	2.01	23.55	26.95	16.40	48.98	99.32	13.52
	3	0.10	2.06	0.01	0.69	1.80	2.44	0.07	1.50	0.00	0.38	0.01	1.98	32.60	27.17	23.42	46.19	99.08	18.68
	2	0.10	2.06	0.01	0.69	1.80	2.44	0.08	1.69	0.01	0.48	0.03	2.13	19.20	11.32	9.44	25.35	98.05	5.81
	1	0.10	2.06	0.01	0.69	1.80	2.44	0.08	1.70	0.01	0.54	0.11	2.06	19.98	17.42	19.47	21.72	94.08	15.57

Table 39: Distribution coefficients from solvent extraction tests at different conditions

D2EHPA (% v/v)	pH	O/A	Al	Co	Cu	Li	Mn	Ni
10	2.5	5	0.176	0.012	0.008	0.014	3.112	0.005
		4	0.134	0.009	0.008	0.009	2.514	0.003
		3	0.152	0.012	0.019	0.011	2.052	0.009
		2	0.096	0.007	0.013	0.004	1.438	0.005
		1	0.118	0.014	0.011	0.006	1.038	0.004
	3	5	0.068	0.038	0.044	0.050	6.189	0.028
		4	0.111	0.041	0.049	0.056	6.386	0.031
		3	0.069	0.025	0.044	0.037	5.091	0.018
		2	0.114	0.065	0.073	0.068	3.004	0.060
		1	0.165	0.151	0.170	0.137	2.239	0.145
	3.5	5	0.063	0.042	0.052	0.093	12.348	0.030
		4	0.103	0.071	0.077	0.124	12.333	0.059
		3	0.103	0.069	0.076	0.106	8.964	0.060
		2	0.112	0.075	0.079	0.094	5.697	0.069
		1	0.201	0.141	0.157	0.121	1.704	0.135
20	2.5	5	0.364	0.073	0.072	0.078	11.975	0.031
		4	0.433	0.045	0.050	0.055	10.328	0.012
		3	0.530	0.090	0.098	0.100	10.887	0.054
		2	0.189	0.084	0.077	0.088	9.055	0.055
		1	0.241	0.095	0.123	0.098	4.734	0.077
	3	5	0.295	0.240	0.178	0.302	39.215	0.149
		4	0.178	0.085	0.067	0.133	25.793	0.031
		3	0.186	0.061	0.049	0.111	22.844	0.016
		2	0.164	0.079	0.050	0.121	19.547	0.040
		1	0.239	0.177	0.189	0.194	10.211	0.153
	3.5	5	0.068	0.095	0.061	0.253	38.373	0.033
		4	0.093	0.109	0.064	0.264	38.327	0.054
		3	0.161	0.124	0.102	0.286	35.871	0.077
		2	0.168	0.109	0.096	0.223	27.138	0.073
		1	0.250	0.211	0.242	0.277	15.879	0.184

Table 40: Separation factors for solvent extraction tests

D2EHPA	pH	O/A	Al	Co	Cu	Li	Ni
10	2.5	5	17.66	266.10	410.21	226.61	676.42
10	2.5	4	18.76	275.17	322.45	276.42	806.25
10	2.5	3	13.48	177.14	107.70	186.98	240.43
10	2.5	2	15.01	204.23	108.43	398.77	270.76
10	2.5	1	8.82	76.25	92.92	162.91	292.14
10	3	5	90.48	161.06	140.35	124.47	223.64
10	3	4	57.65	155.87	129.39	114.37	204.34
10	3	3	73.47	200.76	114.52	137.07	286.98
10	3	2	26.42	46.05	41.17	44.36	50.07
10	3	1	13.55	14.80	13.18	16.34	15.48
10	3.5	5	195.34	295.35	237.21	132.40	413.84
10	3.5	4	120.24	173.56	160.49	99.80	210.00
10	3.5	3	86.84	130.60	117.21	84.71	149.54
10	3.5	2	50.98	75.96	71.75	60.85	82.70
10	3.5	1	8.47	12.06	10.84	14.10	12.59
20	2.5	5	32.87	163.99	166.13	153.21	388.05
20	2.5	4	23.83	227.44	206.94	188.99	873.41
20	2.5	3	20.53	121.34	111.43	109.34	201.29
20	2.5	2	47.85	107.74	117.31	102.78	165.32
20	2.5	1	19.67	49.69	38.49	48.35	61.28
20	3	5	133.00	163.16	220.22	129.78	262.88
20	3	4	144.97	303.67	382.62	194.27	825.98
20	3	3	122.82	376.31	467.28	205.42	1445.28
20	3	2	119.42	246.88	389.93	161.46	490.62
20	3	1	42.76	57.78	54.10	52.63	66.74
20	3.5	5	567.51	404.94	625.21	151.49	1158.58
20	3.5	4	410.61	350.51	598.73	144.92	715.74
20	3.5	3	222.50	288.52	351.92	125.39	468.42
20	3.5	2	161.20	249.11	281.89	121.50	370.04
20	3.5	1	63.59	75.29	65.66	57.24	86.12

8.4 Appendix D: Stripping tests

Table 41: Stripping with 2M Sulphuric acid

A/O	Concentration in organic before stripping (mg/L)						Concentration in aqueous after stripping (mg/L)						Stripping efficiency (%)						
	Al	Co	Cu	Li	Mn	Ni	Al	Co	Cu	Li	Mn	Ni	Al	Co	Cu	Li	Mn	Ni	
1	3.95	10.91	0.17	5.37	236.42	13.80	0.98	10.89	0.11	5.36	216.24	1.81	24.93	99.83	65.24	99.83	91.46	13.11	Test 1
	3.95	10.91	0.17	5.37	236.42	13.80	0.84	10.69	0.10	5.22	227.33	1.63	21.11	98.03	56.58	97.42	96.15	11.83	Test 2
	3.95	10.91	0.17	5.37	236.42	13.80	1.13	10.88	0.11	5.26	222.61	1.98	28.75	99.75	63.06	98.12	94.16	14.39	Test 3
							0.98	10.82	0.10	5.28	222.06	1.81	24.93	99.20	61.63	98.46	93.92	13.11	Average
							0.15	0.11	0.01	0.07	5.56	0.18	3.82	1.02	4.51	1.24	2.35	1.28	STDEV
2	3.95	10.91	0.17	5.37	236.42	13.80	0.80	5.31	0.07	2.68	107.74	1.08	40.67	97.33	81.40	99.80	91.14	15.59	Test 1
	3.95	10.91	0.17	5.37	236.42	13.80	0.89	5.44	0.06	2.68	112.78	0.79	45.35	99.86	76.76	99.92	95.41	11.37	Test 2
	3.95	10.91	0.17	5.37	236.42	13.80	0.71	5.17	0.07	2.65	111.94	1.37	35.99	94.80	86.75	98.90	94.69	19.82	Test 3
							0.80	5.31	0.07	2.67	110.82	1.08	40.67	97.33	81.64	99.54	93.75	15.59	Average
							0.09	0.14	0.00	0.01	2.70	0.29	4.68	2.53	5.00	0.56	2.28	4.22	STDEV
3	3.95	10.91	0.17	5.37	236.42	13.80	0.86	3.63	0.03	1.77	75.09	0.88	64.86	99.75	54.92	99.32	95.29	19.14	Test 1
	3.95	10.91	0.17	5.37	236.42	13.80	0.87	3.58	0.05	1.79	78.04	0.53	66.11	98.59	91.62	99.94	99.03	11.58	Test 2
	3.95	10.91	0.17	5.37	236.42	13.80	0.84	3.61	0.05	1.77	78.30	1.23	63.62	99.34	90.52	98.89	99.36	26.69	Test 3
							0.86	3.61	0.04	1.78	77.15	0.88	64.86	99.23	79.02	99.38	97.89	19.14	Average
							0.01	0.02	0.01	0.01	1.78	0.35	1.24	0.59	20.87	0.52	2.26	7.56	STDEV
4	3.95	10.91	0.17	5.37	236.42	13.80	0.57	2.67	0.03	1.27	53.47	0.54	57.34	97.78	63.98	94.93	90.45	15.78	Test 1
	3.95	10.91	0.17	5.37	236.42	13.80	0.57	2.65	0.03	1.29	56.51	0.36	57.52	97.20	79.50	95.92	95.60	10.37	Test 2
	3.95	10.91	0.17	5.37	236.42	13.80	0.56	2.68	0.02	1.28	57.61	0.73	57.17	98.36	63.09	94.96	97.46	21.19	Test 3
							0.57	2.67	0.03	1.28	55.86	0.54	57.34	97.78	68.85	95.27	94.51	15.78	Average
							0.00	0.01	0.00	0.01	2.15	0.19	0.18	0.58	9.23	0.56	3.63	5.41	STDEV
5	3.95	10.91	0.17	5.37	236.42	13.80	0.51	2.16	0.03	1.07	45.10	0.70	64.26	99.12	98.20	99.08	95.38	25.57	Test 1
	3.95	10.91	0.17	5.37	236.42	13.80	0.62	2.11	0.03	1.06	47.12	0.34	77.68	96.58	96.63	98.51	99.64	12.13	Test 2
	3.95	10.91	0.17	5.37	236.42	13.80	0.40	2.12	0.03	1.07	45.14	1.08	50.84	96.95	98.17	99.20	95.45	39.00	Test 3
							0.51	2.13	0.03	1.06	45.78	0.70	64.26	97.55	97.67	98.93	96.82	25.57	Average
							0.11	0.03	0.00	0.00	1.15	0.37	13.42	1.37	0.90	0.37	2.44	13.44	STDEV

Table 42: Stripping with 0.5M Sulphuric acid

A/O	Concentration in organic before stripping (mg/L)						Concentration in aqueous after stripping (mg/L)						Stripping efficiency (%)						
	Al	Co	Cu	Li	Mn	Ni	Al	Co	Cu	Li	Mn	Ni	Al	Co	Cu	Li	Mn	Ni	
1	3.95	10.91	0.17	5.37	236.42	13.80	0.09	9.52	0.02	4.62	200.48	1.66	2.18	87.23	10.36	86.14	84.80	12.04	Test 1
	3.95	10.91	0.17	5.37	236.42	13.80	0.17	9.43	0.01	4.64	200.33	1.46	4.25	86.46	4.39	86.41	84.73	10.58	Test 2
	3.95	10.91	0.17	5.37	236.42	13.80	0.00	9.60	0.02	4.73	200.64	1.86	0.11	88.00	10.31	88.20	84.86	13.50	Test 3
							0.09	9.52	0.01	4.66	200.48	1.66	2.18	87.23	8.35	86.92	84.80	12.04	Average
							0.08	0.08	0.00	0.06	0.15	0.20	2.07	0.77	3.44	1.12	0.06	1.46	STDV
2	3.95	10.91	0.17	5.37	236.42	13.80	0.04	5.33	0.04	2.45	106.28	0.84	2.33	97.68	52.93	91.41	89.90	12.21	Test 1
	3.95	10.91	0.17	5.37	236.42	13.80	0.06	5.17	0.02	2.46	106.24	0.76	2.91	94.84	22.85	91.85	89.87	11.00	Test 2
	3.95	10.91	0.17	5.37	236.42	13.80	0.03	5.43	0.03	2.55	106.31	0.92	1.76	99.59	39.65	94.87	89.94	13.42	Test 3
							0.04	5.31	0.03	2.49	106.28	0.84	2.33	97.37	38.47	92.71	89.90	12.21	Average
							0.01	0.13	0.01	0.05	0.04	0.08	0.57	2.39	15.07	1.88	0.03	1.21	STDV
3	3.95	10.91	0.17	5.37	236.42	13.80	0.05	3.63	0.02	1.79	78.21	0.63	3.83	99.71	41.36	99.98	99.24	13.60	Test 1
	3.95	10.91	0.17	5.37	236.42	13.80	0.08	3.51	0.03	1.80	78.53	0.55	6.50	96.52	50.51	100.47	99.65	11.92	Test 2
	3.95	10.91	0.17	5.37	236.42	13.80	0.01	3.57	0.03	1.78	78.30	0.70	1.15	98.10	51.63	99.56	99.35	15.28	Test 3
							0.05	3.57	0.03	1.79	78.35	0.63	3.83	98.11	47.84	100.00	99.42	13.60	Average
							0.03	0.06	0.00	0.01	0.17	0.08	2.67	1.60	5.63	0.46	0.21	1.68	STDV
4	3.95	10.91	0.17	5.37	236.42	13.80	0.02	2.73	0.00	1.33	56.49	0.53	1.83	99.99	11.65	99.37	95.57	15.42	Test 1
	3.95	10.91	0.17	5.37	236.42	13.80	0.02	2.69	0.04	1.31	58.91	0.39	2.41	98.68	87.52	98.05	99.67	11.28	Test 2
	3.95	10.91	0.17	5.37	236.42	13.80	0.01	2.70	0.04	1.33	56.58	0.67	1.26	99.05	86.74	99.63	95.73	19.57	Test 3
							0.02	2.71	0.02	1.33	57.33	0.53	1.83	99.24	61.97	99.02	96.99	15.42	Average
							0.00	0.02	0.02	0.01	1.37	0.14	0.58	0.68	43.58	0.84	2.32	4.14	STDV
5	3.95	10.91	0.17	5.37	236.42	13.80	0.04	2.17	0.03	1.06	45.49	0.51	4.72	99.74	96.43	98.82	96.20	18.45	Test 1
	3.95	10.91	0.17	5.37	236.42	13.80	0.05	2.18	0.03	1.07	46.41	0.32	6.37	99.87	91.65	99.49	98.15	11.74	Test 2
	3.95	10.91	0.17	5.37	236.42	13.80	0.02	2.15	0.03	1.07	45.59	0.69	3.07	98.66	92.18	99.49	96.42	25.16	Test 3
							0.04	2.17	0.03	1.07	45.83	0.51	4.72	99.42	93.42	99.27	96.92	18.45	Average
							0.01	0.01	0.00	0.00	0.50	0.19	1.65	0.66	2.62	0.38	1.07	6.71	STDV

8.5 Appendix E: Metal precipitation tests

Table 43: Phosphate precipitation at different temperatures

		Mass of metal precipitated (mg)						Extraction (%)					
		Al	**Co**	**Cu**	**Li**	**Mn**	**Ni**	**Al**	**Co**	**Cu**	**Li**	**Mn**	**Ni**
50 ℃	Test 1	2.14	41.19	0.12	0.11	36.80	49.23	99.73	97.72	65.08	0.76	99.65	98.62
	Test 2	2.07	40.51	0.07	0.93	36.68	48.88	96.58	95.98	35.76	3.79	99.31	97.87
	Test 3	2.08	40.57	0.07	0.86	36.70	48.91	96.98	96.24	36.85	6.04	99.38	98.00
	Average	2.09	40.76	0.09	0.63	36.73	49.01	97.76	96.65	45.90	3.53	99.45	98.16
	Standard deviation	0.04	0.38	0.03	0.46	0.06	0.19	1.72	0.94	16.62	2.65	0.18	0.40
60℃	Test 1	2.10	40.96	0.07	1.02	36.64	49.10	98.07	97.12	35.33	5.82	99.20	98.35
	Test 2	2.06	40.98	0.05	1.20	36.64	49.16	96.31	97.17	27.93	7.10	99.21	98.46
	Test 3	2.10	40.82	0.05	0.99	36.60	49.05	98.09	96.83	28.45	6.94	99.10	98.26
	Average	2.09	40.92	0.06	1.07	36.63	49.10	97.49	97.04	30.57	6.62	99.17	98.36
	Standard deviation	0.02	0.09	0.01	0.12	0.02	0.06	1.02	0.18	4.13	0.70	0.06	0.10
70℃	Test 1	19.93	406.86	0.14	34.60	365.21	488.64	92.91	96.47	6.18	23.13	98.87	97.86
	Test 2	19.43	406.26	0.18	34.33	365.00	488.16	90.85	96.43	11.08	25.28	98.85	97.83
	Test 3	19.99	415.45	0.13	35.97	361.04	489.55	93.40	98.58	8.49	26.41	97.79	98.11
	Average	19.78	409.53	0.15	34.97	363.75	488.78	92.39	97.16	8.58	24.94	98.50	97.93
	Standard deviation	0.30	5.14	0.03	0.88	2.35	0.71	1.35	1.23	2.45	1.67	0.62	0.15
80℃	Test 1	15.69	409.13	0.50	99.15	364.40	493.79	73.75	97.11	27.91	70.20	98.69	98.95
	Test 2	15.87	409.48	0.61	99.66	364.49	494.25	73.58	97.09	31.31	69.43	98.67	99.00
	Test 3	15.69	408.85	0.57	107.65	364.20	493.76	72.73	96.94	29.01	75.14	98.59	98.90
	Average	15.75	409.15	0.56	102.15	364.36	493.93	73.35	97.04	29.41	71.59	98.65	98.95
	Standard deviation	0.10	0.31	0.06	4.77	0.15	0.27	0.55	0.10	1.73	3.10	0.06	0.05

Table 44: Masses of metal precipitated during precipitation tests to investigate the proposed metal separation orders

	Mass of metal precipitated (mg)					
Process description	**Al**	**Co**	**Cu**	**Li**	**Mn**	**Ni**
Phosphate precipitation at 80℃ after Mn extraction with DEHPA	4.70	768.98	2.58	190.78	3.50	992.58
Repeat 1	4.69	765.95	2.56	184.24	3.50	989.25
Repeat 2	4.70	767.39	2.53	185.55	3.50	990.49
Average	4.70	767.44	2.56	186.85	3.50	990.77
SDV	0.01	1.51	0.02	3.46	0.00	1.68
Carbonate precipitation after Mn extraction with DEHPA	3.74	373.11	0.09	1.28	2.82	696.41
Repeat 1	3.52	393.47	0.19	6.74	2.87	686.09
Repeat 2	3.61	356.74	0.13	1.07	2.75	678.48
Average	3.62	374.44	0.14	3.03	2.81	686.99
SDV	0.11	18.40	0.06	3.21	0.06	8.99
Phosphate precipitation at 80℃ after carbonate precipitation and Mn. Al extraction with D2EHPA	0.98	389.72	3.16	180.61	0.63	294.48
Repeat 1	0.98	383.91	3.09	176.24	0.64	286.35
Repeat 2	0.98	389.69	3.13	180.40	0.63	294.44
Average	0.98	387.77	3.13	179.09	0.64	291.76
SDV	0.00	3.35	0.04	2.46	0.01	4.69
Phosphate precipitation at 50 ℃. after Mn extraction with DEHPA	4.72	763.14	2.41	10.66	3.46	987.69
Repeat 1	4.67	754.11	2.32	9.19	3.46	983.95
Repeat 2	4.62	755.21	2.23	7.38	3.44	984.57
Average	4.67	757.48	2.32	9.08	3.46	985.40
SDV	0.05	4.93	0.09	1.64	0.01	2.01
Phosphate precipitation at 80℃ after phosphate precipitation at 50℃ and Mn. Al extraction with D2EHPA	0.00	7.88	0.61	190.71	0.03	6.87
Repeat 1	0.02	16.92	0.70	179.44	0.04	10.61
Repeat 2	0.03	15.82	0.78	193.58	0.05	9.98
Average	0.01	13.54	0.70	187.91	0.04	9.15
SDV	0.01	4.93	0.09	7.47	0.01	2.00
Metal mass in 20ml feed of solution after Mn and Al extraction with DEHPA (mg)	4.72	771.05	3.07	249.29	3.50	994.57

Table 45: Metal extraction during precipitation tests to investigate the proposed metal separation orders

	Extraction (%)					
Process description	**Al**	**Co**	**Cu**	**Li**	**Mn**	**Ni**
Phosphate precipitation at 80℃ after Mn extraction with DEHPA	99.52	99.73	84.12	76.53	99.94	99.80
Repeat 1	99.25	99.34	83.41	73.90	99.93	99.47
Repeat 2	99.54	99.52	82.62	74.43	99.93	99.59
Average	99.44	99.53	83.38	74.95	99.93	99.62
SDV	0.16	0.20	0.75	1.39	0.01	0.17
Carbonate precipitation after Mn extraction with DEHPA	79.24	48.39	2.79	0.51	80.57	70.02
Repeat 1	74.62	51.03	6.35	2.70	82.12	68.98
Repeat 2	76.35	46.27	4.12	0.43	78.62	68.22
Average	76.74	48.56	4.42	1.22	80.44	69.07
SDV	2.33	2.39	1.80	1.29	1.76	0.90
Phosphate precipitation at 80℃ after carbonate precipitation and Mn. Al extraction with D2EHPA	20.76	50.54	100.00	72.45	18.04	29.61
Repeat 1	20.76	49.79	100.00	70.70	18.37	28.79
Repeat 2	20.76	50.54	100.00	72.37	18.04	29.60
Average	20.76	50.29	100.00	71.84	18.15	29.33
SDV	0.00	0.43	0.00	0.99	0.19	0.47
Phosphate precipitation at 50 ℃. after Mn extraction with DEHPA	100.00	98.97	78.67	4.28	99.01	99.31
Repeat 1	98.82	97.80	75.74	3.69	98.90	98.93
Repeat 2	97.92	97.94	72.62	2.96	98.45	98.99
Average	98.91	98.24	75.68	3.64	98.79	99.08
SDV	1.04	0.64	3.02	0.66	0.30	0.20
Phosphate precipitation at 80℃ after phosphate precipitation at 50℃ and Mn. Al extraction with D2EHPA	0.00	1.02	20.04	76.50	0.99	0.69
Repeat 1	0.34	2.19	22.71	71.98	1.10	1.07
Repeat 2	0.61	2.05	25.59	77.65	1.55	1.00
Average	0.32	1.76	22.78	75.38	1.21	0.92
SDV	0.31	0.64	2.77	3.00	0.30	0.20

Appendix F: Mass balance data

Scenario 1

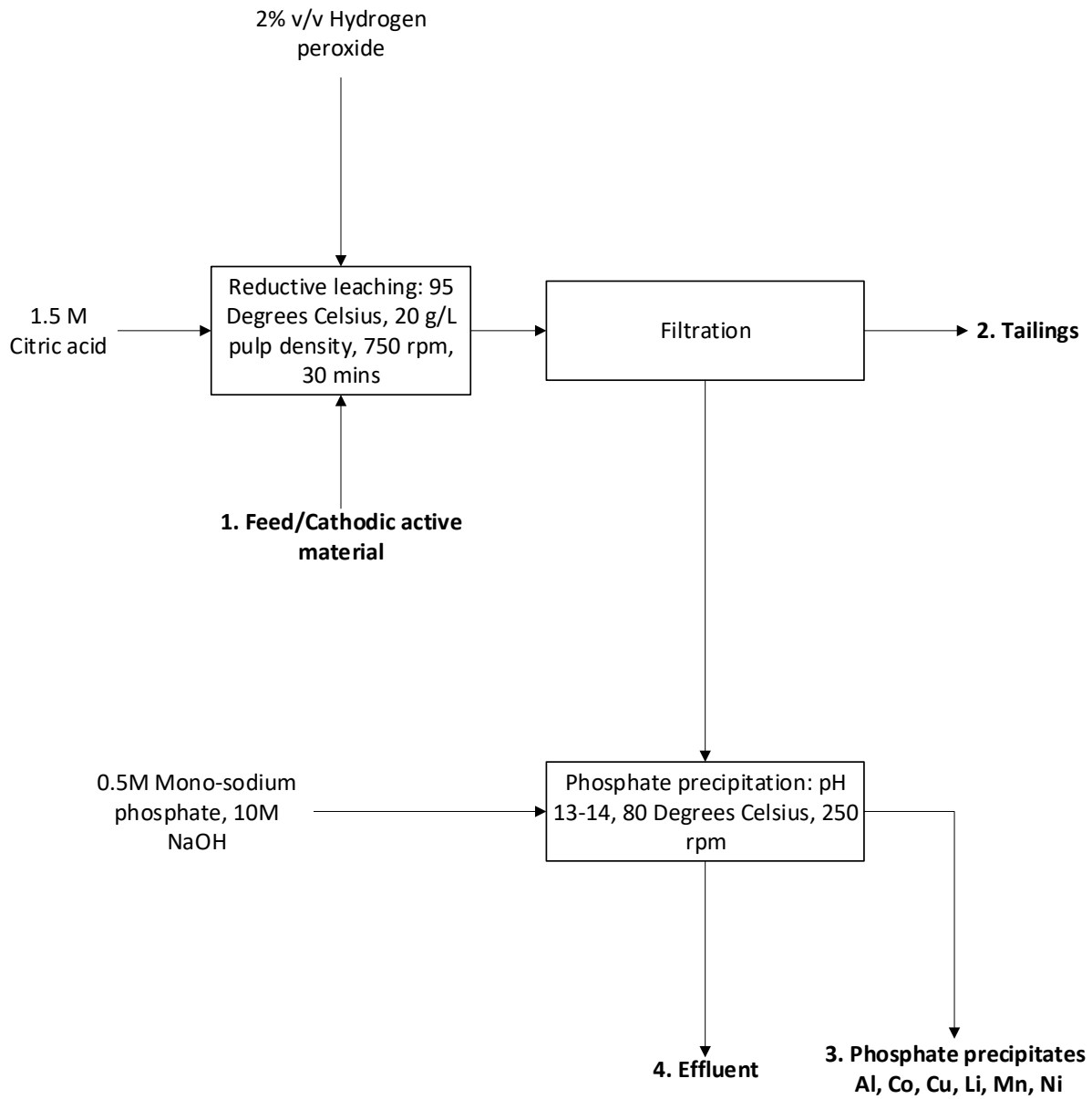

Figure 42: Simple flowsheet showing the streams from scenario 1

Table 46: Mass balance for scenario 1

			Input	Output			
	Stream number		**1**	**2**	**3**	**4**	
	Stream ID		**Feed**	**Tailings**	**Co-Li-Mn-Ni phosphates**	**Effluent**	**Total**
	Solid throughput	t/h	20.00	11.52	8.07	0.41	20.00
Solid composition	Al	%	0.67	0.14	1.06	-	-
	C	%	30.70	53.31	0.00	-	-
	Co	%	12.97	1.30	29.38	-	-
	Cu	%	0.05	0.00	0.04	-	-
	Li	%	4.38	0.29	7.47	-	-
	Mn	%	10.98	1.16	25.19	-	-
	Ni	%	15.26	0.38	36.87	-	-
	O	%	25.00	43.41	0.00	-	-
Liquid composition	Al	mg/L	-	-	-	10.70	-
	C	mg/L	-	-	-	0.00	-
	Co	mg/L	-	-	-	23.36	-
	Cu	mg/L	-	-	-	2.48	-
	Li	mg/L	-	-	-	75.92	-
	Mn	mg/L	-	-	-	9.35	-
	Ni	mg/L	-	-	-	9.83	-
	O	mg/L	-	-	-	0.00	-
Total elemental flow	Al	t/h	0.13	0.02	0.09	0.03	0.13
	C	t/h	6.14	6.14	0.00	0.00	6.14
	Co	t/h	2.59	0.15	2.37	0.07	2.59
	Cu	t/h	0.01	0.00	0.00	0.01	0.01
	Li	t/h	0.88	0.03	0.60	0.24	0.88
	Mn	t/h	2.20	0.13	2.03	0.03	2.20
	Ni	t/h	3.05	0.04	2.98	0.03	3.05
	O	t/h	5.00	5.00	0.00	0.00	5.00

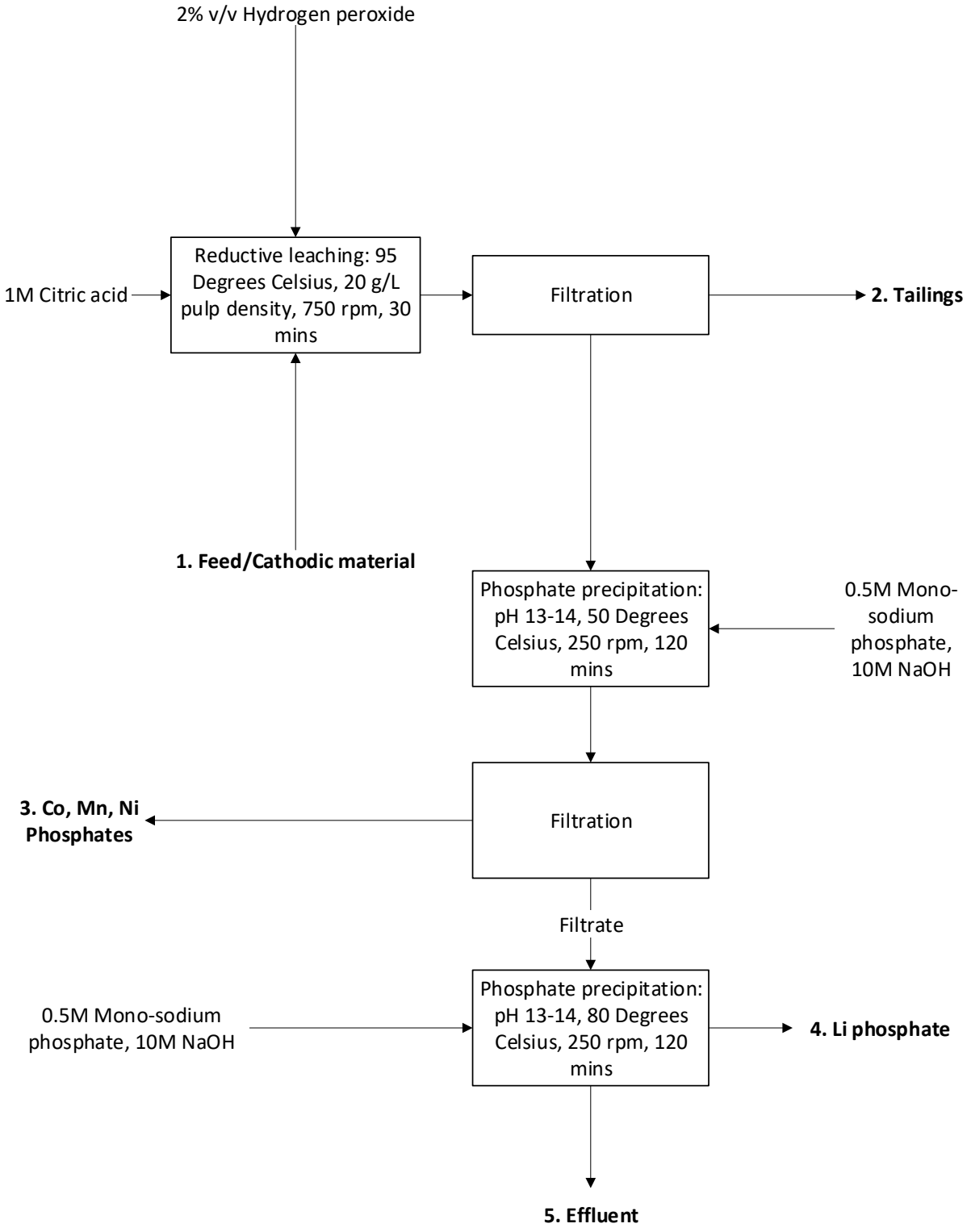

Figure 43: Simple flowsheet showing the streams from scenario 2

Table 47: Mass balance for scenario 2

			Input	Output				
	Stream number		**1**	**2**	**3**	**4**	**5**	
	Stream ID		**Feed**	**Tailings**	**Co, Mn, Ni phosphates**	**Li phosphate**	**Effluent**	**Total**
	Material flow	t/h	20.00	11.30	7.47	0.81	0.43	20.00
Solids composition	Al	%	0.67	0.14	1.53	0.31	-	-
	C	%	30.70	53.31	0.00	0.00	-	-
	Co	%	12.97	1.30	31.59	10.39	-	-
	Cu	%	0.05	0.00	0.07	0.21	-	-
	Li	%	4.38	0.29	0.33	76.15	-	-
	Mn	%	10.98	1.16	26.94	6.17	-	-
	Ni	%	15.26	0.38	39.54	6.75	-	-
	O	%	25.00	43.41	0.00	0.00	-	-
Liquid composition	Al	mg/L	-	-	-	-	0.00	-
	C	mg/L	-	-	-	-	0.00	-
	Co	mg/L	-	-	-	-	0.64	-
	Cu	mg/L	-	-	-	-	1.08	-
	Li	mg/L	-	-	-	-	63.87	-
	Mn	mg/L	-	-	-	-	0.00	-
	Ni	mg/L	-	-	-	-	0.27	-
	O	mg/L	-	-	-	-	0.00	-
Total Elemental flow	Al	t/h	0.13	0.02	0.11	0.00	0.00	0.13
	C	t/h	6.14	6.14	0.00	0.00	0.00	6.14
	Co	t/h	2.59	0.15	2.36	0.08	0.00	2.59
	Cu	t/h	0.01	0.00	0.00	0.00	0.00	0.01
	Li	t/h	0.88	0.03	0.02	0.62	0.20	0.88
	Mn	t/h	2.20	0.13	2.01	0.05	0.00	2.20
	Ni	t/h	3.05	0.04	2.95	0.05	0.00	3.05
	O	t/h	5.00	5.00	0.00	0.00	0.00	5.00

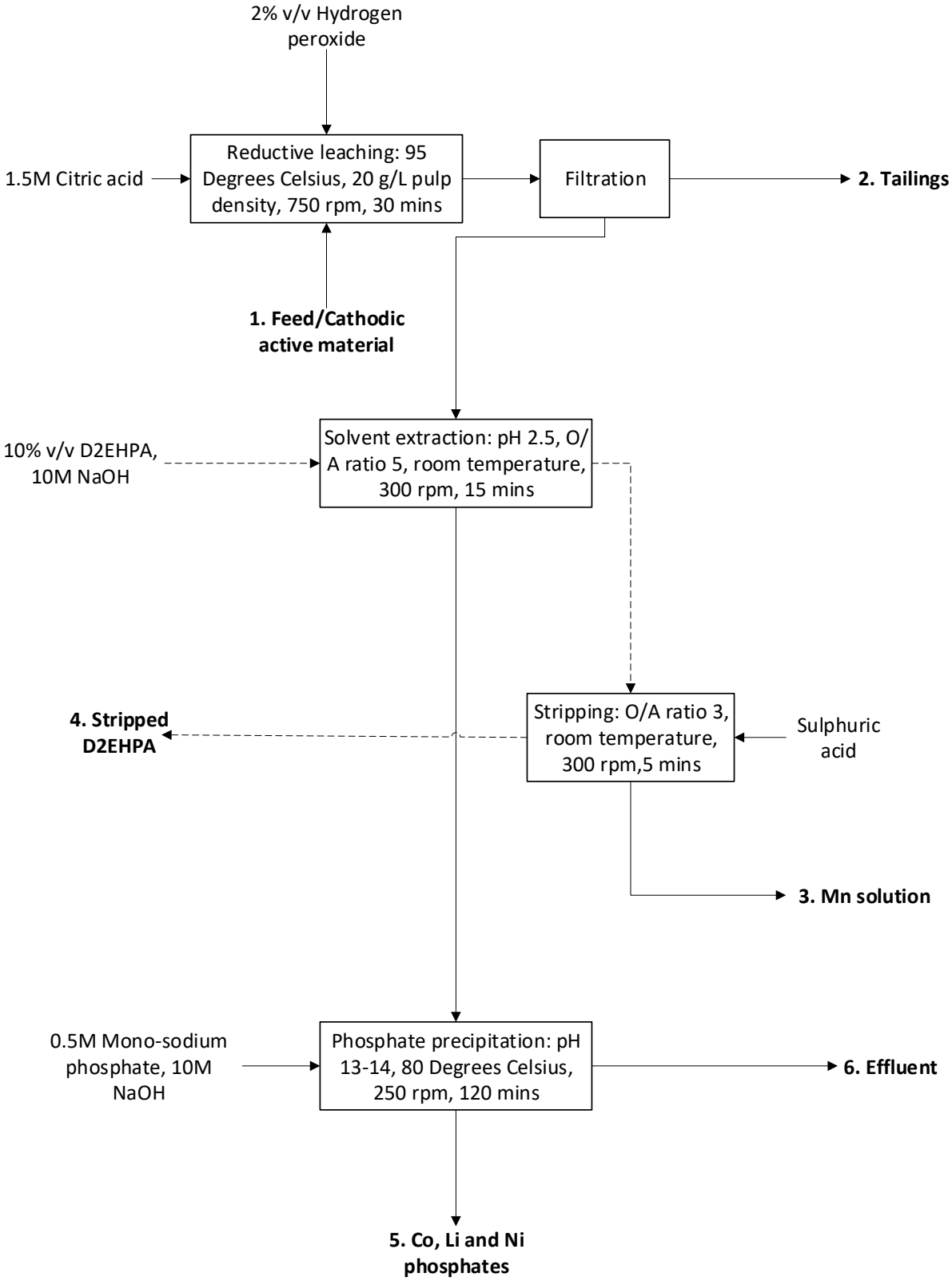

Figure 44: Simple flowsheet showing the streams from scenario 3

Table 48: Mass balance for scenario 3

			Input	Output					
	Steam number		**1**	**2**	**3**	**4**	**5**	**6**	
	Stream ID		**Feed**	**Tailings**	**Mn solution**	**Stripped D2EHPA**	**Co, Li, Ni phosphates**	**Effluent**	**Total**
	Material flow	t/h	20.00	11.52	0.27	2.54	5.47	0.40	20.20
Solids composition	Al	%	0.67	0.14	-	-	0.22	-	-
	C	%	30.70	53.31	-	-	0.00	-	-
	Co	%	12.97	1.30	-	-	38.42	-	-
	Cu	%	0.05	0.00	-	-	0.11	-	-
	Li	%	4.38	0.29	-	-	9.54	-	-
	Mn	%	10.98	1.16	-	-	0.17	-	-
	Ni	%	15.26	0.38	-	-	51.54	-	-
	O	%	25.00	43.41	-	-	0.00	-	-
Liquid composition	Al	mg/L	-	-	9.53	0.05	-	0.10	-
	C	mg/L	-	-	0.00	0.00	-	0.00	-
	Co	mg/L	-	-	18.00	3.71	-	13.90	-
	Cu	mg/L	-	-	0.17	0.02	-	1.96	-
	Li	mg/L	-	-	8.87	1.83	-	64.81	-
	Mn	mg/L	-	-	183.78	80.01	-	0.01	-
	Ni	mg/L	-	-	0.93	0.64	-	14.60	-
	O	mg/L	-	-	0.00	0.00	-	0.00	-
Total Elemental flow	Al	t/h	0.13	0.02	0.10	0.00	0.01	0.00	0.13
	C	t/h	6.14	6.14	0.00	0.00	0.00	0.00	6.14
	Co	t/h	2.59	0.15	0.00	0.33	2.10	0.01	2.59
	Cu	t/h	0.01	0.00	0.00	0.00	0.01	0.00	0.01
	Li	t/h	0.88	0.03	0.00	0.15	0.52	0.17	0.88
	Mn	t/h	2.20	0.13	0.02	2.04	0.01	0.00	2.20
	Ni	t/h	3.05	0.04	0.15	0.02	2.82	0.01	3.05
	O	t/h	5.00	5.00	0.00	0.00	0.00	0.00	5.00

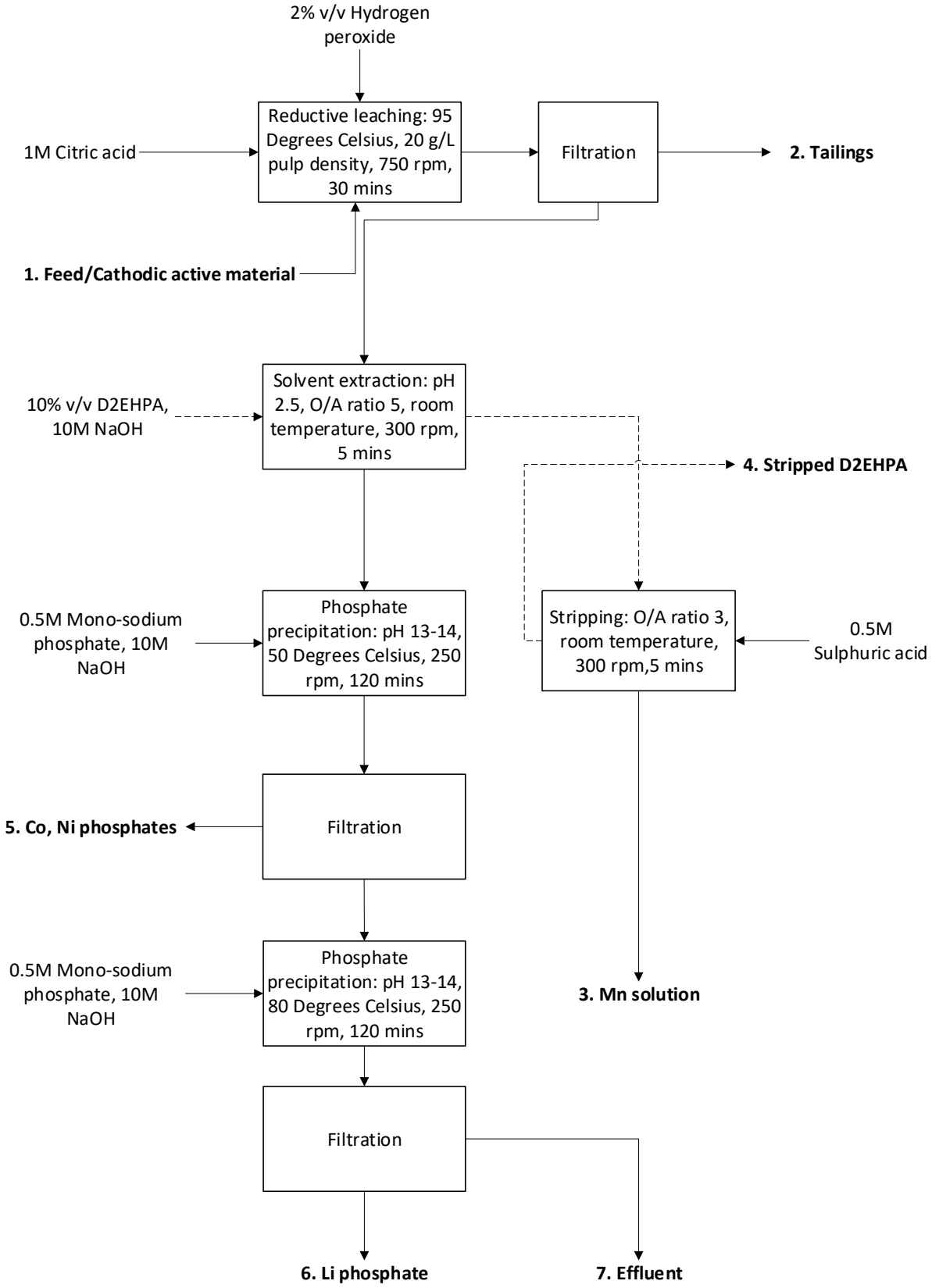

Figure 45: Simple flowsheet showing the streams from scenario 4

Table 49: Mass balance for scenario 4

			Input	Output						
	Stream number		**1**	**2**	**3**	**4**	**5**	**6**	**7**	
	Stream ID		**Feed**	**Tailings**	**Mn solution**	**Stripped D2EHPA**	**Co, Ni phosphate**	**Li phosphate**	**Effluent**	**Total**
	Material flow	t/h	20.00	11.52	2.54	0.27	4.93	0.59	0.15	20.00
Solids composition	Al	%	0.67	0.14	-	-	0.24	0.01	-	-
	C	%	30.70	53.31	-	-	0.00	0.00	-	-
	Co	%	12.97	1.30	-	-	42.07	6.29	-	-
	Cu	%	0.05	0.00	-	-	0.11	0.29	-	-
	Li	%	4.38	0.29	-	-	0.51	88.98	-	-
	Mn	%	10.98	1.16	-	-	0.18	0.02	-	-
	Ni	%	15.26	0.38	-	-	56.87	4.42	-	-
	O	%	25.00	43.41	-	-	0.00	0.00	-	-
Liquid composition	Al	mg/L	-	-	0.05	9.53	-	-	0.00	-
	C	mg/L	-	-	0.00	0.00	-	-	0.00	-
	Co	mg/L	-	-	3.71	18.00	-	-	0.12	-
	Cu	mg/L	-	-	0.02	0.17	-	-	0.20	-
	Li	mg/L	-	-	1.83	8.87	-	-	12.88	-
	Mn	mg/L	-	-	80.01	183.78	-	-	0.00	-
	Ni	mg/L	-	-	0.64	0.93	-	-	0.06	-
	O	mg/L	-	-	0.00	0.00	-	-	0.00	-
Total Elemental flow	Al	t/h	0.13	0.02	0.00	0.10	0.01	0.00	0.00	0.13
	C	t/h	6.14	6.14	0.00	0.00	0.00	0.00	0.00	6.14
	Co	t/h	2.59	0.15	0.33	0.00	2.07	0.04	0.00	2.59
	Cu	t/h	0.01	0.00	0.00	0.00	0.01	0.00	0.00	0.01
	Li	t/h	0.88	0.03	0.15	0.00	0.03	0.52	0.15	0.88
	Mn	t/h	2.20	0.13	2.04	0.02	0.01	0.00	0.00	2.20
	Ni	t/h	3.05	0.04	0.02	0.15	2.80	0.03	0.00	3.05
	O	t/h	5.00	5.00	0.00	0.00	0.00	0.00	0.00	5.00

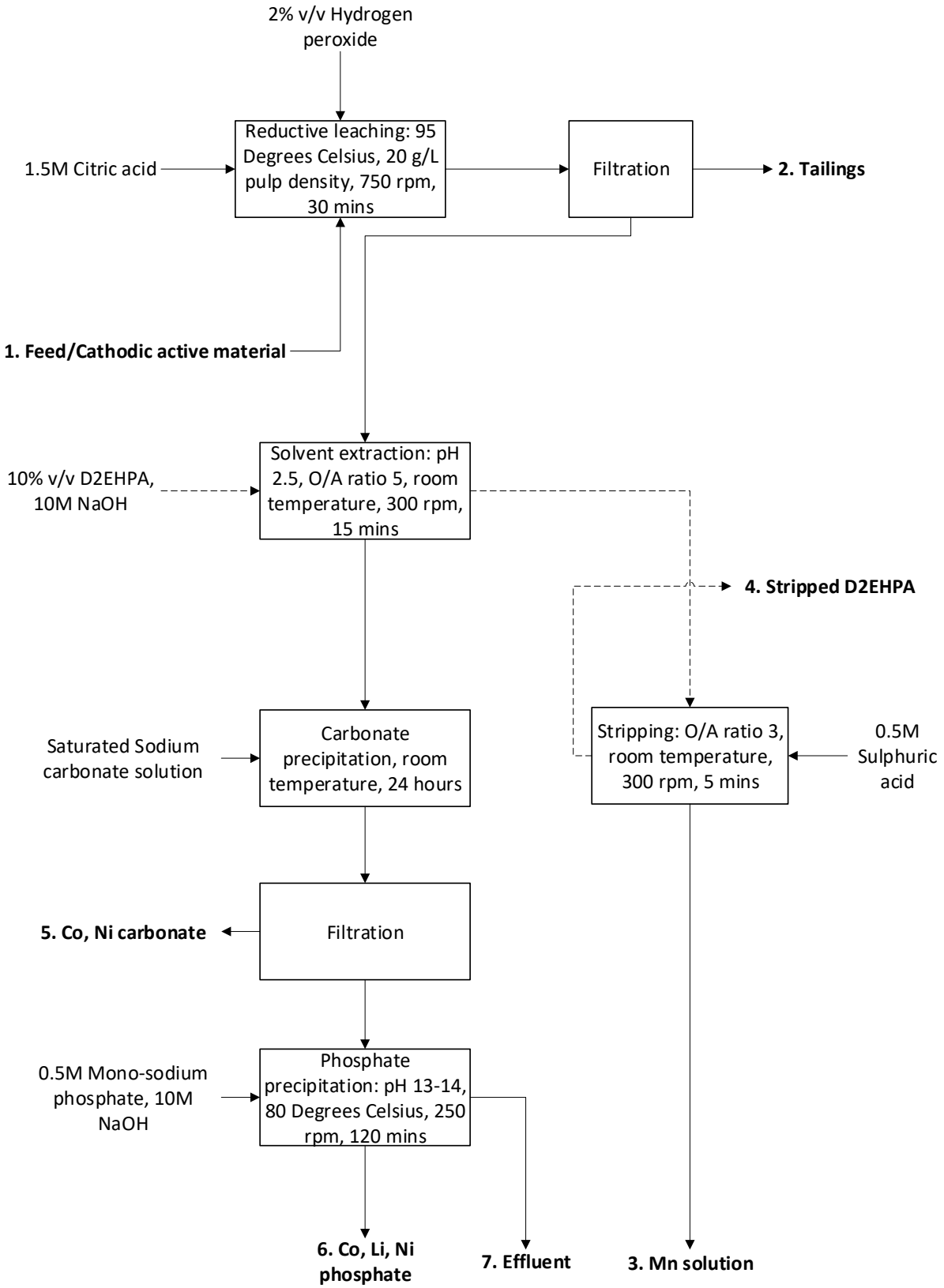

Figure 46: Simple flowsheet showing the streams from scenario 5

Table 50: Mass balance for scenario 5

			Input	Output						
	Stream number		**1**	**2**	**3**	**4**	**5**	**6**	**7**	
	Stream ID		**Feed**	**Tailings**	**Mn solution**	**Stripped D2EHPA**	**Co, Ni carbonate**	**Li phosphate**	**Effluent**	**Total**
	Material flow	t/h	20.00	11.52	2.54	0.27	3.01	2.40	0.26	20.00
Solids composition	Al	%	0.67	0.14	-	-	0.31	0.10	-	-
	C	%	30.70	53.31	-	-	0.00	0.00	-	-
	Co	%	12.97	1.30	-	-	34.11	44.17	-	-
	Cu	%	0.05	0.00	-	-	0.01	0.32	-	-
	Li	%	4.38	0.29	-	-	0.28	20.80	-	-
	Mn	%	10.98	1.16	-	-	0.25	0.07	-	-
	Ni	%	15.26	0.38	-	-	65.04	34.54	-	-
	O	%	25.00	43.41	-	-	0.00	0.00	-	-
Liquid composition	Al	mg/L	-	-	0.05	9.53	-	-	0.00	-
	C	mg/L	-	-	0.00	0.00	-	-	0.00	-
	Co	mg/L	-	-	3.71	18.00	-	-	8.94	-
	Cu	mg/L	-	-	0.02	0.17	-	-	2.08	-
	Li	mg/L	-	-	1.83	8.87	-	-	73.26	-
	Mn	mg/L	-	-	80.01	183.78	-	-	0.05	-
	Ni	mg/L	-	-	0.64	0.93	-	-	4.00	
	O	mg/L	-	-	0.00	0.00	-	-	0.00	
Total Elemental flow	Al	t/h	0.13	0.02	0.00	0.10	0.01	0.00	0.00	0.13
	C	t/h	6.14	6.14	0.00	0.00	0.00	0.00	0.00	6.14
	Co	t/h	2.59	0.15	0.33	0.00	1.03	1.06	0.02	2.59
	Cu	t/h	0.01	0.00	0.00	0.00	0.00	0.01	0.00	0.01
	Li	t/h	0.88	0.03	0.15	0.00	0.01	0.50	0.19	0.88
	Mn	t/h	2.20	0.13	2.04	0.02	0.01	0.00	0.00	2.20
	Ni	t/h	3.05	0.04	0.02	0.15	1.95	0.83	0.05	3.05
	O	t/h	5.00	5.00	0.00	0.00	0.00	0.00	0.00	5.00